PB 86 111606/AS

U.S. Department
of Transportation
**Federal Railroad
Administration**

Analytic Studies of the Effects of Track Geometry Variation

Office of Research and
Development
Washington DC 20590

F. B. Blader
G. L. Mealy

The Analytic Sciences Corporation
One Jacob Way
Reading MA 01867

DOT/FRA/ORD-85/01
DOT-TSC-FRA-84-3

July 1985
Final Report

This document is available to the
Public through the National
Technical Information Service,
Springfield, Virginia 22161

O2 Track/Train
[redacted]s

Notice

This document is disseminated under the sponsorship of the Department of Transportation in the interest of information exchange. The United States Government assumes no liability for its contents or use thereof.

Notice

The United States Government does not endorse products or manufacturers. Trade or manufacturers' names appear herein solely because they are considered essential to the objective of this report.

Technical Report Documentation Page

1. Report No. DOT/FRA/ORD-85/01	**2. Government Accession No.**	**3. Recipient's Catalog No.**

4. Title and Subtitle
ANALYTIC STUDIES OF THE EFFECTS OF TRACK GEOMETRY VARIATION

5. Report Date
July 1985

6. Performing Organization Code
DTS-76

7. Author(s)
F.B. Blader, G.L. Mealy

8. Performing Organization Report No.
DOT-TSC-FRA-84-3

9. Performing Organization Name and Address
The Analytic Sciences Corporation*
One Jacob Way
Reading MA 01867

10. Work Unit No. (TRAIS)
RR419/R4304

11. Contract or Grant No.
TR-1922-4

12. Sponsoring Agency Name and Address
U.S. Department of Transportation
Federal Railroad Administration
Office of Research and Development
Washington DC 20590

13. Type of Report and Period Covered
Final Report
June 1983 - June 1984

14. Sponsoring Agency Code
RRD-10

15. Supplementary Notes
*Under Contract to:
U.S. Department of Transportation
Research and Special Programs Administration
Transportation Systems Center
Cambridge MA 02142

16. Abstract

In this report, analyses are described which were used to aid in the planning of tests carried out on track in Bennington, New Hampshire in August 1982. These tests were designed to provide insight into practical aspects of track safety standards. General results for a fully loaded 100-ton hopper car are used to support the validation of the computer simulation program SIMCAR. In addition, particular results are given for the partially loaded 100-ton car. Extensions beyond existing data are given for response to combined crosslevel and gage cusps and long wavelength alignment sinusoids in tight curves. Conclusions are reached on the limit to geometries beyond which derailment is predicted.

17. Key Words
Computer Simulation, Mathematical Dynamic Curving, Hunting, Wheel/Rail Forces, Profiles, Derailment, Track Geometry, Track Safety Standards

18. Distribution Statement
DOCUMENT IS AVAILABLE TO THE PUBLIC THROUGH THE NATIONAL TECHNICAL INFORMATION SERVICE, SPRINGFIELD, VIRGINIA 22161

19. Security Classif. (of this report) UNCLASSIFIED	**20. Security Classif. (of this page)** UNCLASSIFIED	**21. No. of Pages** 76	**22. Price**

Form DOT F 1700.7 (8-72)   Reproduction of completed page authorized

PREFACE

Under the Track Safety Research Program conducted for the Federal Railroad Administration (FRA) at the Transportation Systems Center (TSC), new guidelines are being developed to provide a basis for improved track and maintenance safety specifications. These new "Track Safety Performance Specifications" are being constructed using both analysis and experimental data to provide an assessment of track geometry and whether it will guide the vehicle safely under the loads imposed by revenue traffic. Efforts conducted under this program have included:

- Statistical Correlation of Railcar Accident Data and Freight Car Characteristics (Conducted at TSC, Ref. 1)
- Development of a data base of engineering parameters characterizing the physical parameters and configurations of railway rolling stock by Pullman-Standard Corporation. (Ref. 2)
- Development of analytic characterizations of track geometry variations found in existing track by ENSCO, INC. (Ref. 3)
- Field tests and demonstrations conducted in cooperation with the railroad industry and the American Railway Engineering Association (AREA)
- Analytic studies of the relation between track geometry variations and derailment potential conducted by The Analytic Sciences Corporation (TASC). (Ref. 4).

This report describes the continuation of work commenced earlier (Ref. 4). In particular, the work includes analysis of the results and support of the vehicle/track interaction test at Bennington, New Hampshire in August 1982, a new study of the effect of curvature on the limits in gage and crosslevel variations set to prevent derailment, and the extension of studies of alignment variations with constant gage into curves.

The work described in the report is primarily intended to support the study of track safety and can be used by those in government (FRA, TSC), the American Railway Engineering Association (AREA) and the railroad industry, particularly the Association of American Railroads (AAR), responsible for addressing safety in rail transportation. The results will also aid the rail vehicle manufacturing industry in assessing the response of particular vehicles to track geometry.

The authors wish to thank Dr. Herbert Weinstock, the TSC Technical Monitor, for his advice and support in guiding the work and for providing the framework within which the work was carried out.

METRIC CONVERSION FACTORS

Approximate Conversions to Metric Measures

LENGTH

Symbol	When You Know	Multiply by	To Find	Symbol
in	inches	*2.5	centimeters	cm
ft	feet	30	centimeters	cm
yd	yards	0.9	meters	m
mi	miles	1.6	kilometers	km

AREA

Symbol	When You Know	Multiply by	To Find	Symbol
in^2	square inches	6.5	square centimeters	cm^2
ft^2	square feet	0.09	square meters	m^2
yd^2	square yards	0.8	square meters	m^2
mi^2	square miles	2.6	square kilometers	km^2
	acres	0.4	hectares	ha

MASS (weight)

Symbol	When You Know	Multiply by	To Find	Symbol
oz	ounces	28	grams	g
lb	pounds	0.45	kilograms	kg
	short tons (2000 lb)	0.9	tonnes	t

VOLUME

Symbol	When You Know	Multiply by	To Find	Symbol
tsp	teaspoons	5	milliliters	ml
Tbsp	tablespoons	15	milliliters	ml
fl oz	fluid ounces	30	milliliters	ml
c	cups	0.24	liters	l
pt	pints	0.47	liters	l
qt	quarts	0.95	liters	l
gal	gallons	3.8	liters	l
ft^3	cubic feet	0.03	cubic meters	m^3
yd^3	cubic yards	0.76	cubic meters	m^3

TEMPERATURE (exact)

Symbol	When You Know	Multiply by	To Find	Symbol
°F	Fahrenheit temperature	5/9 (after subtracting 32)	Celsius temperature	°C

---

*1 in. = 2.54 cm (exactly). For other exact conversions and more detail tables see NBS Misc. Publ. 286. Units of Weight and Measures. Price $2.25 SD Catalog No. C13 10 286.

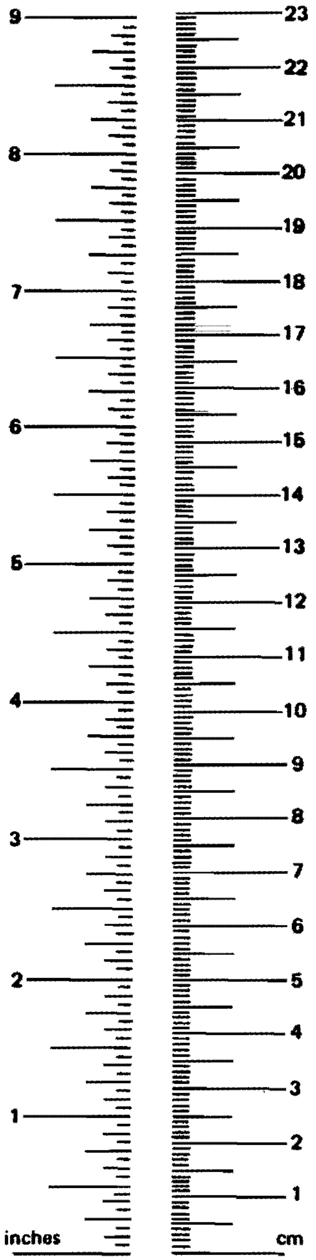

Approximate Conversions from Metric Measures

LENGTH

Symbol	When You Know	Multiply by	To Find	Symbol
mm	millimeters	0.04	inches	in
cm	centimeters	0.4	inches	in
m	meters	3.3	feet	ft
m	meters	1.1	yards	yd
km	kilometers	0.6	miles	mi

AREA

Symbol	When You Know	Multiply by	To Find	Symbol
cm^2	square centimeters	0.16	square inches	in^2
m^2	square meters	1.2	square yards	yd^2
km^2	square kilometers	0.4	square miles	mi^2
ha	hectares (10,000 m^2)	2.5	acres	

MASS (weight)

Symbol	When You Know	Multiply by	To Find	Symbol
g	grams	0.035	ounces	oz
kg	kilograms	2.2	pounds	lb
t	tonnes (1000 kg)	1.1	short tons	

VOLUME

Symbol	When You Know	Multiply by	To Find	Symbol
ml	milliliters	0.03	fluid ounces	fl oz
l	liters	2.1	pints	pt
l	liters	1.06	quarts	qt
l	liters	0.26	gallons	gal
m^3	cubic meters	36	cubic feet	ft^3
m^3	cubic meters	1.3	cubic yards	yd^3

TEMPERATURE (exact)

Symbol	When You Know	Multiply by	To Find	Symbol
°C	Celsius temperature	9/5 (then add 32)	Fahrenheit temperature	°F

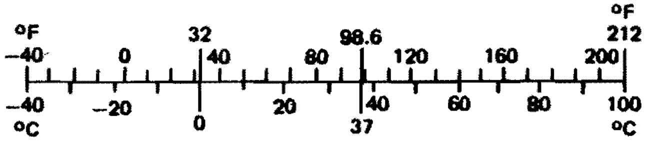

TABLE OF CONTENTS

Page No.

1. INTRODUCTION 1-1

2. STUDY METHODOLOGY 2-1
   - 2.1 Introduction 2-1
     - 2.1.1 Scenario A 2-2
     - 2.1.2 Scenario B 2-2
     - 2.1.3 Scenario C 2-2
     - 2.1.4 Scenario D 2-2
   - 2.2 Derailment Processes and Measures 2-2
     - 2.2.1 Body Roll Angle 2-3
     - 2.2.2 Wheel Lift and Wheel Climb 2-3
     - 2.2.3 Wheel Drop 2-3

3. ANALYTIC RESULTS FOR 100 TON HOPPER CAR 3-1
   - 3.1 Scenario Description 3-1
     - 3.1.1 Alignment, Gage and Crosslevel in Tight Curves 3-1
     - 3.1.2 Sinusoidal Alignment Variations 3-1
   - 3.2 Results for Alignment, Gage and Crosslevel in Tight Curves 3-1
   - 3.3 Results for Sinusoidal Alignment Variations 3-20

4. SIMULATION RESULTS FOR BENNINGTON TEST 4-1
   - 4.1 Alignment Sinusoids on Tangent Track 4-1
   - 4.2 Cusps and Crosslevel in a Twelve Degree Curve 4-5

5. CONCLUSIONS AND RECOMMENDATIONS 5-1
   - 5.1 Dynamic Curving with Crosslevel and Gage Variation in Tight Curves at Low Speed 5-1
   - 5.2 Dynamic Curving with Alignment Sinusoids and Constant Gage at Low Speed 5-1
   - 5.3 Recommendations 5-2

APPENDIX A PARAMETER VALUES USED IN THE SIMCAR MODEL A-1

REFERENCES R-1

LIST OF FIGURES

Figure No.		Page No.
2.1-1	Track Scenarios	2-1
2.2-1	Severe Roll in a 10 Degree Curve at 14 mph	2-3
2.2-2	Wheel Lift vs Lateral Displacement New AAR Wide Flange Wheel Profile	2-4
2.2-3	Severe Wheel Climb Under Severe Crosslevel and Alignment Perturbations in a 10 Degree Curve	2-4
2.2-4	Wheel/Rail Contact Geometry for AAR Standard Freight Car Wheel on AREA Standard Rail at 59 in. Rail Gage with Wheelset Displaced Laterally 1.5 in.	2-5
2.2-5	Instantaneous Clearance with Severe Lateral Rail Cusps on a 15 Degree Curve	2-5
2.2-6	Leading Outer Wheel Lateral Force Against Distance to Wheel Drop - 15 Degree Curve with Outer Rail Cusps (See Also Fig. 2.2-4)	2-6
3.1-1	Separate Effects of Alignment and Crosslevel in Curves (The Data Points for Crosslevel Variation Correspond to a 15 mph Speed and Do Not Represent a Worst Case.)	3-2
3.1-2	Vertical Forces on Leading Wheels (Response to 3/4 in. Crosslevel Variation, 15 mph)	3-3
3.1-3	Lateral Forces on Leading Wheels (Response to 3/4 in. Crosslevel Variation, 15 mph)	3-4
3.1-4	Incipient Wheel Drop Prediction (3 in. Peak/Peak Sinusoidal Amplitude at 25 mph Tangent Track with 58.0 in. gage)	3-6
3.2-1	Carbody Roll Angle, Leading Axle Vertical Force and Wheel Climb Tendency (Ten Degree Curve, 15 mph Speed, 5/8 in. Crosslevel Variation, 1 1/4 in. Lateral Cusp Outer Rail, 57 3/4 in. Maximum Gage)	3-10
3.2-2	Roll Angle of 100 Ton Loaded Carbody (Response to Crosslevel and Gage Variation/Curvature 5 Degrees/Crosslevel Variation 5/8 in./Maximum Gage 57.75 in./Outer Rail Lat. Cusp 1.75 in.)	3-11
3.2-3	Vertical Forces on Leading Wheels (Response to Crosslevel and Gage Variation, Curvature 5 Degrees/Crosslevel Variation 5/8 in./Maximum Gage 57.75 in./Outer Rail Lat. Cusp 1.75 in.)	3-12
3.2-4	Lateral Forces on Leading Wheels (Response to Crosslevel and Gage Variation, Curvature 5 Degrees/Crosslevel Variation 5/8 in./Maximum Gage 57.75 in./Outer Rail Lat. Cusp 1.75 in.)	3-13
3.2-5	Wheel Climb Tendency (Response to Crosslevel and Gage Variation, Curvature 5 Degrees/Crosslevel Variation 5/8 in./Maximum Gage 57.75 in./Outer Rail Lat. Cusp 1.75 in.)	3-14
3.2-6	Roll Angle of 100 Ton Loaded Carbody (Response to Crosslevel and Gage Variation, Curvature 5 Degrees/Crosslevel Variation 5/8 in./Maximum Gage 57.75 in./Outer Rail Lat. Cusp 1.25 in.)	3-15
3.2-7	Vertical Forces on Leading Wheels (Response to Crosslevel and Gage Variation, Curvature 5 Degrees/Crosslevel Variation 5/8 in./Maximum Gage 57.75 in./Outer Rail Lat. Cusp 1.25 in.)	3-15
3.2-8	Lateral Forces on Leading Wheels (Response to Crosslevel and Gage Variation, Curvature 5 Degrees/Crosslevel Variation 5/8 in./Maximum Gage 57.75 in./Outer Rail Lat. Cusp 1.25 in.)	3-16

LIST OF FIGURES (Continued)

Figure No.		Page No.
3.2-9	Wheel Climb Tendency (Response to Crosslevel and Gage Variation, Curvature 5 Degrees/Crosslevel Variation 5/8 in./Maximum Gage 57.75 in./Outer Rail Lat. Cusp 1.25 in.)	3-16
3.2-10	Roll Angle of 100 Ton Loaded Carbody (Response to Crosslevel and Gage Variation, Curvature 3 Degrees/Crosslevel Variation 5/8 in./Maximum Gage 57.75 in./Outer Rail Lat. Cusp 1.75 in.)	3-17
3.2-11	Vertical Forces on Leading Wheels (Response to Crosslevel and Gage Variation, Curvature 3 Degrees/Crosslevel Variation 5/8 in./Maximum Gage 57.75 in./Outer Rail Lat. Cusp 1.75 in.)	3-17
3.2-12	Lateral Forces on Leading Wheels (Response to Crosslevel and Gage Variation, Curvature 3 Degrees/Crosslevel Variation 5/8 in./Maximum Gage 57.75 in./Outer Rail Lat. Cusp 1.75 in.)	3-18
3.2-13	Wheel Climb Tendency (Response to Crosslevel and Gage Variation, Curvature 3 Degrees/Crosslevel Variation 5/8 in./Maximum Gage 57.75 in./Outer Rail Lat. Cusp 1.75 in.)	3-18
3.2-14	Wheel Climb Tendency (Response to Crosslevel and Gage Variation, Curvature 10 Degrees/56.5 in. Minimum Gage/Lat. Cusp 1.25 in.)	3-19
3.2-15	Roll Angle of 100 Ton Loaded Carbody (Response to Crosslevel and Gage Variation, Curvature 10 Degrees)	3-20
3.2-16	Vertical Forces on Leading Wheels (Response to Crosslevel and Gage Variation, Curvature 10 Degrees)	3-20
3.2-17	Lateral Forces on Leading Wheels (Response to Crosslevel and Gage Variation, Curvature 10 Degrees)	3-21
3.2-18	Wheel Climb Tendency (Response to Crosslevel and Gage Variation, Curvature 10 Degrees)	3-21
3.2-19	Roll Angle of 100 Ton Loaded Carbody (Response to Crosslevel and Gage Variation, Crosslevel Variation 1/2 in.)	3-22
3.2-20	Vertical Forces on Leading Wheels (Response to Crosslevel and Gage Variation, Crosslevel Variation 1/2 in.)	3-23
3.2-21	Lateral Forces on Leading Wheels (Response to Crosslevel and Gage Variation, Crosslevel Variation 1/2 in.)	3-24
3.2-22	Wheel Climb Tendency (Response to Crosslevel and Gage Variation, Crosslevel Variation 1/2 in.)	3-25
3.3-1	Severe Roll Response from 3 in. Peak/Peak Alignment Variation (15 mph/Tangent Track/Wavelength 39 ft/Gage 58.0 in.)	3-27
3.3-2	Response to Sinusoidal Alignment with Varying Gage (Tangent Track/Amplitude 3 in. Peak/Peak/Wavelength 39 ft/Speed 20 mph.)	3-28
3.3-3	Response to Sinusoidal Alignment with Wide Gage (10 Degree Curve/Amplitude 4.5 in. Peak/Peak/Wavelength 90 ft/Speed 25 mph at Balance)	3-29
3.3-4	Variation in Wheel Drop Tendency with Speed (Tangent Track/Amplitude 1.125 in. Peak/Peak/Wavelength 50 ft/Gage 57.75 in.)	3-30
3.3-5	Variation in Wheel Drop Tendency with Speed (Tangent Track/Amplitude 1.125 in. Peak/Peak/Wavelength 50 ft/Gage 57.75 in.)	3-31
3.3-6	Variation in Vertical Force Due to Unbalance (15 Deg Curve/Amplitude 3 in. Peak/Peak/Wavelength 75 ft/Run Speed 25 mph)	3-32

LIST OF FIGURES (Continued)

Figure No.		Page No.
3.3-7	Effect of Unbalance on Wheel Drop Tendency (15 deg Curve/Amplitude 3 in. Peak/Peak/Wavelength 75 ft/Run Speed 25 mph)	3-33
3.3-8	Lateral Motion of First Axle in Curves with Sinusoidal Alignment Variation (Amplitude 1 in. Peak/Peak/Wavelength 39 ft/Speed 25 mph at Balance/Gage 57.75 in.)	3-34
3.3-9	Wheel Drop Tendency of First Axle in Curves with Sinusoidal Alignment Variation (Amplitude 1 in. Peak/Peak/Wavelength 39 ft/Speed 25 mph at Balance/Gage 57.75 in.)	3-35
3.3-10	Lead Outer Wheel Peak Lateral Force with Increasing Curvature	3-35
3.3-11	Maximum Combined Gage Spreading Force with Increasing Curvature	3-35
3.3-12	Variation of Lateral Force on First Axle with Amplitude of Sinusoidal Alignment (10 deg Curve/75 ft Wavelength/25 mph at Balance/ Gage 57.75 in.)	3-36
3.3-13	Wheel Drop Tendency on First Axle with Amplitude of Sinusoidal Alignment (10 deg Curve/75 ft Wavelength/25 mph at Balance/ Gage 57.75 in.)	3-37
3.3-14	Limiting Cases for Wheel Drop Avoidance (Tangent Track/25 mph at Balance/Gage 57.75 in.)	3-38
3.3-15	Limiting Cases for Wheel Drop Avoidance (5 deg Curve/25 mph at Balance/Gage 57.75 in.)	3-39
3.3-16	Limiting Cases for Wheel Drop Avoidance (10 deg Curve/25 mph at Balance/Gage 57.75 in.)	3-40
3.3-17	Limiting Cases for Wheel Drop Avoidance (15 deg Curve/25 mph at Balance/Gage 57.75 in.)	3-41
3.3-18	Limiting Cases for Wheel Drop Avoidance (10 deg Curve/25 mph at Balance/Gage 57.5 in.)	3-42
3.3-19	Limiting Cases for Wheel Drop Avoidance (15 deg Curve/25 mph at Balance/Gage 57.5 in.)	3-43/3-44
4.1-1	Comparison of Test with Simulated Peak Lateral Force in Alignment Sinusoids (Tangent Track/50 ft Wavelength/1.25 in. Peak/Peak)	4-2
4.1-2	Comparison of Test with Simulated Peak Lateral Force in Alignment Sinusoids (Tangent Track/90 ft Wavelength/4.5 in. Peak/Peak)	4-2
4.1-3	Comparison of Vertical Forces in Alignment Sinusoids (Tangent Track/50 ft Wavelength/1.25 in. Peak/Peak)	4-3
4.1-4	Comparison of Vertical Forces in Alignment Sinusoids (Tangent Track/90 ft Wavelength/4.5 in. Peak/Peak)	4-4
4.2-1	Peak Lateral Wheel Forces in the 12 Deg Curve (21 mph Balance/Outer Rail Cusp 1.25 in./Crosslevel (Nominal) 0.75 in.)	4-5
4.2-2	Vertical Wheel Forces on Low Rail in the 12 Deg Curve (21 mph Balance/Outer Rail Cusp 1.25 in./Crosslevel (Nominal) 0.75 in.)	4-6
4.2-3	Vertical Wheel Forces on High Rail in the 12 Deg Curve (21 mph Balance/Outer Rail Cusp 1.25 in./Crosslevel (Nominal) 0.75 in.)	4-6

LIST OF TABLES

Table No.		Page No.
3.1-1	Summary Crosslevel, Gage, Curvature Runs 100 Ton Loaded Hopper - cg 98 in. Above Rails	3-5
3.1-2	Run List for Sinusoidal Alignment Variation	3-7
3.1-3	Run List for Sinusoidal Alignment Variation 5 Degree Curve	3-8
3.1-4	Run List for Sinusoidal Alignment Variation 10 Degree Curve	3-8
3.1-5	Run List for Sinusoidal Alignment Variation 15 Degree Curve	3-9
3.3-1	Limiting Values of Alignment Amplitude Wheel Drop at Low Speed on Tangent Track Having a Minimum Restraint Capability	3-26
4-1	Run List for the Bennington Test Simulations	4-1
5.1-1	Limits Predicted for Track Geometry for Combined Outer Rail Cusps and Staggered Joint Crosslevel in Curves	5-1
5.2-1	Maximum Peak/Peak Amplitudes of Sinusoidal Track Alignment Variations Which do not Give Incipient Wheel Drop Derailments on Track Having a Minimum Restraint Capability to a Loaded 100 Ton Hopper Car (25 mph at Balance Speed)	5-2

1. INTRODUCTION

In support of the Federal Railroad Administration (FRA), Transportation Systems Center (TSC) is conducting studies of the relationships between track geometry variations and rail car dynamic response as related to safety, in order to recommend limits on acceptable track geometry variations and track strength requirements. The primary tool for conducting the analytic studies has been a computer program developed for TSC by The Analytic Sciences Corporation (TASC). This program, named SIMCAR, is based upon a sixteen degree-of-freedom analytical model of a freight car. As reported in Ref. 4, the SIMCAR parameters were initially adjusted to provide good agreement with the field test data available on steady-state curving behavior, rail cars and specially conducted perturbed track tests. The program was applied by TSC to the development of preliminary recommendations of limits on track gage and crosslevel variations as a function of track curvature for the 10-25 mph speed range. Relationships were also established between wheel/rail forces, peak-to-peak amplitude and wavelength for sinusoidal track alignment variations to recommend limits on track geometry alignment variation wavelengths of greater than 39 feet. In addition, general test requirements were defined to:

- Verify force predictions at high track curvatures and limiting gage and cross-level geometry variations for the 10-25 mph range
- Verify and demonstrate the large amplitude and long wavelength results obtained and extend these into a full range of curvatures
- Provide baseline data that would permit extending the 10-25 mph study results into higher speed regimes.

Further investigations on the low speed gage requirements necessary to evaluate the influence of a specific minimum track strength and the assumption of clean dry friction coefficients on the results presented are also identified. The sinusoid was used to describe typical alignment variations representative of railroad experience and to define the applicability of a chordal measurement to control these variations.

The objective of the work reported here is to provide details of the analysis supporting the tests conducted at Bennington in August 1982, and discuss the extensions of the study as required by this analysis, especially in the range of high track curvatures.

2. STUDY METHODOLOGY

2.1 INTRODUCTION

The study reported here constitutes a continuation of work on the safety-related dynamic response of freight cars, subjected to track geometry variations representing operating conditions that are felt to be typical of train derailment situations. As such, the work described complements work carried out and reported previously (Ref. 4) under the Track Safety Research Program.

The method used has been to identify derailment scenarios, typical of service derailments, indicated in the FRA Railroad Accident/Incident Reporting System, and to choose quantitative measures of dynamic response which can be directly related to the proximity to derailment.

To this point in the work reported, the 100 ton hopper car has been chosen as the study vehicle. It was known to have suffered a significant number of derailments, especially when loaded and responding in roll to large crosslevel variations. The derailment scenarios in order of severity (determined from a review of FRA data and industry experience) may be summarized as follows:

i Crosslevel on loaded high c.g. cars, 10-25 mph

ii Alignment-gage response of loaded high c.g. cars, 10-25 mph

iii Alignment-gage response of unloaded hopper cars in curves, 25-40 mph

iv Crosslevel induced response of unloaded hopper cars on tangent track, 25-40 mph

v Alignment-gage response of light box cars on tangent track, 40-60 mph

vi Lateral-yaw response of locomotives during spiral entry-exit, 40-60 mph.

Specific track geometries which may produce track-induced derailments, are used to investigate vehicle response and proximity to derailment and to establish safe bounds on track geometry variation. Typical of these have been (see Fig. 2.1-1):

- Outward rail cusps at joints for studies of limits to gage variation on tangent track and, more importantly, in curves to prevent wheel climb and/or wheel drop

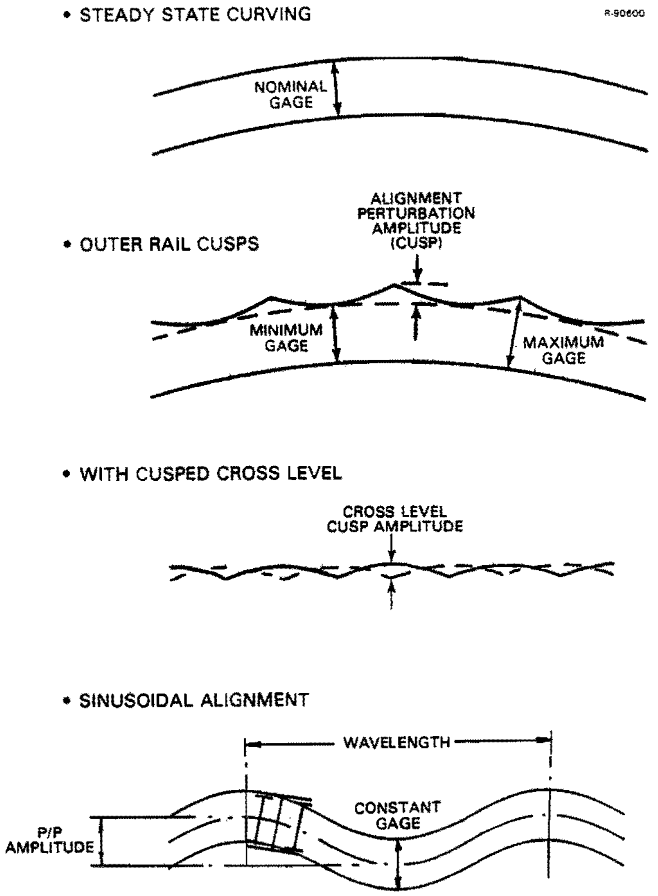

Figure 2.1-1 Track Scenarios

- Downward rail cusps at joints for studies of limits to crosslevel variation to prevent excessive wheel lift and wheel climb in curves due to rail roll resonance
- Sinusoidal alignment variations for studies of limits to alignment variation to prevent wheel climb and wheel drop under dynamic gage widening forces.

The terms wheel lift, wheel climb and wheel drop are defined in Section 2.2.

The model used to simulate the dynamic response of the car represents a typical freight vehicle having two 3-piece trucks and is described in Ref. 4. The computer code is called SIMCAR. The methodology used herein has been to:

- run the program for typical scenarios at various levels of severity of track geometry variation
- predict the safe bounds

- design tests or use existing test data to validate the results
- use simulation results to provide as complete a picture of track geometry and response as possible
- modify or improve the model and rerun the program until a satisfactory set of limiting geometries covering the range of scenarios has been achieved.

Previous studies identified safe variations in track geometry with the minimum rail restraint conditions defined in Section 2.2.3 in the low speed range, for the 100 ton hopper car with new wheel profile, in the following scenarios.

2.1.1 Scenario A

Dynamic curving without crosslevel but with gage variation, 10-25 mph to prevent wheel drop on track with minimum rail restraint.

SAFE LIMITS

Degree of Curve	Cusp Amplitude	Maximum Gage
0-5	1.75 in.	57.75 in.
5-10	1.75 in.	57.75 in.
10-15	1.00 in.	57.5 in.

2.1.2 Scenario B

Sinusoidal alignment variation at constant gage to prevent wheel drop on track with maximum gage (57.75 in) and minimum rail restraint.

SAFE LIMITS

Degree of Curve	Wavelength	Peak/Peak Amplitude
0	39 ft	1.33 in.
0,5	50 ft	1.25 in.
0,5	75 ft	3.25 in.
10	90 ft	4.5 in.
10	39 ft	1.0 in.
10	50 ft	1.0 in.
10	75 ft	2.7 in.
10	90 ft	3.75 in.

2.1.3 Scenario C

Crosslevel alone on tangent track to prevent wheel lift greater than 1/2 in. from continuous low joints.

SAFE LIMIT

Continuous variation in crosslevel of 0.625 in. (This would result in a value for TSC's crosslevel index, CLI, of 0.3 in.)

2.1.4 Scenario D

Dynamic curving with crosslevel and gage variation to prevent wheel climb on rigid track.

SAFE LIMIT

On a ten degree curve it was found that the combination of crosslevel and gage variation provided a greater hazard than the above limits for them individually. Several alternative combinations were possible and require further investigation.

2.2 DERAILMENT PROCESSES AND MEASURES

Section 2.1 sets out the nature of the derailment process for the particular scenarios identified from a review of derailment data. In this section, the derailment processes are identified and related to the measures used in the model described in Ref. 4. Derailment represents the cessation of guidance provided by the rails to the wheelsets and is characterized by movement perpendicular to the direction of travel. In particular, the wheel may lift from the rail surface, and/or may move laterally as when the flange climbs over the rail, or when the outside of the non-flanging wheel moves inside the gage face of the rail. These three derailment conditions are referred to as wheel lift, wheel climb and wheel drop.

Wheel lift is principally associated with the static and dynamic effects of variation in crosslevel. Dynamic wheel lift occurs when the vehicle suspension rolls about a low center excited by crosslevel variation at low joints on staggered jointed track or at high overbalance speed in curves. Wheel lift is therefore descriptive of an impending carbody rollover or of a potential unrestrained lateral movement.

Wheel climb or the climbing of the rail by the wheel in flange contact is frequently associated with partial wheel unloading. Statically, a torsionally-stiff freight car can exhibit wheel unloading and wheel lift if the rate of crosslevel variation along its length exceeds the capability of the suspension and body to twist under its load. This condition is more prevalent with lightly loaded cars having constant contact sidebearers. In this situation, derailment may follow unloading of the flanging wheel in curves where a lateral force is sustained. With the wheelset in flange contact with the rail, and the flanging wheel lightly loaded vertically, the non-flanging wheel carries an increase over its static load and the lateral force developed by the non-flanging wheel may drive the flanging wheel onto and over the rail. Dynamic unloading of the flanging wheel can occur and is found to be important in tight curves with large roll response due to crosslevel variation at joints. The wheel lateral to vertical force ratio, L/V, is frequently used to indicate proximity to derailment conditions in this mode and is especially important for monitoring test measurements.

Wheel drop occurs as a result of gage increase due to static curving and/or dynamic gage widening forces. Track with a minimum restraint capability contributes to incipient wheel drop by permitting wider gages to be developed for the same lateral force.

2.2.1 Body Roll Angle

Derailment indices pertinent to this study are discussed in this and the following subsections. A threshold for body roll angle was chosen from the experience gained from other studies of the rock and roll phenomenon (Ref. 5).

A value of ±5.0 degrees is considered excessive. For the loaded hopper car investigated, this angle occurs well after commencement of rotation over the sidebearing and centerplate separation. A typical plot of carbody roll angle against time from the SIMCAR model is given in Fig. 2.2-1 for severe roll in a ten degree curve with gage and alignment variation. Although roll derailment is predicted, i.e., the angle exceeds +5.0 degrees, it is accompanied by wheel climb as seen in Fig. 2.2-3.

2.2.2 Wheel Lift and Wheel Climb

In earlier studies (Ref. 5), a value of 0.5 inch was used to signify an excessive height of the wheel tread above the rail in crosslevel response. For the AAR 1/20 profile, 0.5 inch approximates the height beyond which the flange angle decreases. The value of wheel lift at the tapeline during wheel climb may be calculated from the lateral wheel/rail movement and knowledge of the profiles as given in Fig. 2.2-2. It suggests derailment if the wheel moves more than 0.1 inch beyond initial flange contact for new AAR 1/20 wheels on AREA 132 lb. rail. Distance beyond flange contact is calculated in SIMCAR. Figure 2.2-3 illustrates the results for the same case shown in Fig. 2.2-1. The graph indicates the time history of the position of the flange beyond initial contact with the rail. Wheel climb is seen to occur simultaneously with a roll angle exceeding five degrees (see Fig. 2.2-1).

2.2.3 Wheel Drop

The "distance to wheel drop" (in inches) for new wide-flange wheels is defined by the equation,

$$\mathrm{DISTDROP} = 0.5\,(64.5 \pm 0.3 - \text{instantaneous track gage}) - y_{\mathrm{wheel}}$$

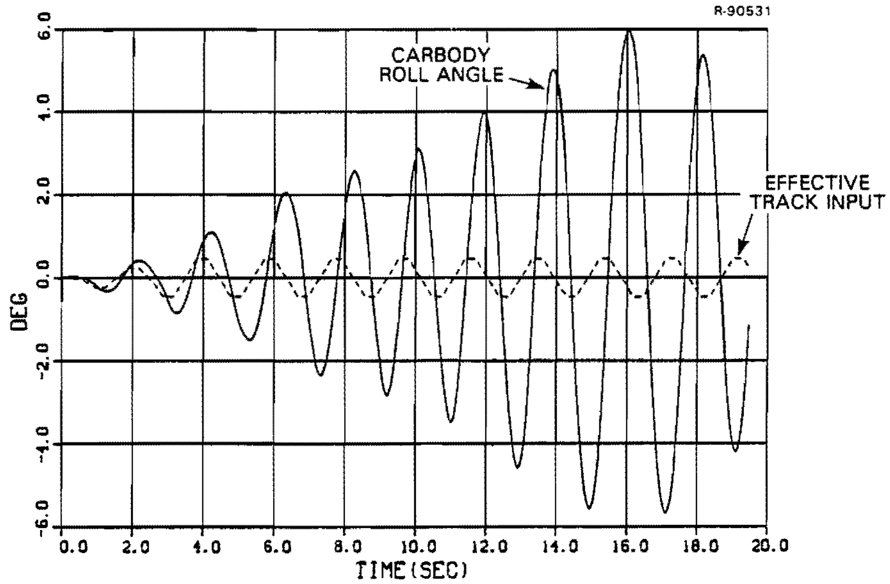

Figure 2.2-1 Severe Roll in a 10 Degree Curve at 14 mph

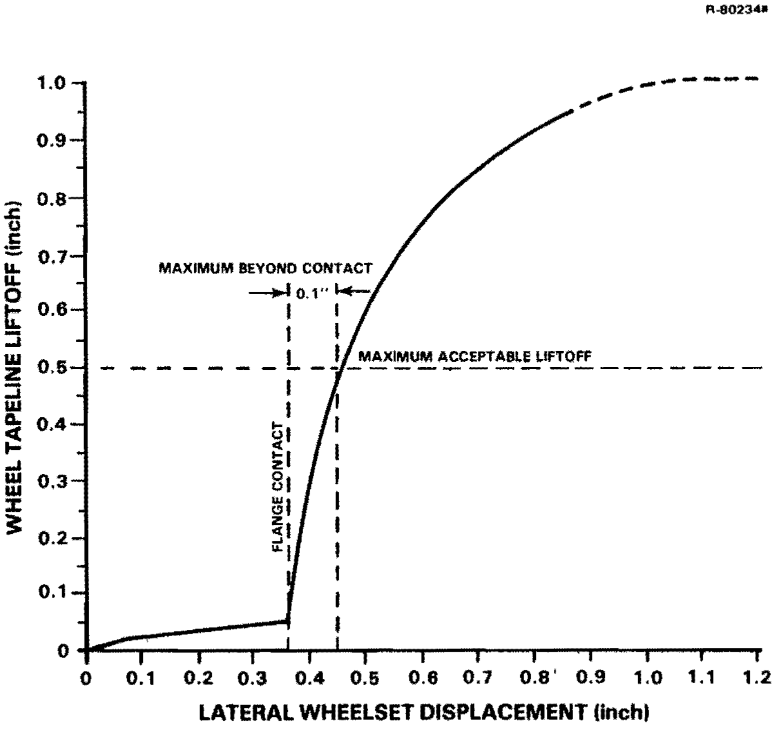

Figure 2.2-2 Wheel Lift vs Lateral Displacement, New AAR Wide Flange Wheel Profile

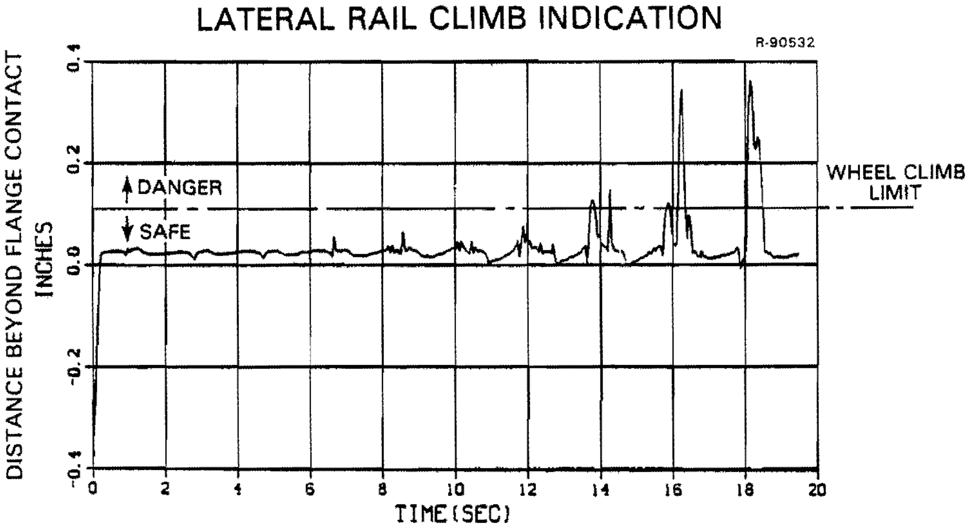

Figure 2.2-3 Severe Wheel Climb Under Severe Crosslevel and Alignment Perturbations in a 10 Degree Curve

where y_{wheel} is the wheelset lateral position relative to the track centerline. The wheelset must also avoid approaching wheel drop by a safety margin. A value of zero represents a wheel drop derailment. The safety margin of 1.25 in. (shown in Fig. 2.2-4) represents a maximum gage of 59 in. and has been used for the cases studied. This gives the distance to the wheel drop limit as,

DISTDROP = 3.07 in. - instantaneous flangeway clearance.

The instantaneous flangeway clearance for rigid track is available from the computer program SIMCAR, and is illustrated in Fig. 2.2-5. The true clearance will have additional gage increases due to each rail deflection. A representation of this effect as computed in the program plots lateral force against distance to wheel drop directly and is given in Fig. 2.2-6. The limiting lateral rail deflection curve for the minimum rail restraint that is chosen as acceptable is added to the computed output plot and the value of the deflection for the low rail is established. The rail

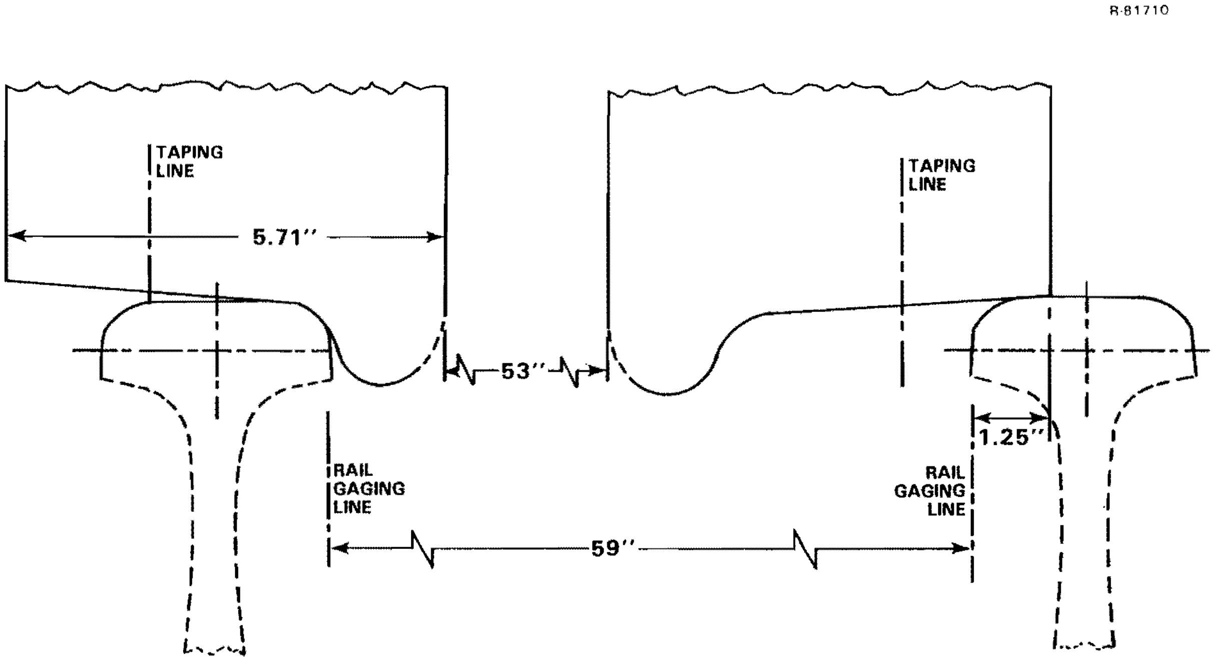
R-81710
TAPING LINE
5.71"
TAPING LINE
53"
1.25"
RAIL GAGING LINE
RAIL GAGING LINE
59"

Figure 2.2-4 Wheel/Rail Contact Geometry for AAR Standard Freight Car Wheel on AREA Standard Rail at 59 in. Rail Gage with Wheelset Displaced Laterally 1.5 in.

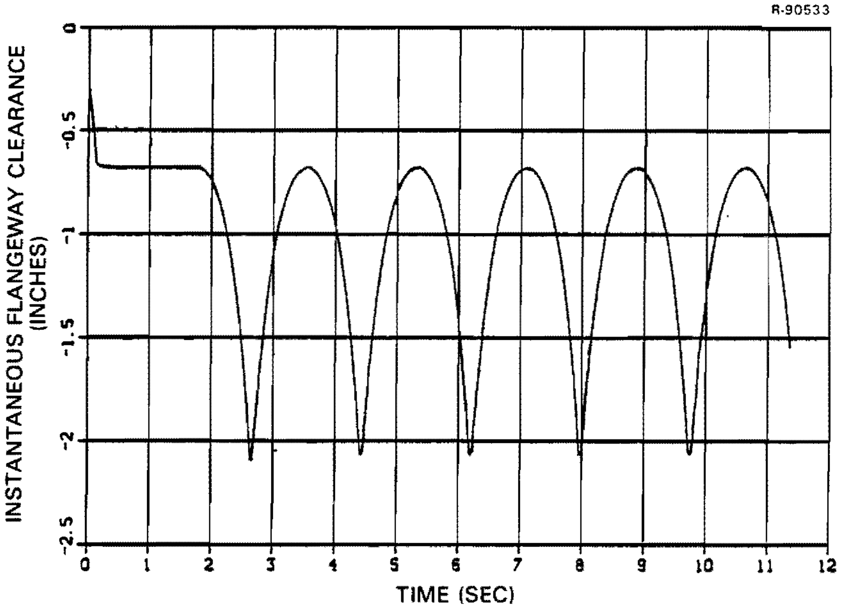

Figure 2.2-5 Instantaneous Clearance with Severe Lateral Rail Cusps on a 15 Degree Curve

deflection curve for the high rail is then plotted from the low rail deflection point and gives a limit above which the computed points indicate a possible derailment.

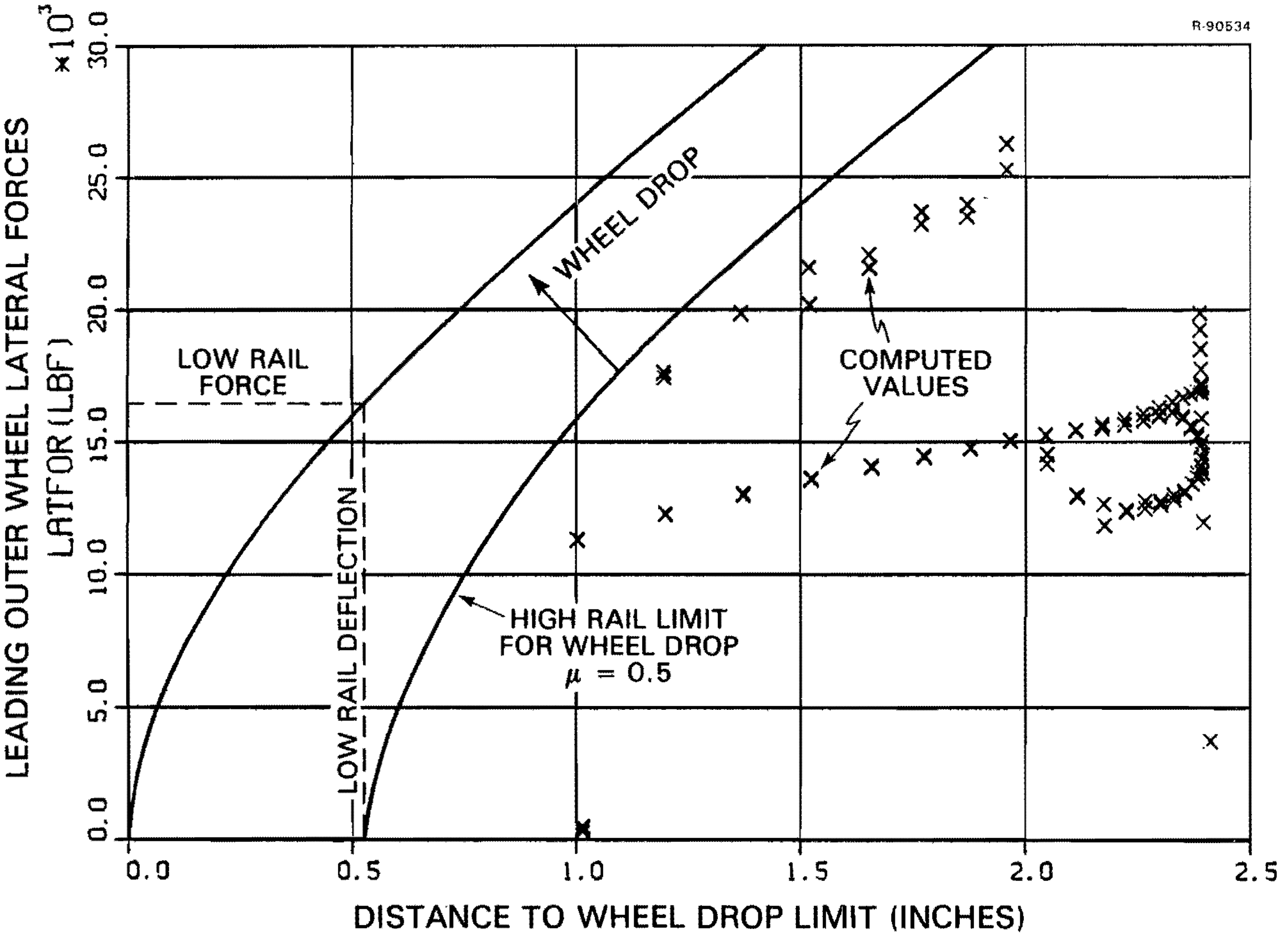

Figure 2.2-6 Leading Outer Wheel Lateral Force Against Distance to Wheel Drop - 15 Degree Curve with Outer Rail Cusps (See Also Fig. 2.2-4)

3. ANALYTIC RESULTS FOR 100 TON HOPPER CAR

3.1 SCENARIO DESCRIPTION

This study continues the scenario approach described in Ref. 4. Two scenarios are addressed which relate directly to track geometry as it affects safety from derailment. These are the combination of variations in alignment, gage and crosslevel in curves, especially tight curves, and the variation of alignment alone on both tangent and curved track. A standard loaded 100 ton hopper car was chosen for the study. Its parameters are given in Appendix A. The study methodology is described below.

3.1.1 Alignment, Gage and Crosslevel in Tight Curves

The major reason for the choice of this scenario is that it provides a severe environment to identify limits to gage and crosslevel in curves which, if exceeded, would cause possible derailment in the speed range of 10-25 mph. The mode of derailment found to be most likely in this scenario includes a large lateral force and unloading of a flanging wheel. The rail geometry chosen is that of the exponential cusp, outward and downward at the outer rail joint and downward only at the inner rail joint with staggered rails. Thus, the crosslevel due to the downward cusps excites the roll of the vehicle body and the outward cusp on the outer rail causes large dynamic lateral forces associated with gage and alignment variation. This combination can result in a large lateral (L) and small vertical force (V), hence a large L/V ratio and the danger of incipient rail climb by the wheel.

The process is illustrated in Fig. 3.1-1, which shows the separate effects of outer rail alignment and crosslevel. A similar result is apparent in the results shown in Figs. 3.1-2 and 3.1-3 for crosslevel excitation on tangent track and a ten degree curve. However, with additional lateral excitation due to outer rail cusps, the minimum vertical force may not be coincident with the maximum lateral force and a computer study was carried out using the SIMCAR program to identify the proximity to incipient wheel climb in tight curves. A summary of these runs is given in Table 3.1-1. This matrix of runs was designed to establish the largest values of alignment, gage and crosslevel which do not exhibit incipient wheel climb. One significant additional variable was included in the runs, namely speed. Differences in the results were apparent from small speed changes around the roll resonance, especially in the time and duration of peak lateral and minimum vertical wheel forces. A range of speeds was therefore examined for certain cases. This table identifies the results discussed later in this chapter. The computed output of greatest interest -- representing proximity to wheel climb -- was illustrated previously in Fig. 2.2-3.

3.1.2 Sinusoidal Alignment Variations

A more severe alignment environment than the lateral cusp of the preceeding scenario is that provided by track having constant gage and large sinusoidal alignment variations with wavelengths between 39 and 90 ft, especially where the track has a minimum restraint capability. The limiting derailment mode in this scenario, in the 10-25 mph speed range, is wheel drop.

Figure 3.1-4, illustrates the prediction of incipient wheel drop as a function of variation wavelength for constant gage. It also shows the occurrence of wheel climb beyond the rail restraint line which suggests that wheel climb is also possible on stiff track for large variations in alignment geometry. The cases investigated here are associated with track having a minimum restraint capability. Also seen from Fig. 3.1-4 is the widely differing response to different wavelengths. The study reported here uses 39, 50, 75 and 90 ft to cover the range of interest and provides preliminary results at a higher speed and for curves up to 15 degrees. The new list is given in Tables 3.1-2 to 3.1-5 for the four wavelengths. As in the previous scenario, summaries of the results are given in the tables. The runs were arranged to find the values of amplitude at each wavelength, which was "just safe" from incipient wheel drop derailment for the given rail restraint curve.

3.2 RESULTS FOR ALIGNMENT, GAGE AND CROSSLEVEL IN TIGHT CURVES

The potential for wheel climb as a result of the combination of dynamic wheel unloading and lateral force was discussed in Ref. 4 as a baseline case. Figure 3.2-1 shows that the limit of 0.1 in. set for the lateral wheel displacement beyond initial flange contact (DYLF 12) is exceeded. Wheel lift is also apparent (negative vertical force on the wheel occurs due to the fact that the model permits snubbing to exist beyond wheel lift). The speed of 15 mph is chosen here and the gage, cusp amplitude and crosslevel were those previously chosen in separate studies as limiting

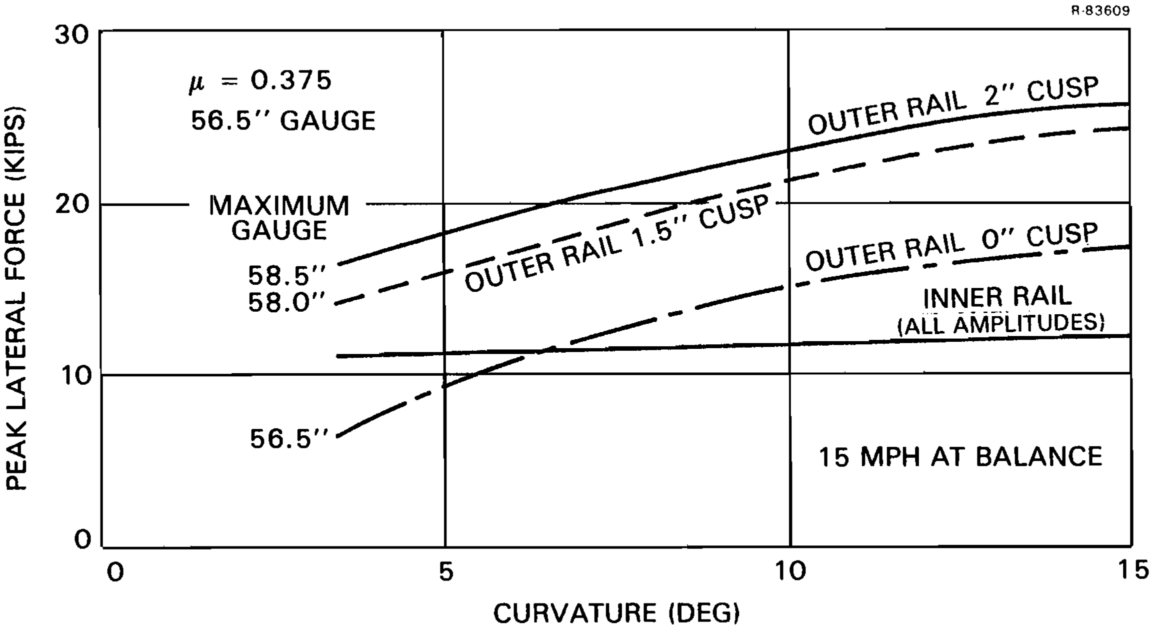

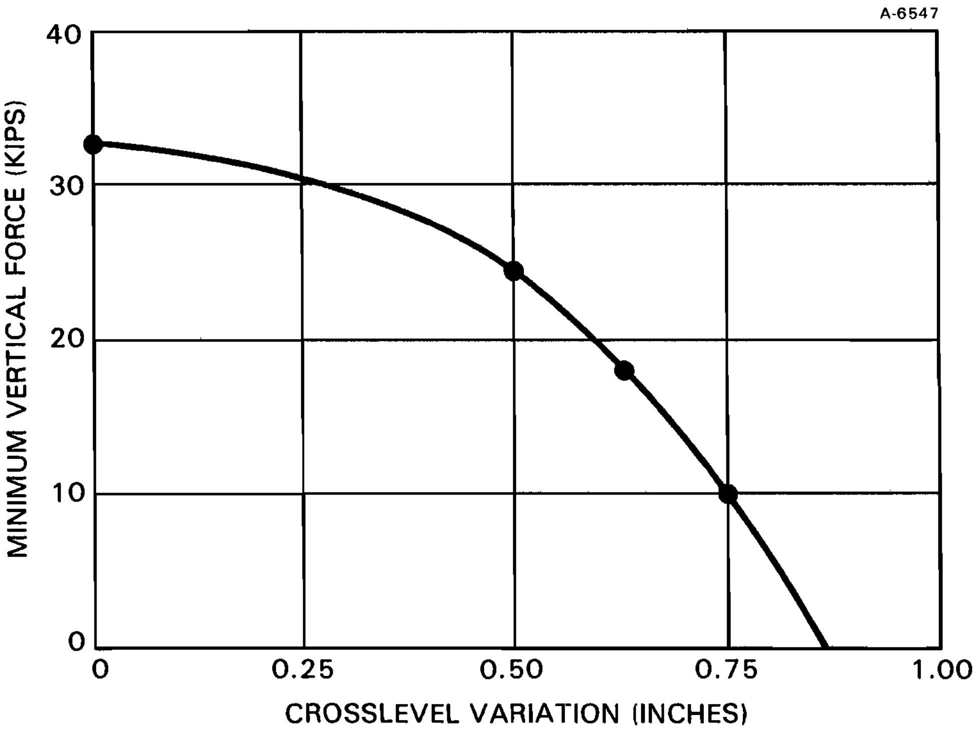

Figure 3.1-1 Separate Effects of Alignment and Crosslevel in Curves (The Data Points for Crosslevel Variation Correspond to a 15 mph Speed and Do Not Represent a Worst Case.)

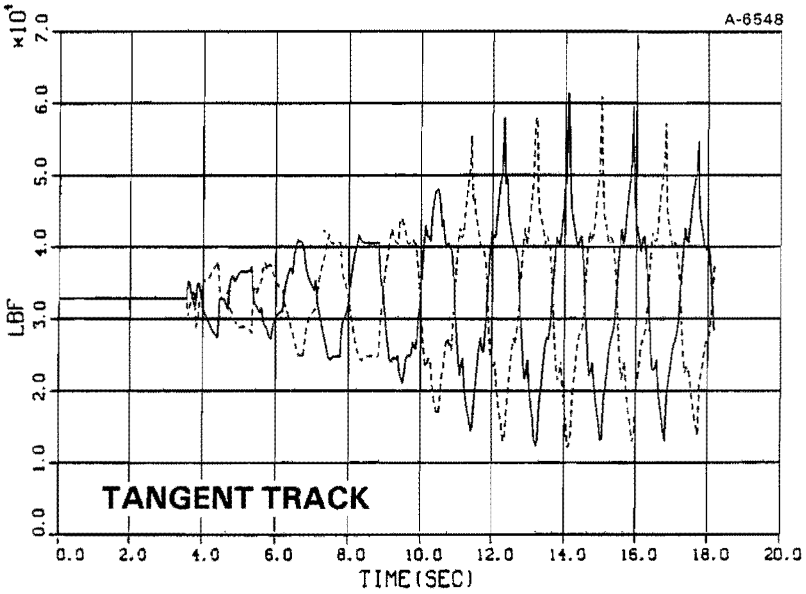

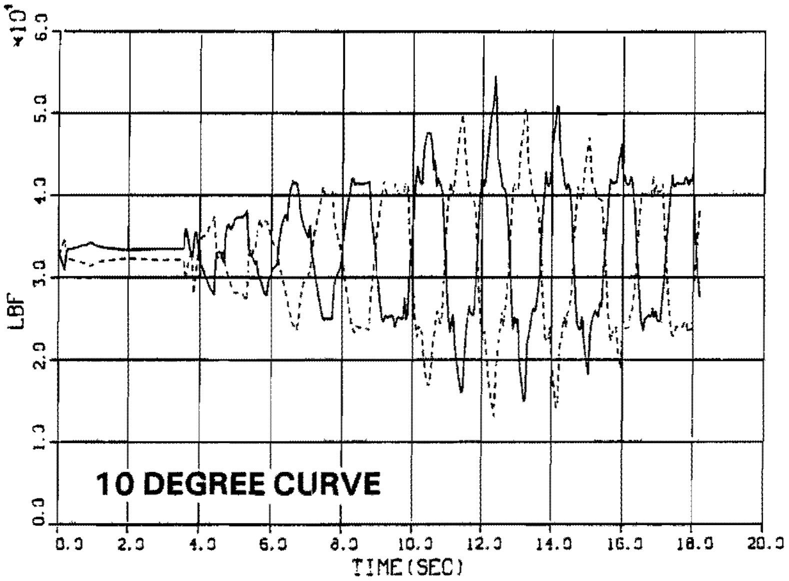

Figure 3.1-2 Vertical Forces on Leading Wheels (Response to 3/4 in. Crosslevel Variation, 15 mph)

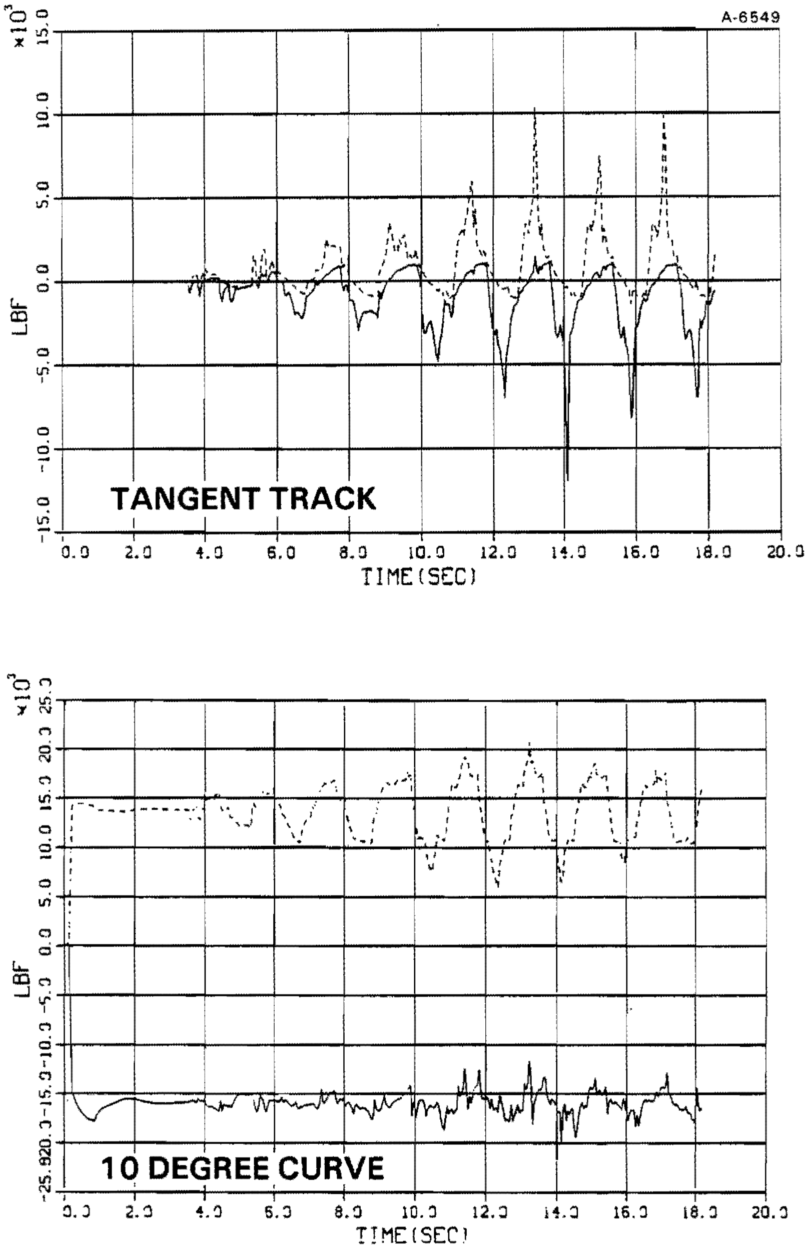

Figure 3.1-3 Lateral Forces on Leading Wheels (Response to 3/4 in. Crosslevel Variation, 15 mph)

TABLE 3.1-1
SUMMARY CROSSLEVEL, GAGE, CURVATURE RUNS
100 TON LOADED HOPPER - CG 98 in. ABOVE RAILS

BATCH NO.	CURVE degree	CROSSLEVEL in.	MIN. GAGE in.	MAX. GAGE in.	LAT. CUSP in.	MIN. SPEED mph	MAX. SPEED mph	COMMENT
0/1	0	1	TIGHT		0	11 →	17	Roll angle increasing after 7 cycles > 7 deg at 13.5 mph. Substantial wheel lift.
0/2	0	1	58	58	0	14	-	Wide gauge reduces angle but still > 5 deg. Substantial wheel lift.
0/3	0	$\frac{3}{4}$	TIGHT		0	15	-	Max. roll angle 2 deg. Min. vert force 12 kips. No incipient wheel climb.
0/4	0	$\frac{5}{8}$	TIGHT		0	14 →	16	Max. roll angle 1.5 deg at 16 mph might peak at 15.5 mph. Crosslevel below threshold input.
0/5	0	$\frac{3}{4}$	56	$57\frac{3}{4}$	$1\frac{3}{4}$	15	-	Roll angle moderate (as 0/3), increase in lat. force but no incipient wheel climb.
3/1	3	$\frac{5}{8}$	56	$57\frac{3}{4}$	$1\frac{3}{4}$	14 →	16	Large roll angle >3 deg. no incipient wheel climb.
5/1	5	$\frac{5}{8}$	56	$57\frac{3}{4}$	$1\frac{3}{4}$	13 →	16	Large roll angle 6 deg at 15 mph, wheel lift. Serious climb at 16 mph.
5/2	5	$\frac{5}{8}$	$56\frac{1}{2}$	$57\frac{3}{4}$	$1\frac{1}{4}$	14 →	16	Large roll angle 4 deg at 14 mph, min. vert. force zero. No incipient wheel climb.
10/1	10	0	$56\frac{1}{2}$	$57\frac{3}{4}$	$1\frac{1}{4}$	15	-	Very little roll < 0.15 deg. No incipient wheel climb.
10/2	10	$\frac{1}{2}$	$56\frac{1}{2}$	$57\frac{3}{4}$	$1\frac{1}{4}$	14 →	16	Moderate roll 2 deg at 15 mph. No incipient wheel climb.
10/3	10	$\frac{5}{8}$	$56\frac{1}{2}$	$57\frac{3}{4}$	$1\frac{1}{4}$	15	-	Large roll > 4 deg, serious climb.
10/4	10	see comment	$56\frac{1}{2}$	$56\frac{1}{2}$	0	15	-	Crosslevels $\frac{1}{2}$ in., $\frac{5}{8}$., $\frac{3}{4}$ in., moderate max. roll at $\frac{3}{4}$ in. No incipient wheel climb.
15/1	15	$\frac{1}{2}$	$56\frac{1}{2}$	$56\frac{1}{2}$	0	15	-	Small roll, no incipient wheel climb.
15/2	15	$\frac{5}{8}$	$56\frac{1}{2}$	$56\frac{1}{2}$	0	15 →	16	Moderate roll 1.5 deg at 15.5 mph, no incipient wheel climb.
15/3	15	$\frac{3}{4}$	$56\frac{1}{2}$	$56\frac{1}{2}$	0	14 →	16	Moderate increasing roll at 14 mph, min. vert. force < 10 kips. Serious climb at 14 mph.
15/4	15	$\frac{1}{2}$	$56\frac{1}{2}$	$57\frac{1}{2}$	1	13 →	16	Moderate roll at 15-16 mph, wheel climb just to 0.1 in. limit. No incipient derailment.

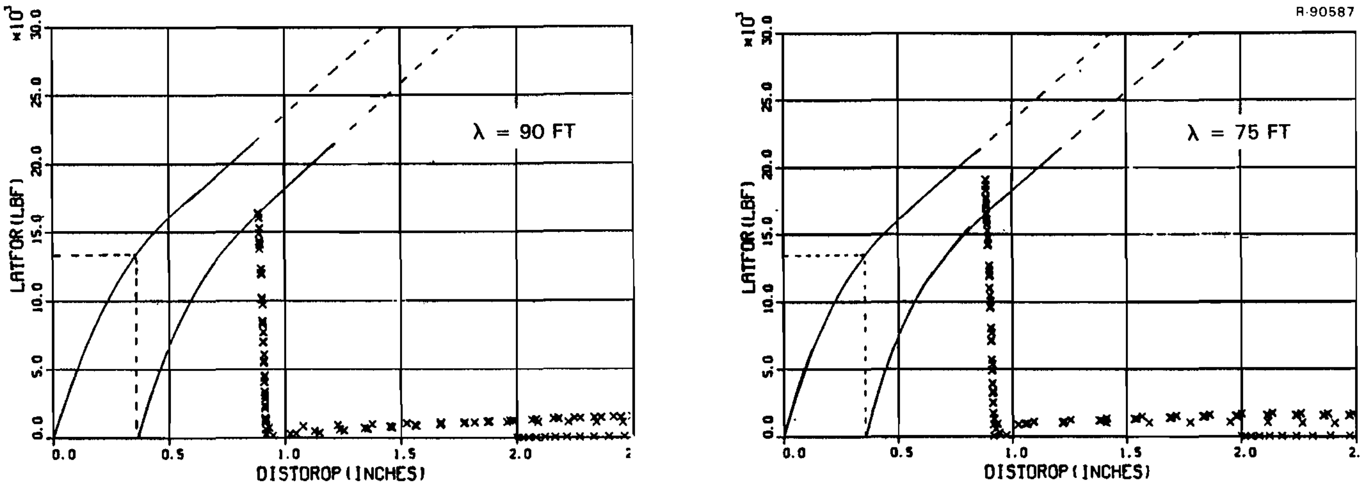

a) 90 ft Wavelength

b) 75 ft Wavelength

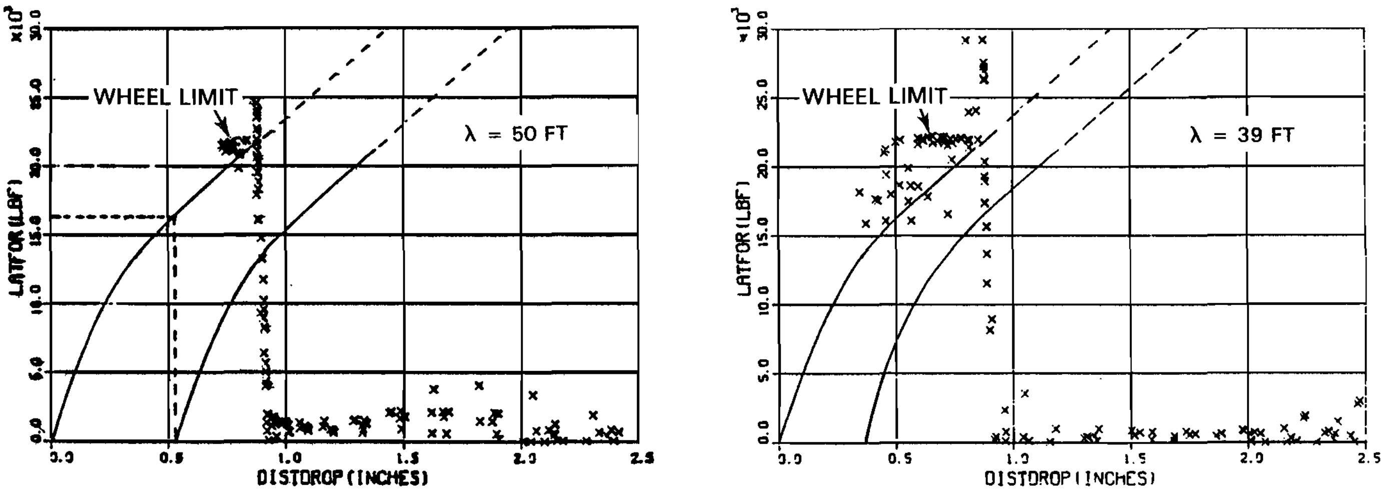

c) 50 ft Wavelength

d) 39 ft Wavelength

Figure 3.1-4 Incipient Wheel Drop Prediction (3 in. Peak/Peak Sinusoidal Amplitude at 25 mph Tangent Track with 58.0 in. gage.)

TABLE 3.1-2
RUN LIST FOR SINUSOIDAL ALIGNMENT VARIATION

RUN	ALIGNMENT PERTURBATION		GAGE	SPEED	COMMENTS
NO.	WAVE-LENGTH	P/P AMPLITUDE	CONST.	MPH	C - CLIMB D - DROP S - SAFE J - JUST V - VERY
T-1	39	5.0	58.0	25	C + D
2	↓	3.0	↓	↓	C + D
3	↓	3.0	↓	15	C + D
4	↓	1.33	57.75	25	JS(D)
5	↓	1.00	↓	10→95	Very little flanging
6	↓	1.00	56.5	10→95	No C or D, 26 kips Lat (Axle 1) 95 mph
T-7	50	5.0	58.0	25	C + D
8	↓	3.0	↓	↓	C + D
9	↓		↓	15	D
10	↓	2.0	57.75	25	D JS(C)
11	↓	↓	58.0	↓	D JS(C)
12	↓	1.75	57.75	↓	D
13	↓	1.50	↓	↓	D
14	↓	1.25	↓	↓	JS(D)
15	↓	1.125	↓	5→100	D (45 mph up) No C.
16	↓	1.00	58.0	25	JS(D)
T-17	75	5.0	58.0	25	D
18	↓	3.5	57.75	↓	JS(D)
19	↓	3.25	↓	↓	S
20	↓	3.0	58.0	↓	D
21	↓	↓	↓	15	JS(D)
22	↓	1.5	57.75	10→95	JS(D) 70 mph. D - 95 mph.
T-23	90	5.0	58.0	25	D
24	↓	4.5	57.75	↓	S
25	↓	4.5	57.5	↓	VS
26	↓	3.5	↓	↓	VS
27	↓	3.0	58.0	↓	VS
28	↓	↓	↓	15	VS
29	↓	↓	56.5	25	VVS

TABLE 3.1-3
RUN LIST FOR SINUSOIDAL ALIGNMENT VARIATION
5 DEGREE CURVE

RUN	BASIC CURVE		ALIGNMENT PERTURBATION		GAGE	SPEED	COMMENTS
NO.	deg	BAL. SPEED	WAVE-LENGTH	P/P AMPLITUDE	CONST.	mph	C - CLIMB D - DROP S - SAFE J - JUST V - VERY
5-1	5	25	39	1.33	57.75	25	D
2	↓	↓	↓	↓	↓	15	D
3	↓	↓	↓	1.0	↓	25	JS(D)
4	↓	↓	↓	0.75	↓	↓	S
5-5	5	25	50	1.25	57.75	25	JS(D)
6	↓	↓	↓	1.125	↓	↓	VS
5-7	5	25	75	3.25	57.75	25	JS(D)
5-8	5	25	90	4.50	57.75	25	S

TABLE 3.1-4
RUN LIST FOR SINUSOIDAL ALIGNMENT VARIATION
10 DEGREE CURVE

RUN	BASIC CURVE		ALIGNMENT PERTURBATION		GAGE	SPEED	COMMENTS
NO.	deg	BAL. SPEED	WAVE-LENGTH	P/P AMPLITUDE	CONST.	mph	C - CLIMB D - DROP S - SAFE J - JUST V - VERY
10-1	10	25	39	1.33	57.75	25	D
2	↓	↓	↓	↓	57.5	↓	D
3	↓	↓	↓	1.25	↓	↓	JS(D)
4	↓	↓	↓	1.0	↓	↓	S
5	↓	15	↓	↓	↓	↓	VS
6	↓	25	↓	↓	57.75	↓	JD
7	↓	↓	↓	0.75	↓	↓	JS(D)
10-8	10	25	50	1.75	57.5	25	S
9	↓	↓	↓	1.5	↓	↓	VS
10	↓	↓	↓	1.25	↓	↓	VS
11	↓	↓	↓	↓	57.75	↓	JD
12	↓	↓	↓	1.0	↓	↓	JS(D)
10-13	10	25	75	3.5	57.5	25	S
14	↓	↓	↓	3.25	57.75	↓	D
15	↓	↓	↓	2.7	↓	↓	D
16	↓	↓	↓	2.5	↓	↓	D
17	↓	↓	↓	2.25	↓	↓	JS(D)
10-18	10	25	90	4.5	57.75	25	D
19	↓	↓	↓		57.5	↓	S
20	↓	↓	↓	3.75	↓	↓	JD
21	↓	↓	↓	3.5	57.75	↓	JS(D)

TABLE 3.1-5
RUN LIST FOR SINUSOIDAL ALIGNMENT VARIATION
15 DEGREE CURVE

RUN	BASIC CURVE		ALIGNMENT PERTURBATION		GAGE	SPEED	COMMENTS
NO.	deg	BAL. SPEED	WAVE LENGTH	P/P AMPLITUDE	CONST.	mph	C - CLIMB D - DROP S - SAFE J - JUST V - VERY
15-1	15	25	39	1.33	57.75	25	D
2	↓	↓	↓	↓	57.5	↓	D
3	↓	↓	↓	1.0	57.75	↓	D
4	↓	↓	↓	↓	57.5	↓	D, JS(D)
5	↓	↓	↓	0.875	↓	↓	S
6	↓	↓	↓	0.75	57.75	↓	D
7	↓	↓	↓	↓	57.5	↓	S
8	↓	↓	↓	0.625	57.75	↓	D
9	↓	↓	↓	0.375	↓	↓	JD
10	↓	↓	↓	0.25	↓	↓	JS(D)
11	15	25	50	1.5	57.5	25	JS(D)
12	↓	↓	↓	1.25	57.75	↓	D
10-13	↓	↓	↓	1.125	57.5	↓	S
14	↓	↓	↓	1.0	↓	↓	S
15	↓	↓	↓	0.75	57.75	↓	D
16	↓	↓	↓	0.625	↓	↓	D
17	↓	↓	↓	0.5	↓	↓	JD
18	↓	↓	↓	0.375	↓	↓	JS(D)
10-19	15	25	75	3.25	57.75	25	D
20	↓	↓	↓	↓	57.5	↓	JS(D)
21	↓	↓	↓	3.00	↓	↓	JS(D)
22	↓	↓	↓	1.75	57.75	↓	D
23	↓	↓	↓	1.5	↓	↓	D
24	↓	↓	↓	1.25	↓	↓	JS(D)
25	15	25	90	4.5	57.75	25	D
26	↓	↓	↓	↓	57.5	↓	JS(D)
27	↓	↓	↓	3.5	↓	↓	S
28	↓	↓	↓	2.5	57.75	↓	D
29	↓	↓	↓	2.25	↓	↓	D
30	↓	↓	↓	2.00	↓	↓	D
31	↓	↓	↓	1.75	↓	↓	JS(D)

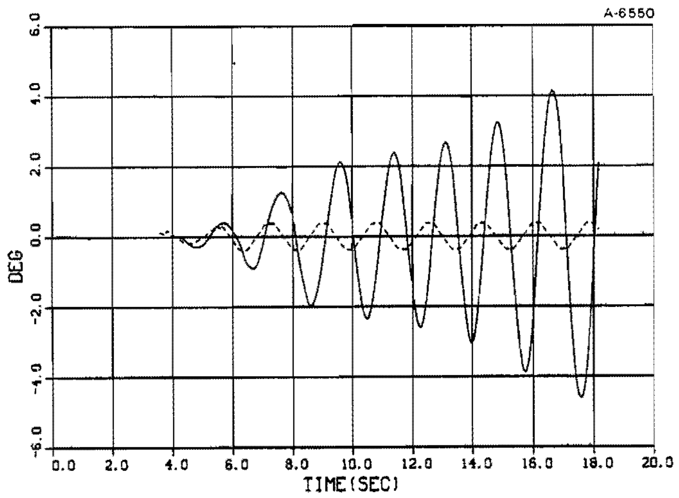

a) Roll Angle

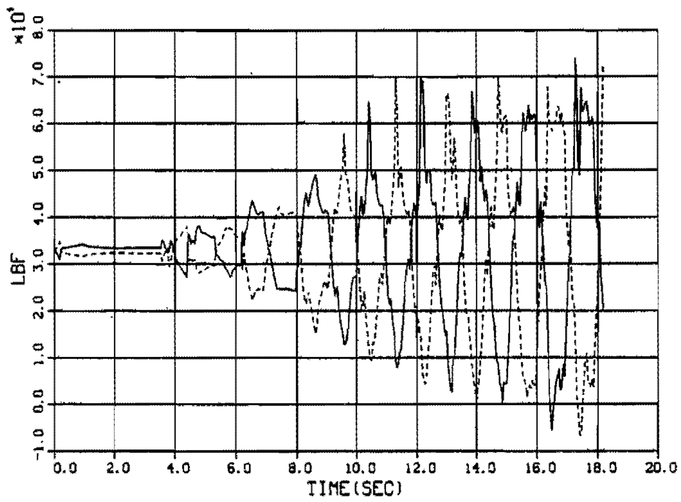

b) Leading Axle Vertical Force

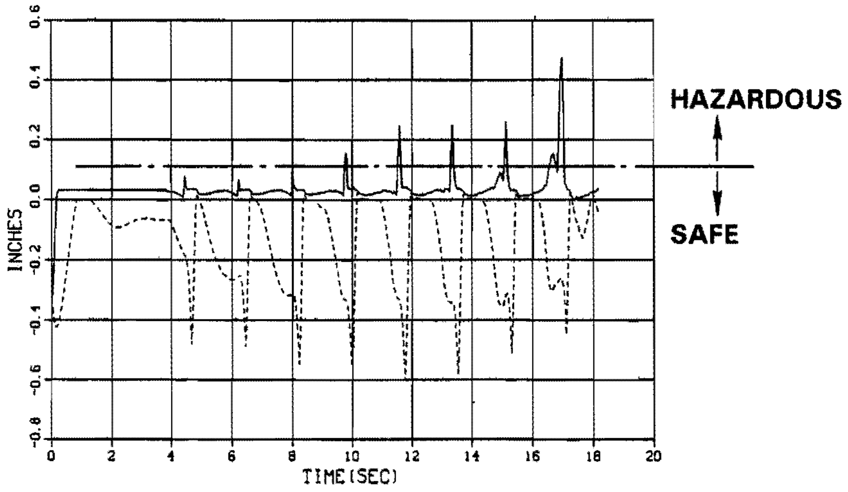

c) Wheel Climb Tendency

Figure 3.2-1 Carbody Roll Angle, Leading Axle Vertical Force and Wheel Climb Tendency (Ten Degree Curve, 15 mph Speed, 5/8 in. Crosslevel Variation, 1 1/4 in. Lateral Cusp Outer Rail, 57 3/4 in. Maximum Gage)

conditions to prevent derailment. The combination of crosslevel and outer rail lateral cusps in tight curves is found to represent a more severe environment than the separate variation of vertical (crosslevel) and lateral rail position (alignment and gage).

Similar results were obtained for other curvatures. Figures 3.2-2 through 3.2-5 show the effect of speed near roll resonance, in a five degree curve. The largest roll angle occurs near 14 mph although 15 mph is also large. Similarly, large variations are observed in the vertical load leading to dynamic unloading. The lateral forces shown in Fig. 3.2-4 are also large at both 14 and 15 mph. However, the 15 mph speed provides a combination of large lateral force with wheel unloading which leads to wheel climb (i.e., DYLF > 0.1) as indicated in Fig. 3.2-5. Again, values of 5/8 in. crosslevel or 1 3/4 in. lateral outer rail cusp were found previously to be insufficient to cause derailment under separate excitation.

A further study was undertaken on the five degree curve to establish a reduced lateral cusp which, together with the 5/8 in. crosslevel variation, would give the maximum cusp amplitude that does not lead to wheel climb. The computer output is summarized in Figs. 3.2-6 through 3.2-9. The peak roll again appears to occur at a speed between 14 and 15 mph. However, the roll angle (Fig. 3.2-6) is reduced significantly and the wheel unloading (Fig. 3.2-7) is less severe than for the previous case. This result illustrates the coupling between lateral excitation and roll response since the crosslevel is unaltered from the previous simulation. Reducing the lateral outer rail cusp amplitude produces the

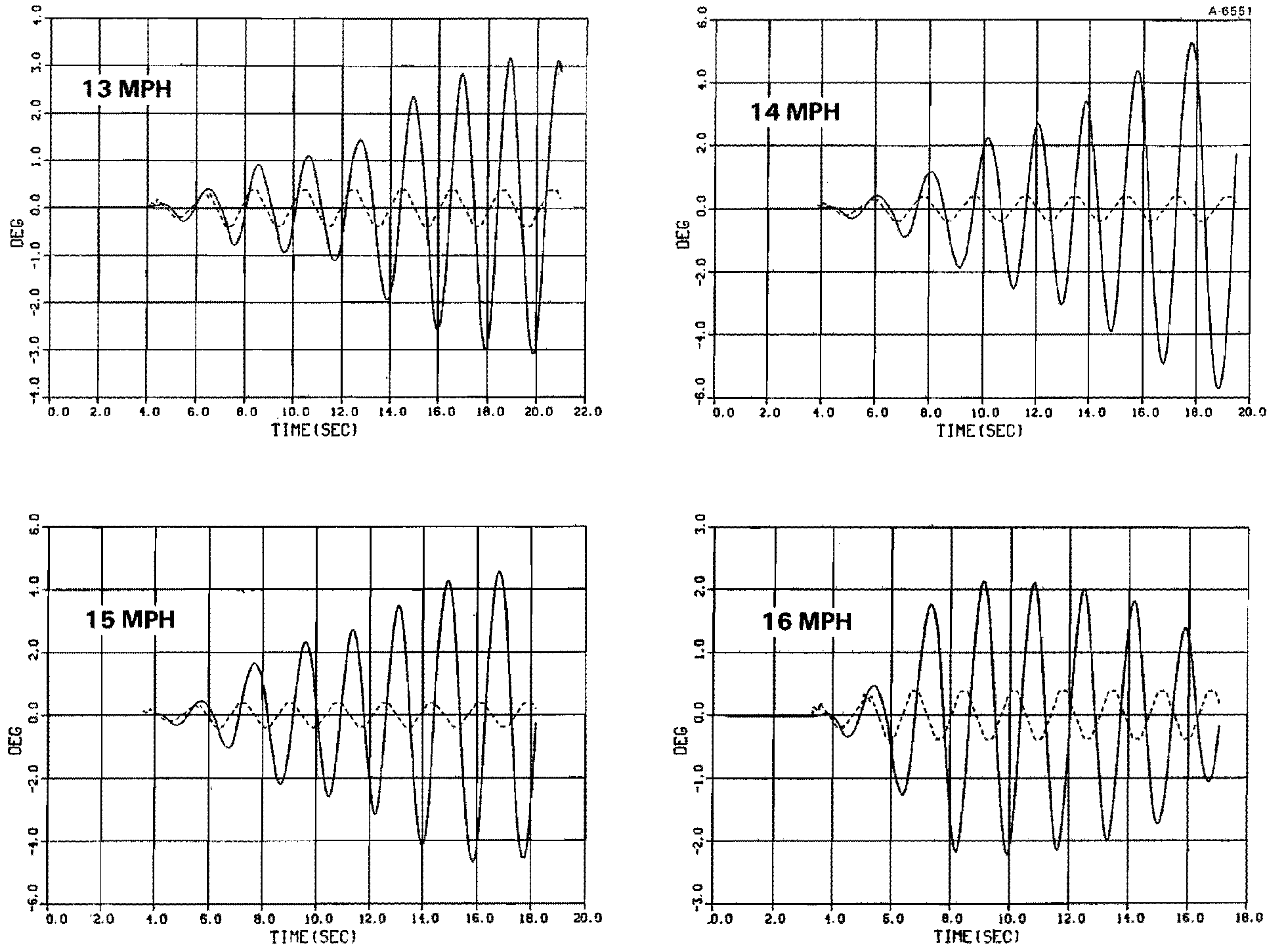

Figure 3.2-2 Roll Angle of 100 Ton Loaded Carbody (Response to Crosslevel and Gage Variation/Curvature 5 Degrees/Crosslevel Variation 5/8 in./Maximum Gage 57.75 in./Outer Rail Lat. Cusp 1.75 in.)

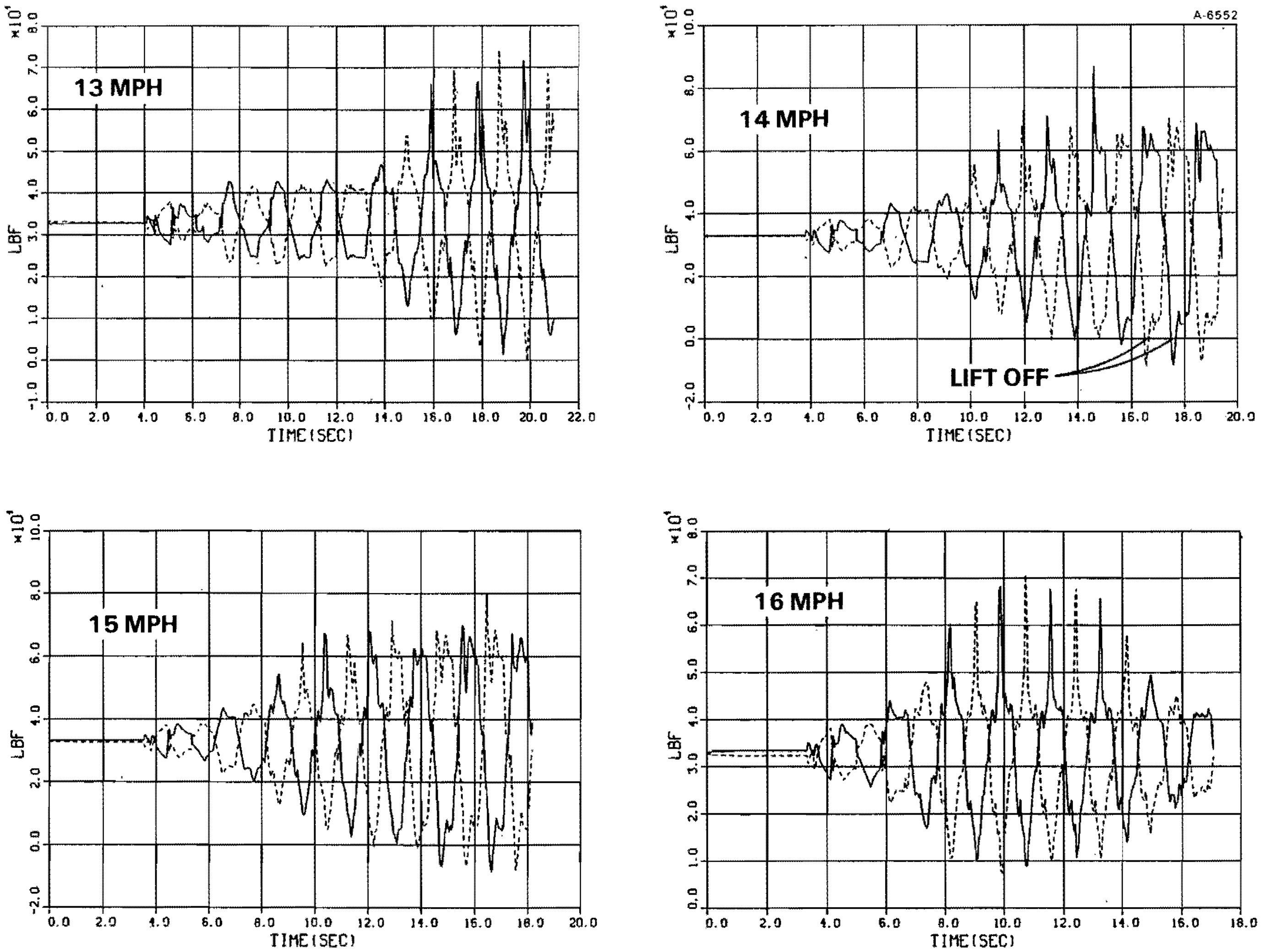

Figure 3.2-3 Vertical Forces on Leading Wheels (Response to Crosslevel and Gage Variation, Curvature 5 Degrees/ Crosslevel Variation 5/8 in./Maximum Gage 57.75 in./ Outer Rail Lat. Cusp 1.75 in.)

same effect as increasing the minimum gage to 56.5 in. from the previous value of 56.0 in. The lateral force is also less than that for the larger lateral cusp, but the major difference is that the large lateral forces (cf. Fig. 3.2-8) persist over a smaller time, which permits a time difference between the occurrence of wheel unloading and lateral thrust. This result is seen as the absence of incipient wheel climb in Fig. 3.2-9.

These results suggest that by reducing the amplitude of outer rail cusps at five degrees of curvature together with further reductions in crosslevel variation at higher values of curvature, it is possible to significantly reduce the likelihood of wheel climb. Since the original outer rail cusp at low curvatures was 1 3/4 in., results were sought for this amplitude on a three degree curve with the previously used crosslevel variation of 5/8 in. The results are remarkably similar to those of the previous five degree curve with the smaller lateral cusp amplitude as shown in Figs. 3.2-9 through 3.2-12. The wheels barely unload and the lateral forces are not sustained to coincide with the unloading. No wheel climb is predicted.

For the ten degree curve the incipient wheel climb derailment is eliminated by

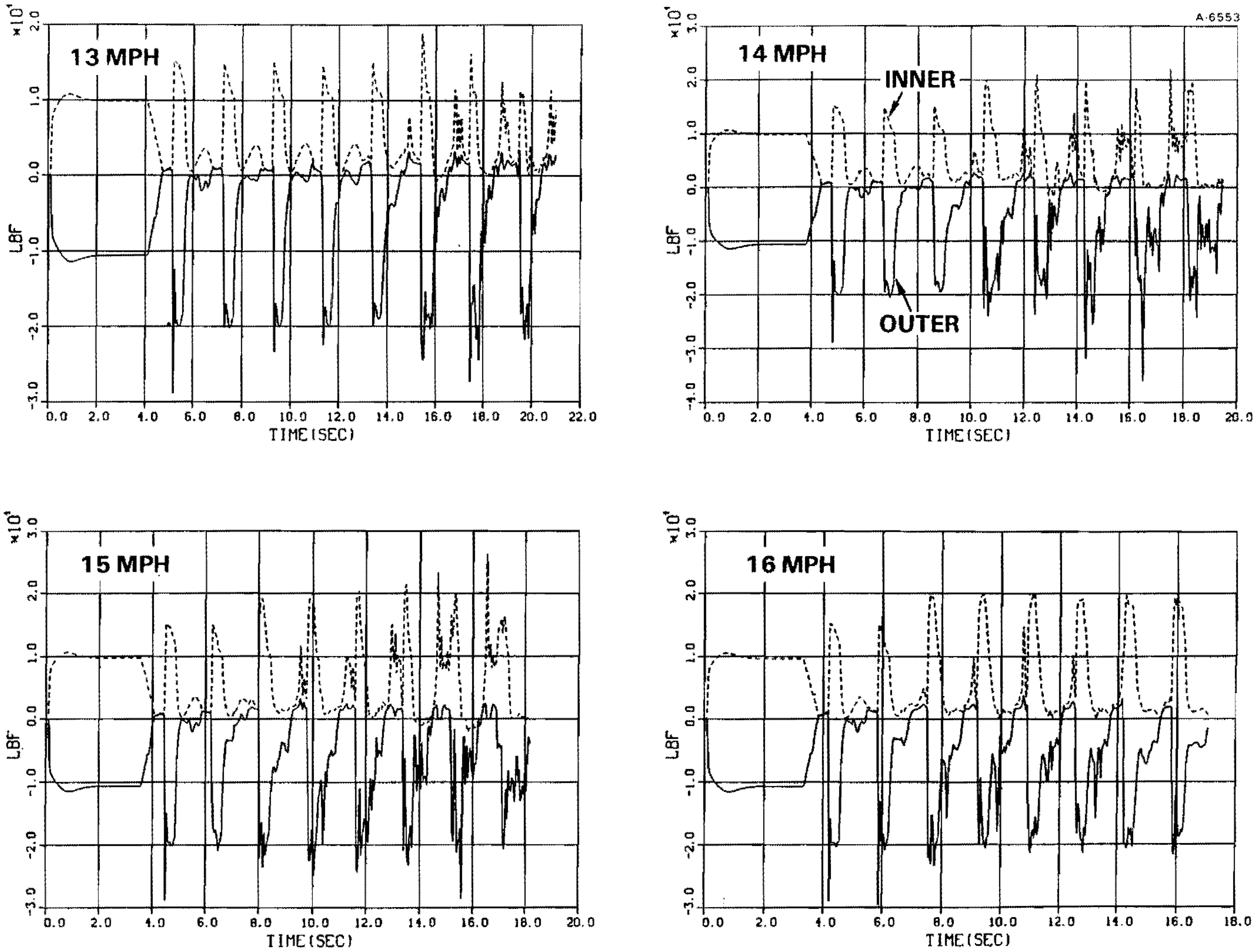

Figure 3.2-4 Lateral Forces on Leading Wheels (Response to Crosslevel and Gage Variation, Curvature 5 Degrees/ Crosslevel Variation 5/8 in./Maximum Gage 57.75 in./ Outer Rail Lat. Cusp 1.75 in.)

the reduction of crosslevel variation from 5/8 in. to 1/2 in. as compared in Fig. 3.2-14. This raises the question of a possible equivalence in the effect of reducing crosslevel and lateral cusp amplitude variations. Figures 3.2-15 through 3.2-18 show, respectively, the history of roll, vertical force, lateral force and lateral excursion beyond flange contact for different track perturbations that are near derailment on a ten degree curve. The roll angle and vertical force responses are similar. However, differences are apparent in the lateral force due to the large difference in track. The two cases are:

	CROSSLEVEL	OUTER RAIL CUSP
Case 1	$\frac{3}{4}$ in	0 in
Case 2	$\frac{1}{2}$ in	$1\frac{1}{4}$ in

It would appear that when a severe tendency to derail exists, a reduction in 1/4 in. of cross level variation is equivalent to about 1-1/4 in. of lateral cusp reduction, supporting the suggestion that limiting lateral cusp amplitude

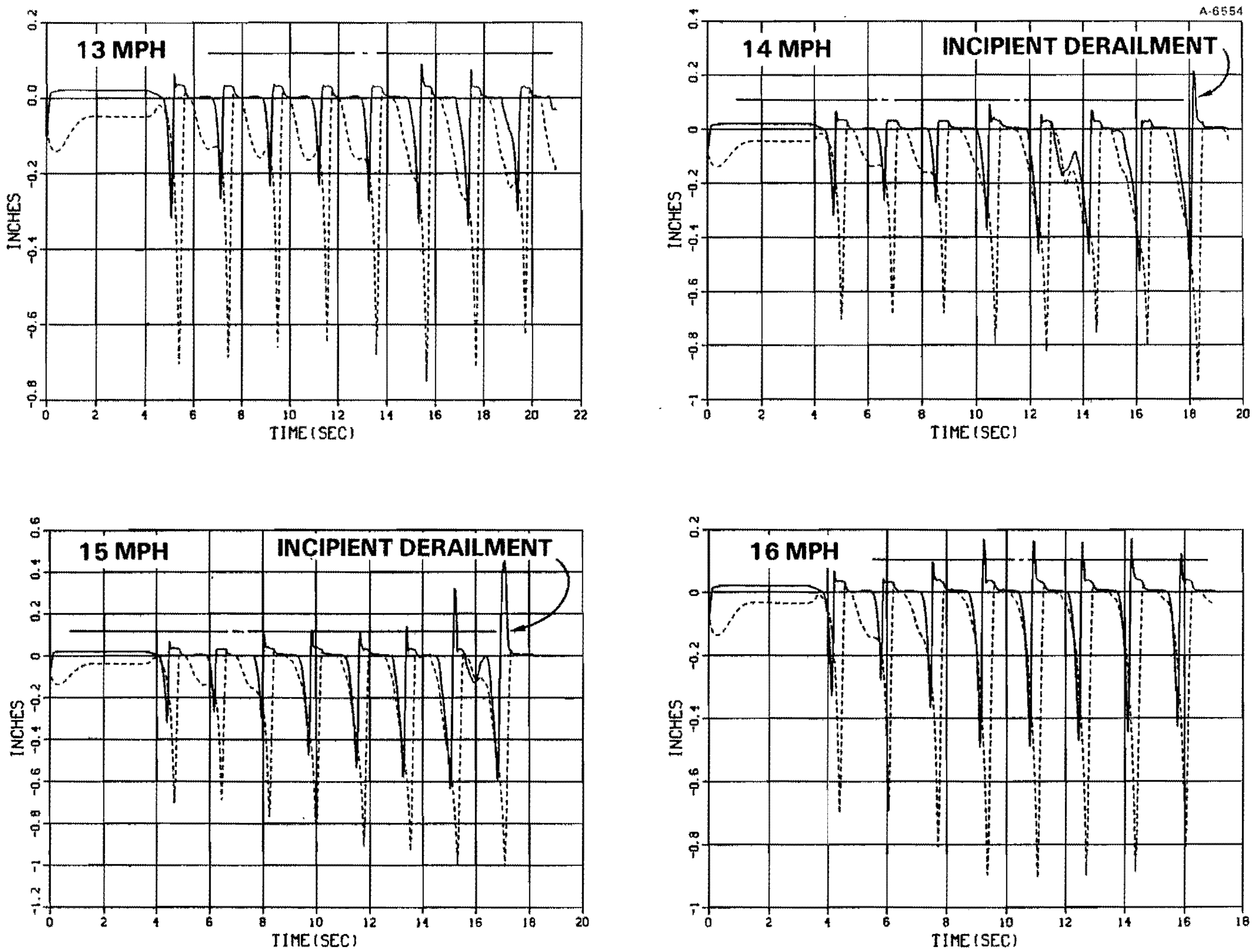

Figure 3.2-5 Wheel Climb Tendency (Response to Crosslevel and Gage Variation, Curvature 5 Degrees/Crosslevel Variation 5/8 in./Maximum Gage 57.75 in./Outer Rail Lat. Cusp 1.75 in.)

alone in high curvatures would impose a track gage impossible to maintain for these tests. The result also suggests that incipient rail climb is more consistent with wheel unloading than excessive lateral force in the range of normal track tolerances.

At the higher curvature of 15 degrees a further reduction in lateral cusp amplitude to 1.0 in. is necessary to prevent wheel climb, even with the reduced crosslevel variation of $\frac{1}{2}$ in. A comparison of results for the four output variables on ten and 15 degree curves are given in Figs. 3.2-19 through 3.2-22, for 15 and 16 mph. The lateral cusp amplitude is $1\frac{1}{4}$ in. for the ten degree curve and 1.0 in. for the 15 degree curve. Complete unloading of the wheel does not occur. However, the combination of high curvature and lateral cusps are sufficient to give large lateral forces but not enough to provide incipient wheel climb (cf. Fig. 3.2-22).

The results in the ten degree curve were used as a basis for planning the test carried out in Bennington, New Hampshire in July and August 1982.

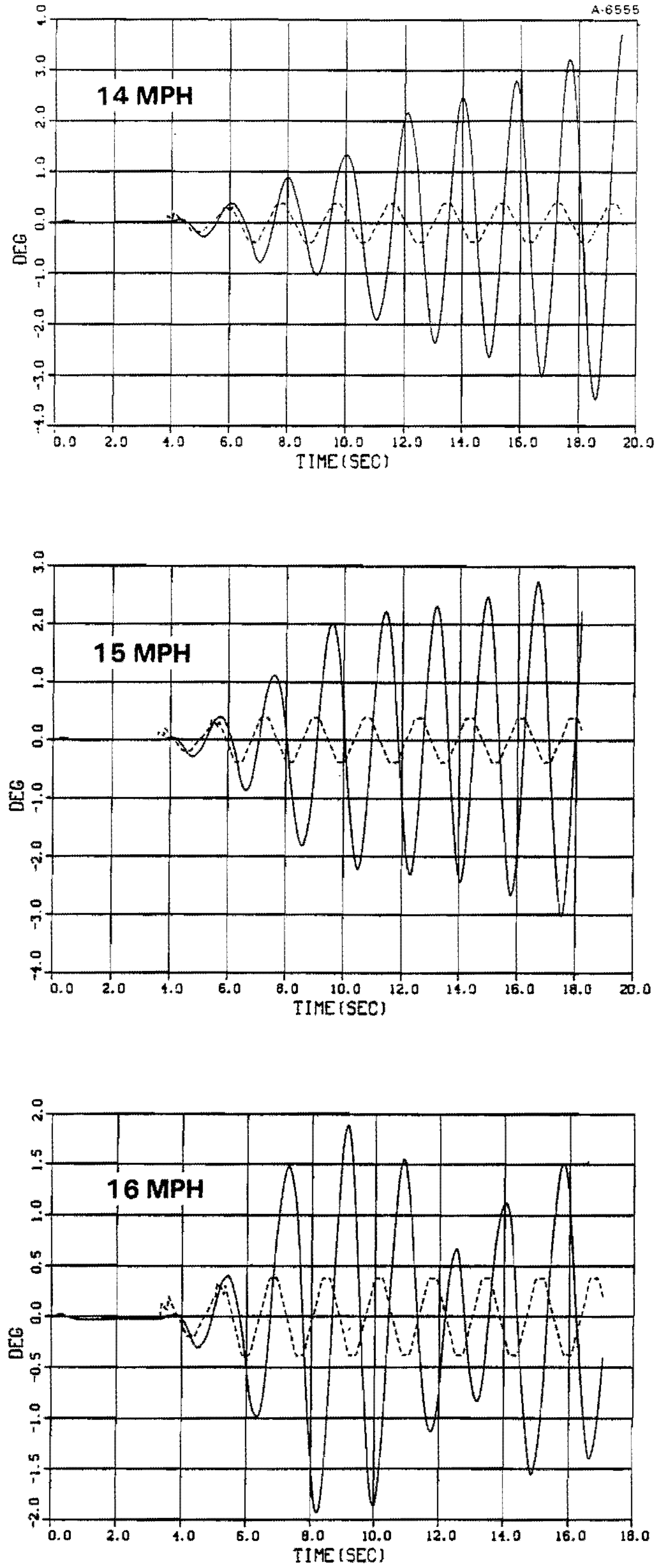

Figure 3.2-6 Roll Angle of 100 Ton Loaded Carbody (Response to Crosslevel and Gage Variation, Curvature 5 Degrees/Crosslevel Variation 5/8 in./Maximum Gage 57.75 in./Outer Rail Lat. Cusp 1.25 in.)

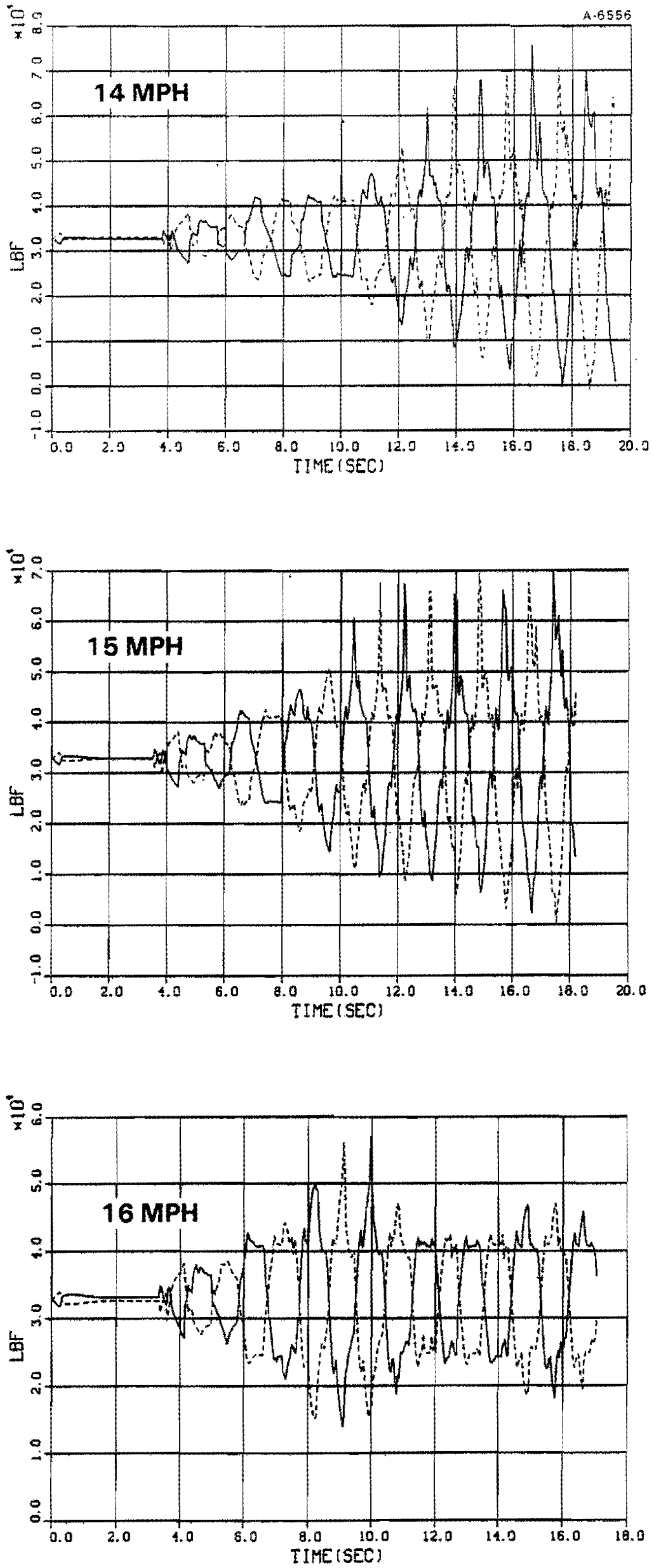

Figure 3.2-7 Vertical Forces on Leading Wheels (Response to Crosslevel and Gage Variation, Curvature 5 Degrees/Crosslevel Variation 5/8 in./Maximum Gage 57.75 in./Outer Rail Lat. Cusp 1.25 in.)

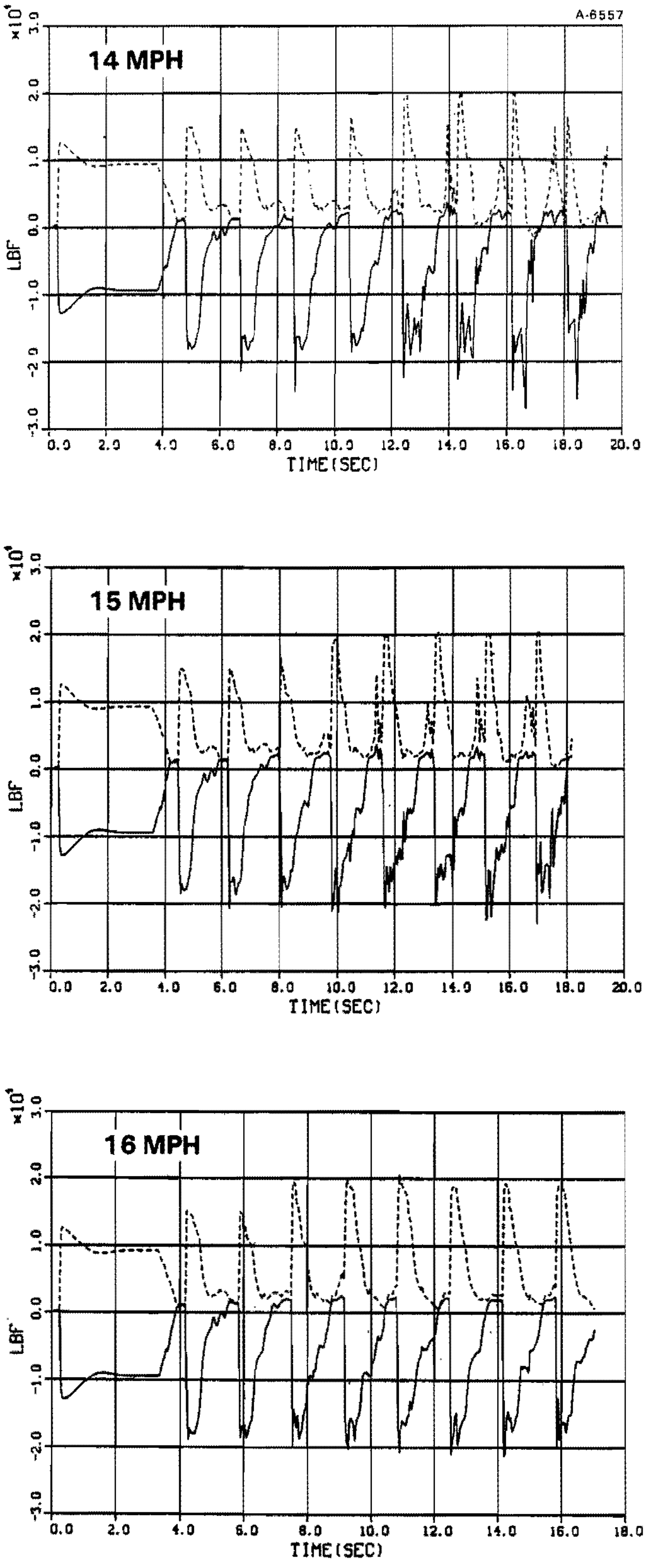

Figure 3.2-8 Lateral Forces on Leading Wheels (Response to Crosslevel and Gage Variation, Curvature 5 Degrees/ Crosslevel Variation 5/8 in./ Maximum Gage 57.75 in./Outer Rail Lat. Cusp 1.25 in.)

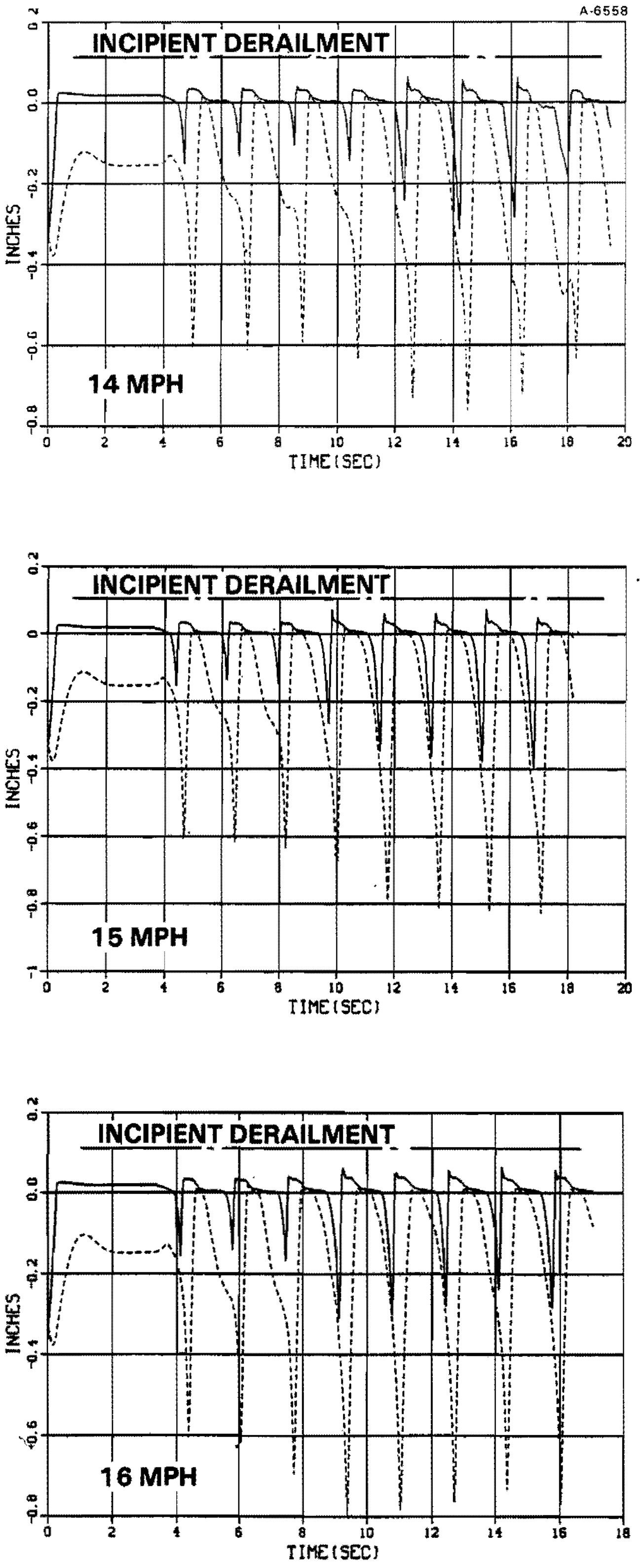

Figure 3.2-9 Wheel Climb Tendency (Response to Crosslevel and Gage Variation, Curvature 5 Degrees/Crosslevel Variation 5/8 in./Maximum Gage 57.75 in./Outer Rail Lat. Cusp 1.25 in.)

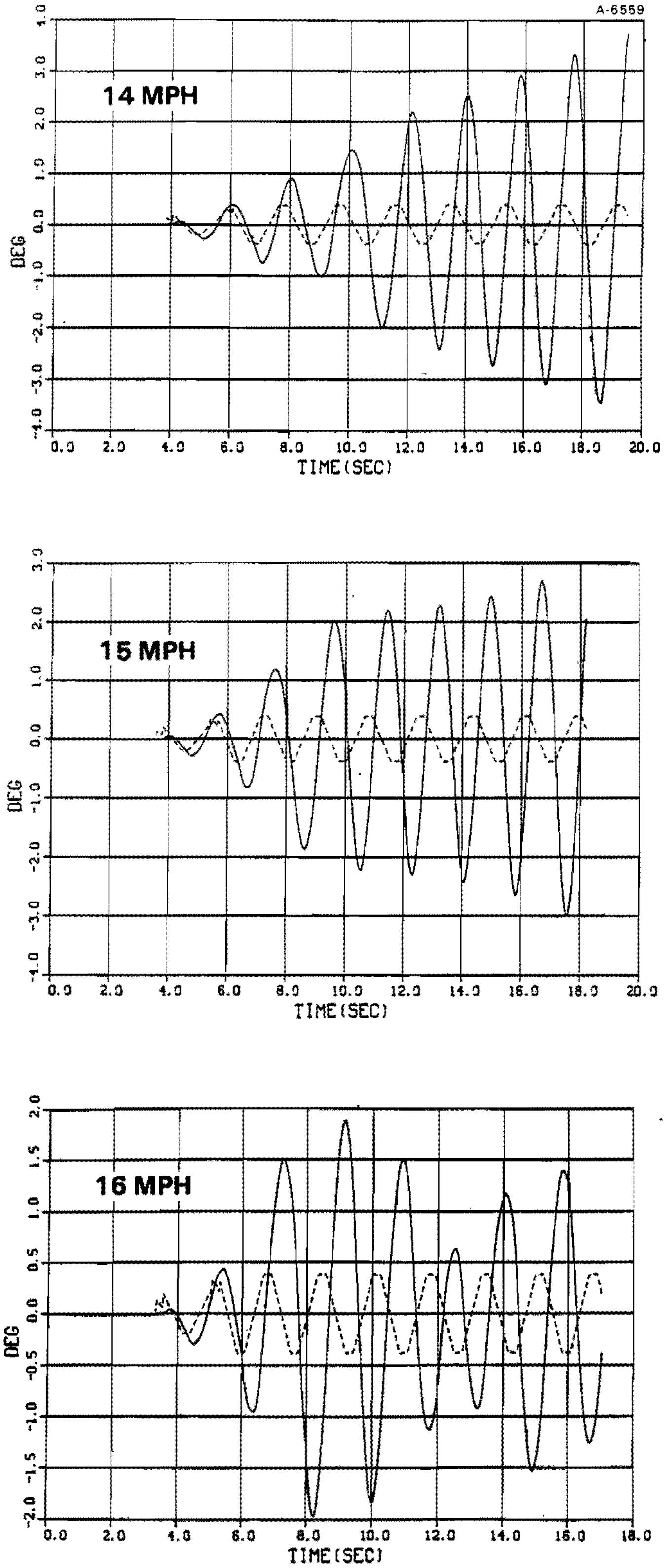

Figure 3.2-10 Roll Angle of 100 Ton Loaded Carbody (Response to Crosslevel and Gage Variation, Curvature 3 Degrees/Crosslevel Variation 5/8 in./Maximum Gage 57.75 in./ Outer Rail Lat. Cusp 1.75 in.)

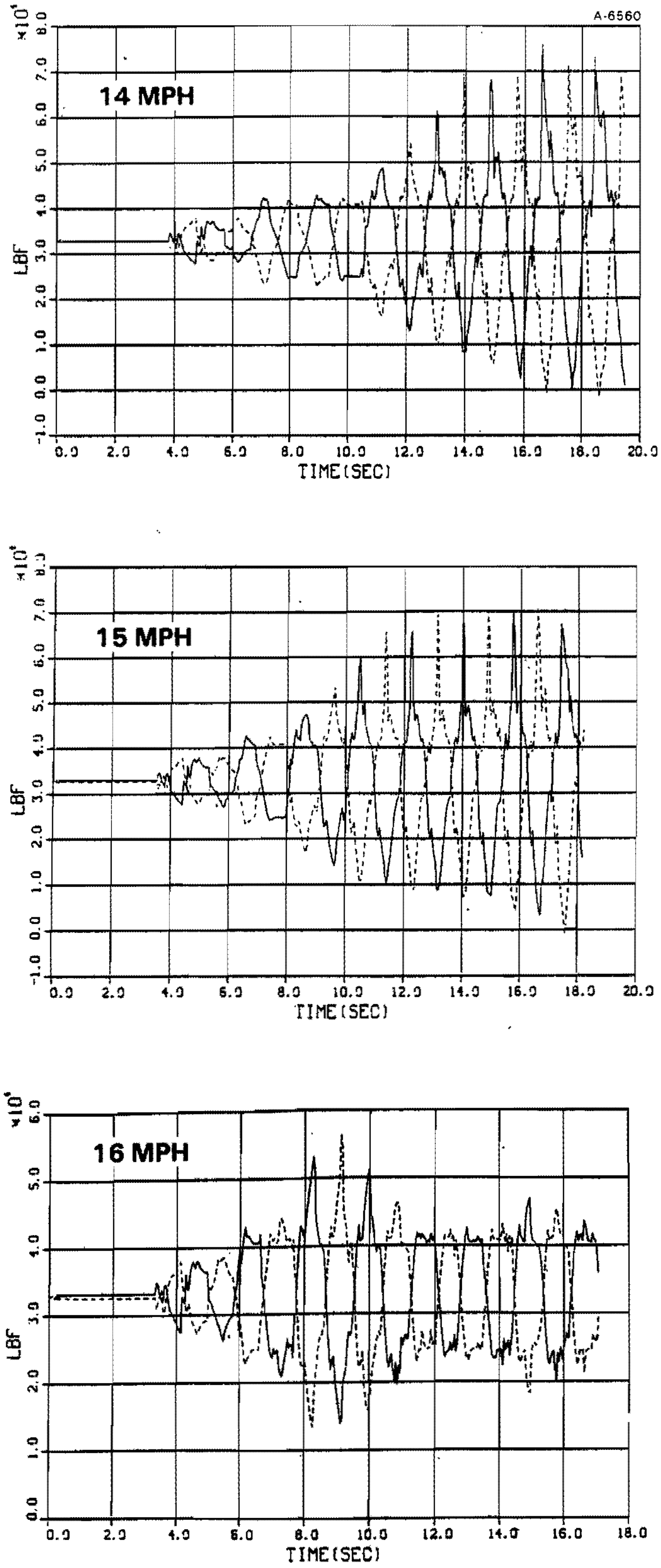

Figure 3.2-11 Vertical Forces on Leading Wheels (Response to Crosslevel and Gage Variation, Curvature 3 Degrees/ Crosslevel Variation 5/8 in./ Maximum Gage 57.75 in./Outer Rail Lat. Cusp 1.75 in.)

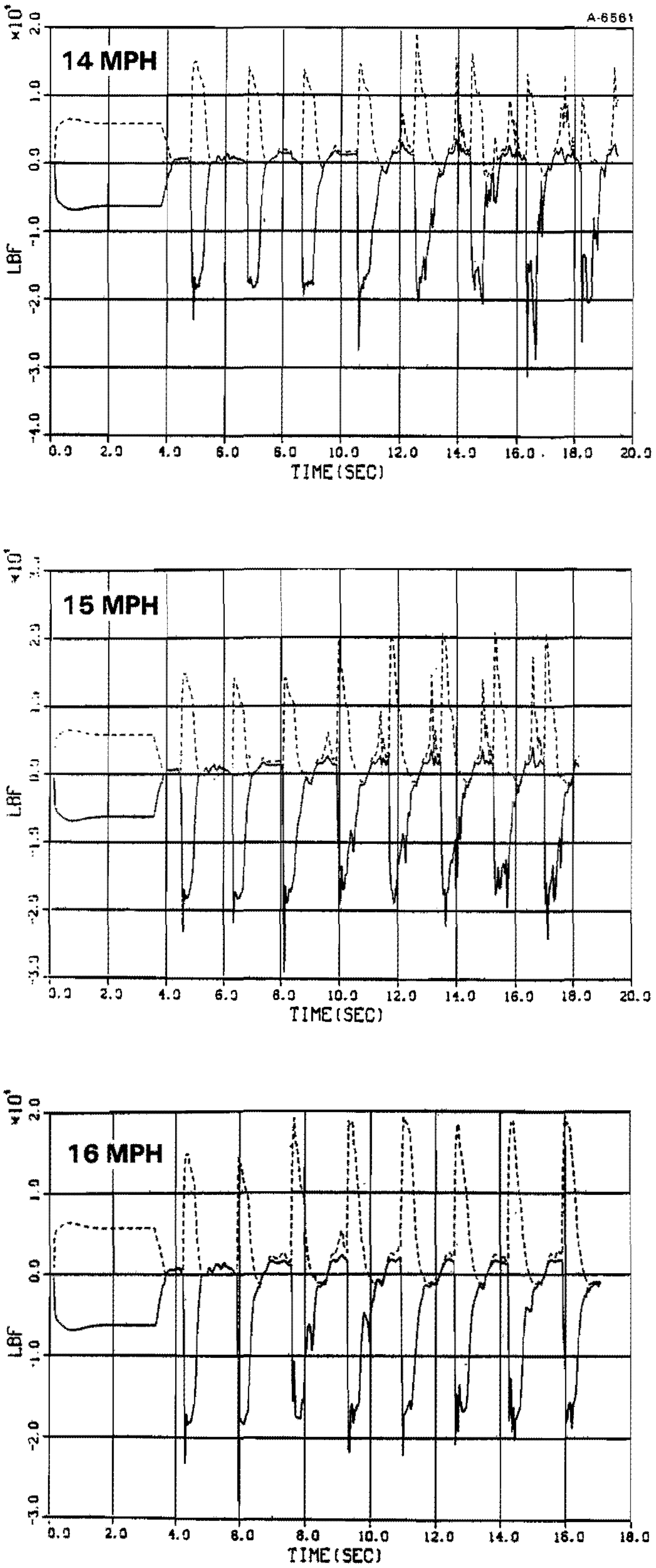

Figure 3.2-12 Lateral Forces on Leading Wheels (Response to Crosslevel and Gage Variation, Curvature 3 Degrees/ Crosslevel Variation 5/8 in./ Maximum Gage 57.75 in./Outer Rail Lat. Cusp 1.75 in.)

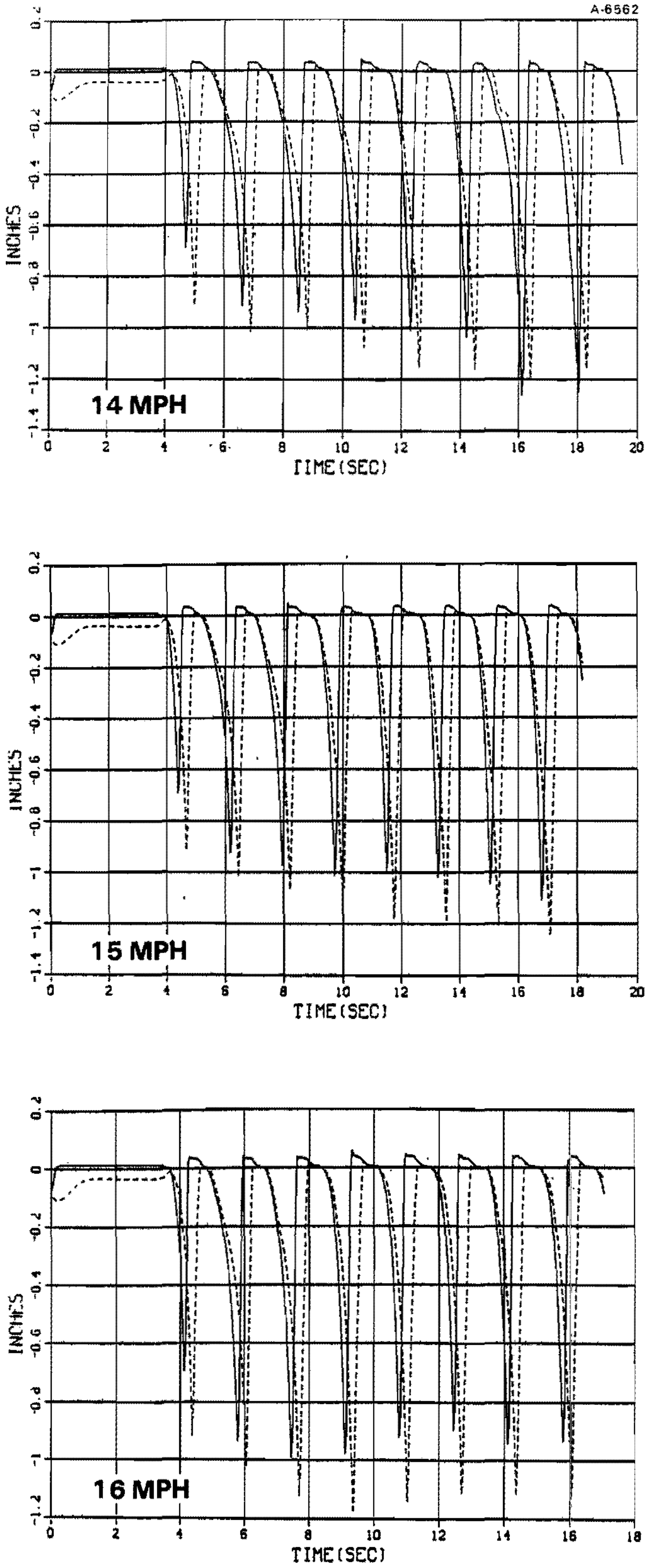

Figure 3.2-13 Wheel Climb Tendency (Response to Crosslevel and Gage Variation, Curvature 3 Degrees/Crosslevel Variation 5/8 in./Maximum Gage 57.75 in./Outer Rail Lat. Cusp 1.75 in.)

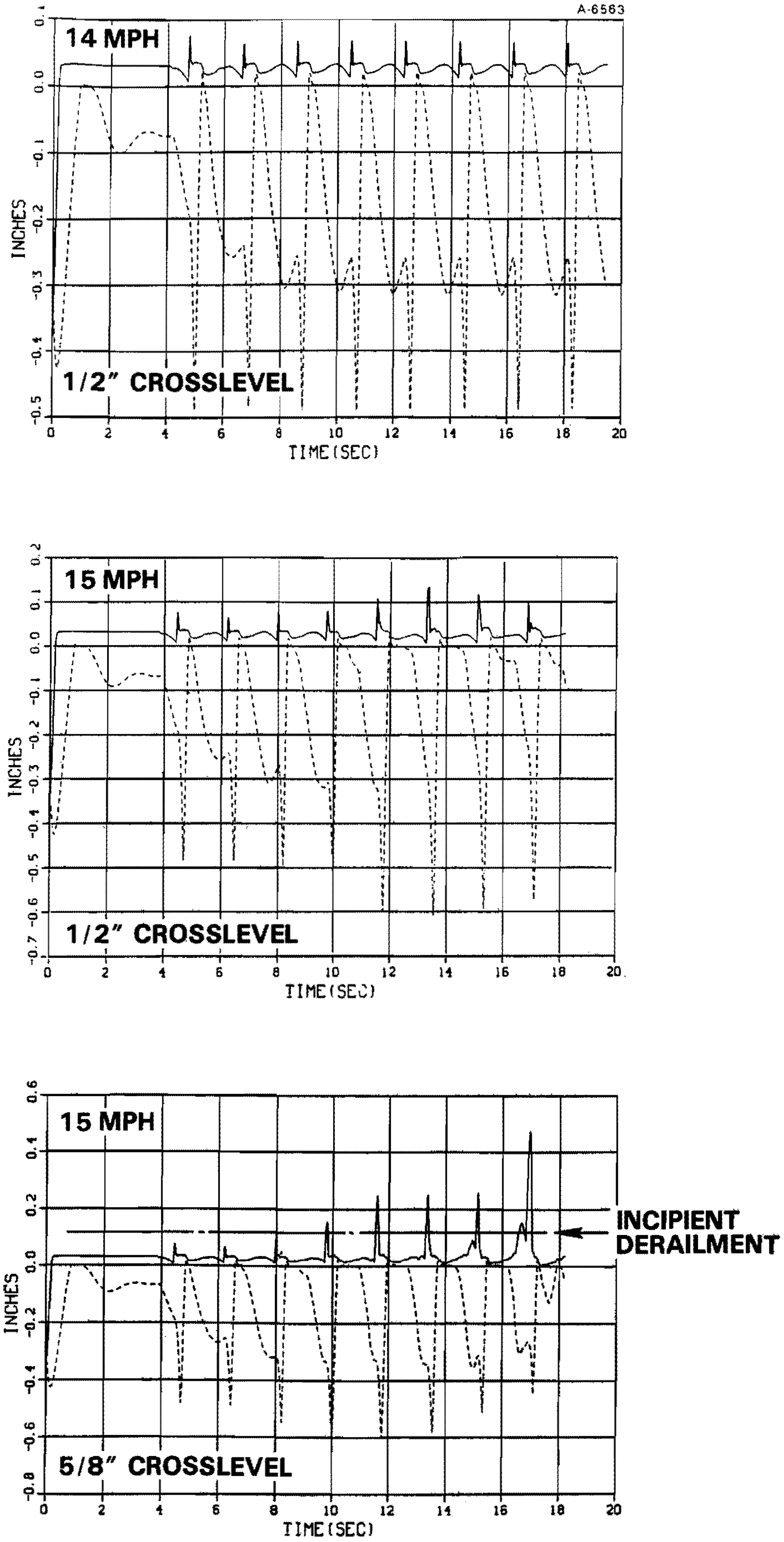

Figure 3.2-14 Wheel Climb Tendency (Response to Crosslevel and Gage Variation, Curvature 10 Degrees/56.5 in. Minimum Gage/Lat. Cusp 1.25 in.)

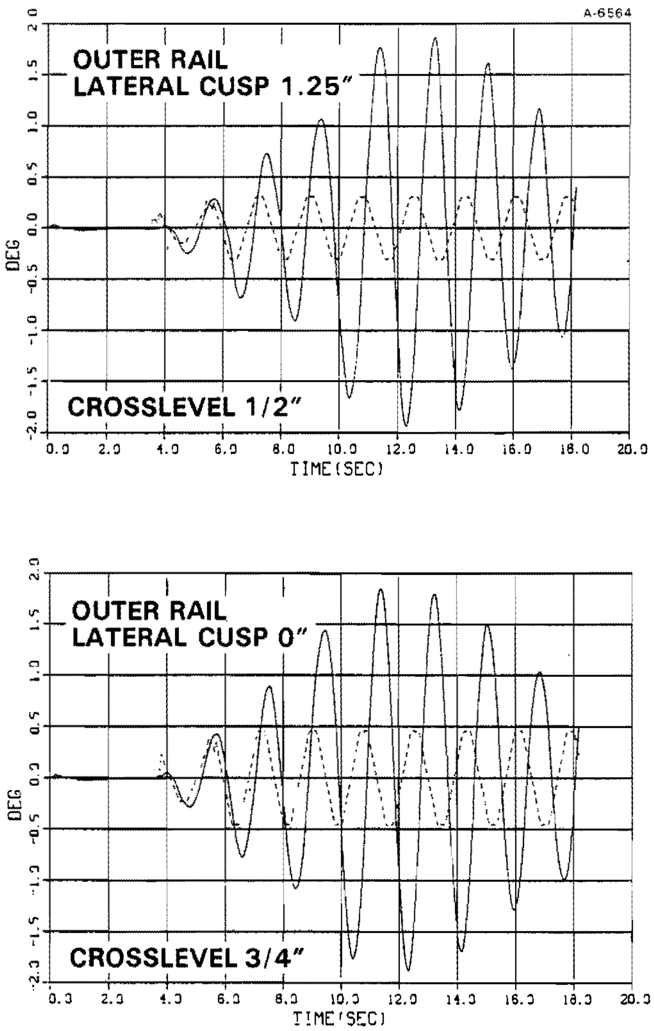

Figure 3.2-15 Roll Angle of 100 Ton Loaded Carbody (Response to Crosslevel and Gage Variation, Curvature 10 Degrees)

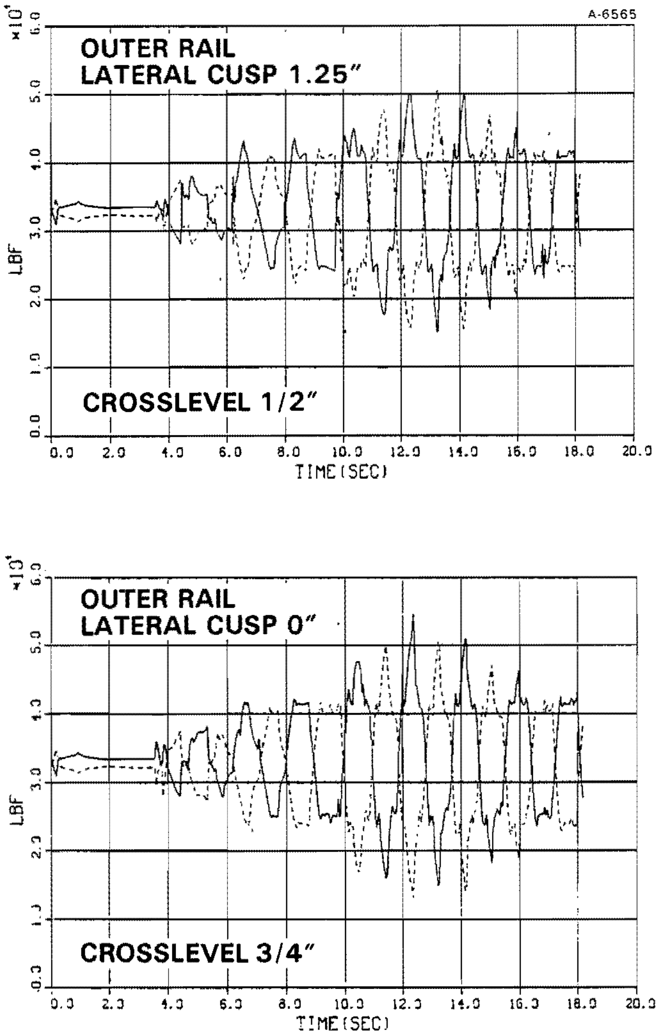

Figure 3.2-16 Vertical Forces on Leading Wheels (Response to Crosslevel and Gage Variation, Curvature 10 degrees)

3.3 RESULTS FOR SINUSOIDAL ALIGNMENT VARIATIONS

Sinusoidal alignment variations on tangent track having a minimum restraint capability at low speed were reconsidered in order to confirm and extend the results given previously in Ref. 4. The limiting derailment scenario is that of wheel drop following dynamic wide gage. The results given in Table 3.3-1 represent the best assessment for tangent track for a fixed wide gage of 57 3/4 in.

During this investigation a search was made to establish the coupling between sinusoidal alignment variation and roll response. The results are shown in Fig. 3.3-1. Severe roll response is apparent at 15 mph for a peak/peak alignment amplitude of 3 in. at a 39 ft wavelength. However, this amplitude is more than twice that which creates forces large enough to cause a wheel drop derailment on the track identified. The wheel climb resulting from large roll response is therefore not critical in this work.

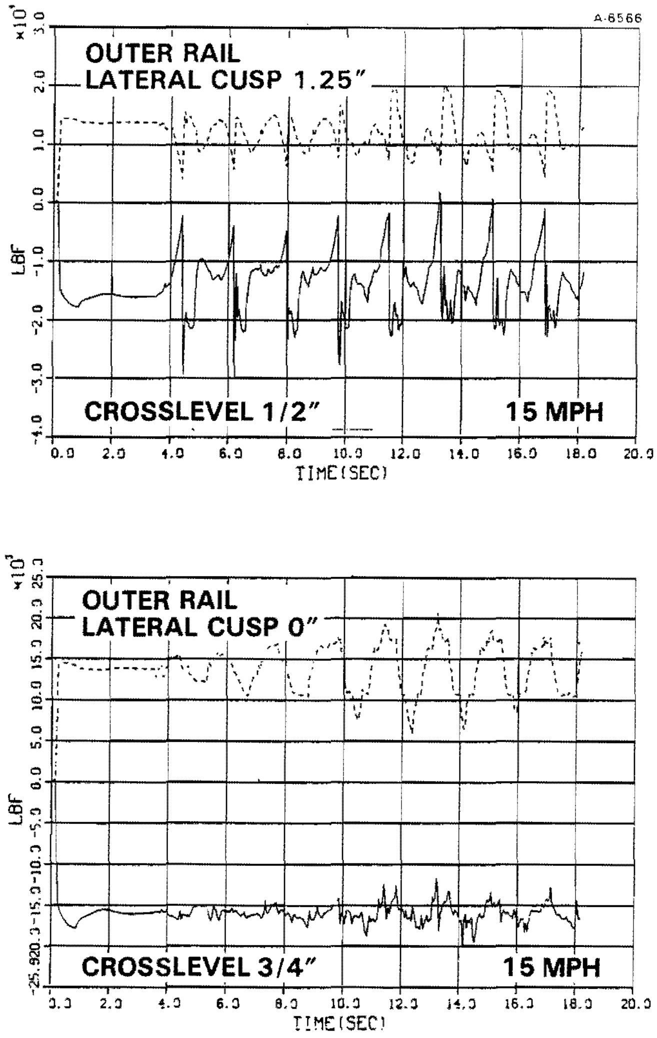

Figure 3.2-17 Lateral Forces on Leading Wheels (Response to Crosslevel and Gage Variation, Curvature 10 degrees)

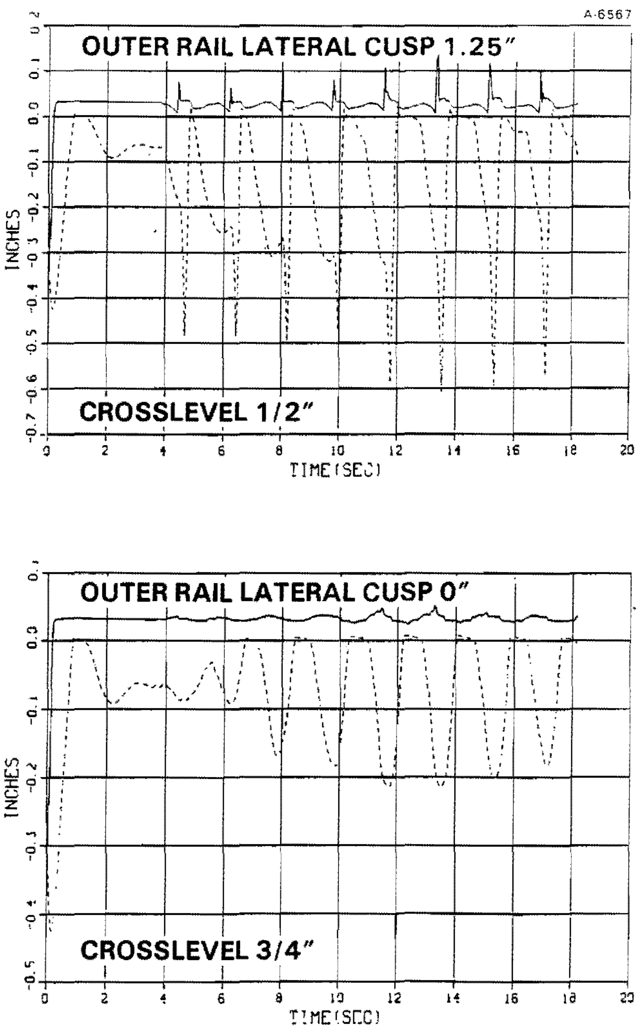

Figure 3.2-18 Wheel Climb Tendency (Response to Crosslevel and Gage Variation, Curvature 10 Degrees)

At the much smaller alignment peak/peak amplitude of 1 in., the simulation program predicted that a wide gage on tangent track would permit the wheelset to ignore the alignment variation with little or no flange contact while at normal gage repeated flange contact occurs. This result is shown in Fig. 3.3-2. However, the trend of larger forces from tighter gages only exists where flange contact can be avoided.

In general, under incipient wheel drop conditions and, in particular, in curves where flange contact occurs with modest alignment variation, larger gages result in smaller distances to wheel drop from the rail restraint curve. This becomes the dominant influence as shown in Fig. 3.3-3.

In a preliminary investigation of the effect of speed on response, it was shown that higher speeds generally cause larger forces. An example is given in Figs. 3.3-4 and 3.3-5 for a 50 ft wavelength alignment sinusoid on tangent track. With the peak/peak amplitude of 1.125 in. shown, a speed of 45 mph just provides the prediction of wheel drop. At 100 mph, on stiffer track with a higher rail restraint curve than that given, the prediction shows the beginnings of a wheel climbing tendency. This is indicated by results with a reduction in DISTDROP, or distance to wheel drop, at

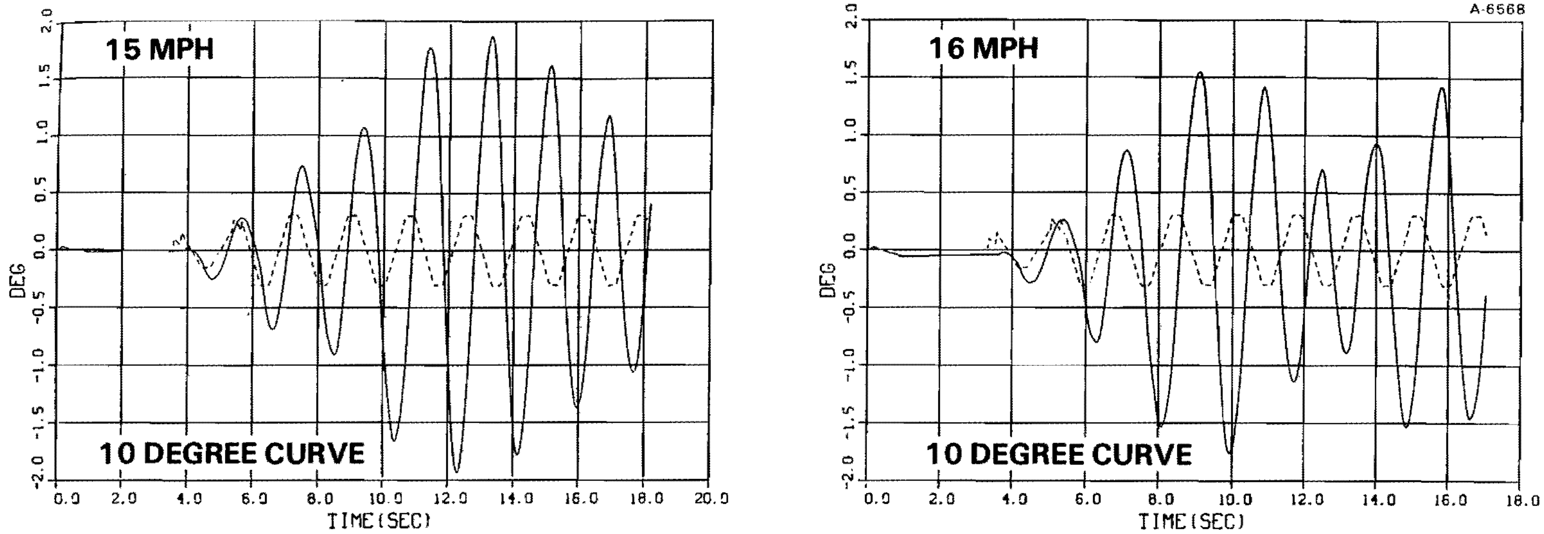

a) Lat. Cusp 1.25 in.

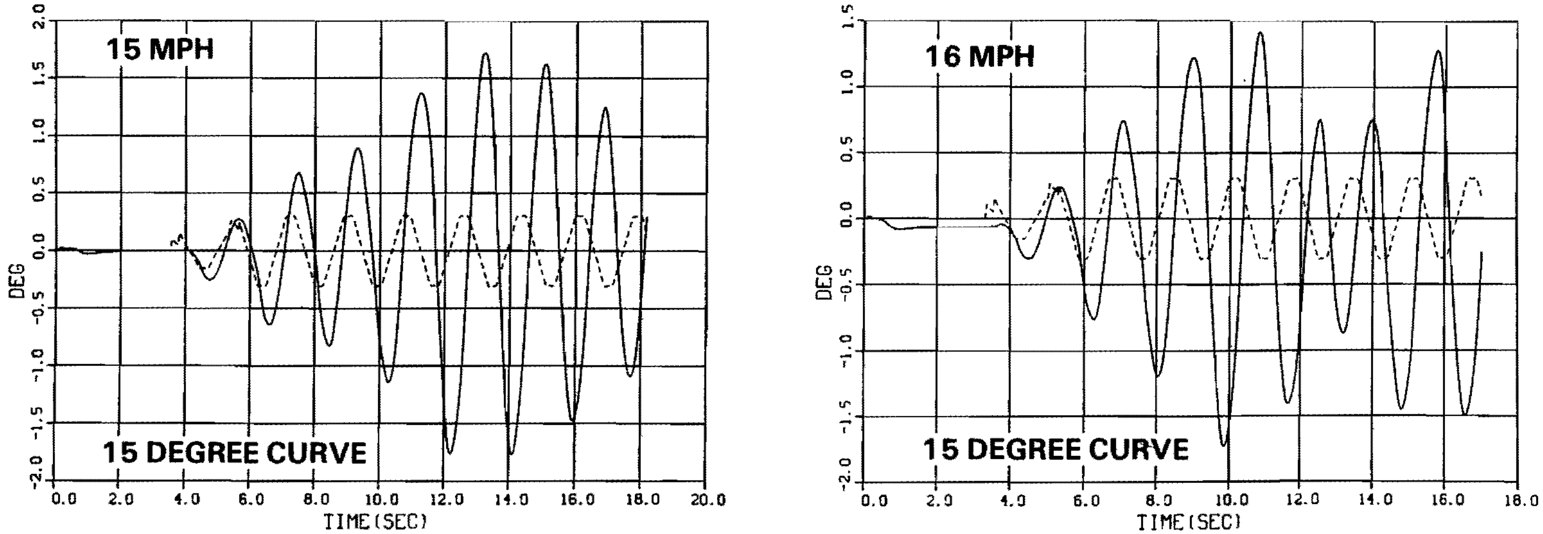

b) Lat. Cusp 1.0 in.

Figure 3.2-19 Roll Angle of 100 Ton Loaded Carbody (Response to Crosslevel and Gage Variation, Crosslevel Variation 1/2 in.)

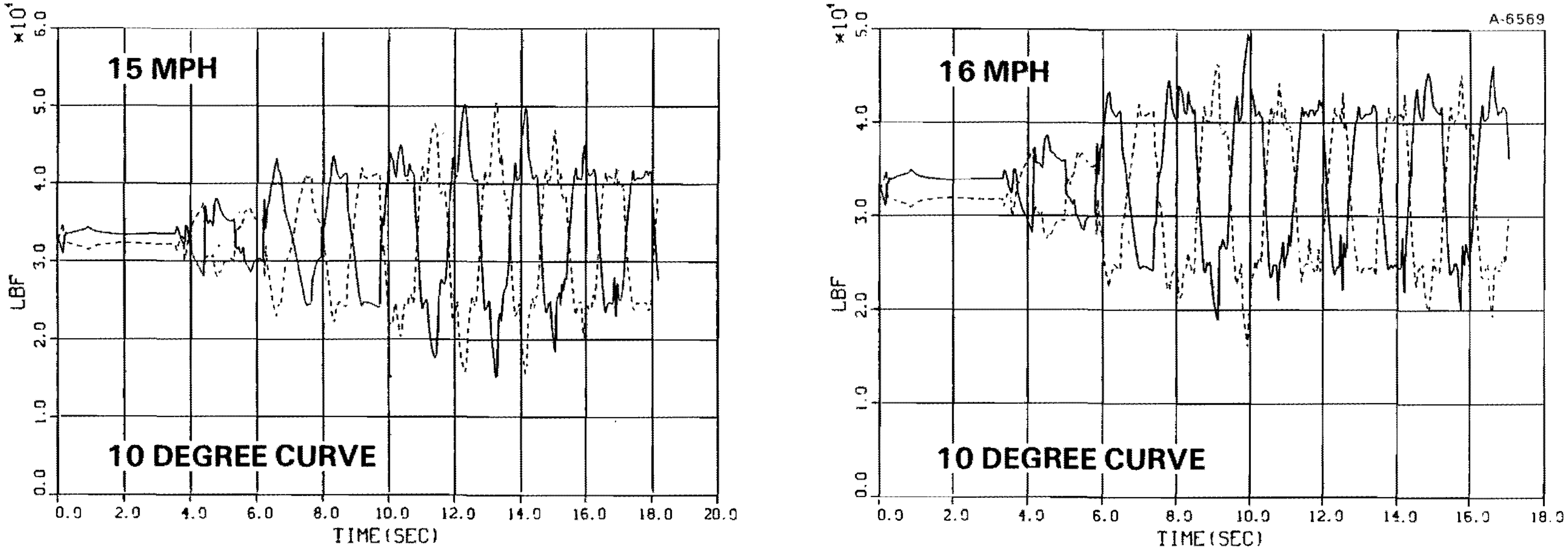

a) Lat. Cusp 1.25 in.

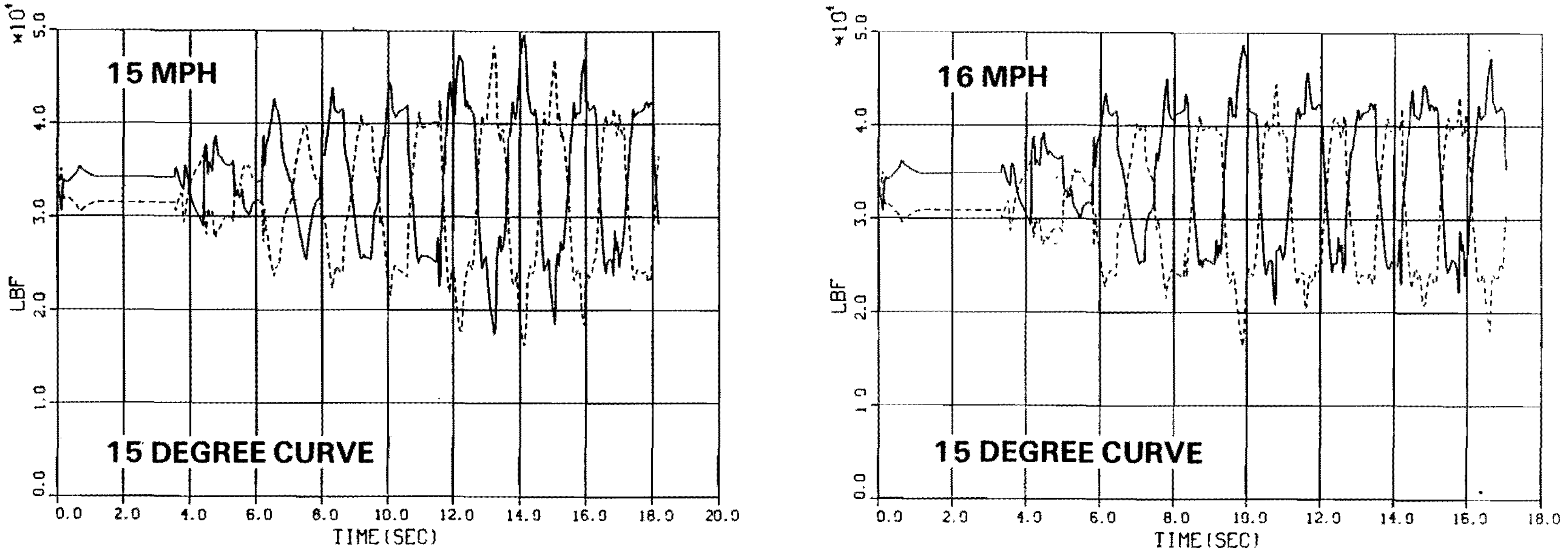

b) Lat. Cusp 1.0 in.

Figure 3.2-20 Vertical Forces on Leading Wheels (Response to Crosslevel and Gage Variation, Crosslevel Variation 1/2 in.)

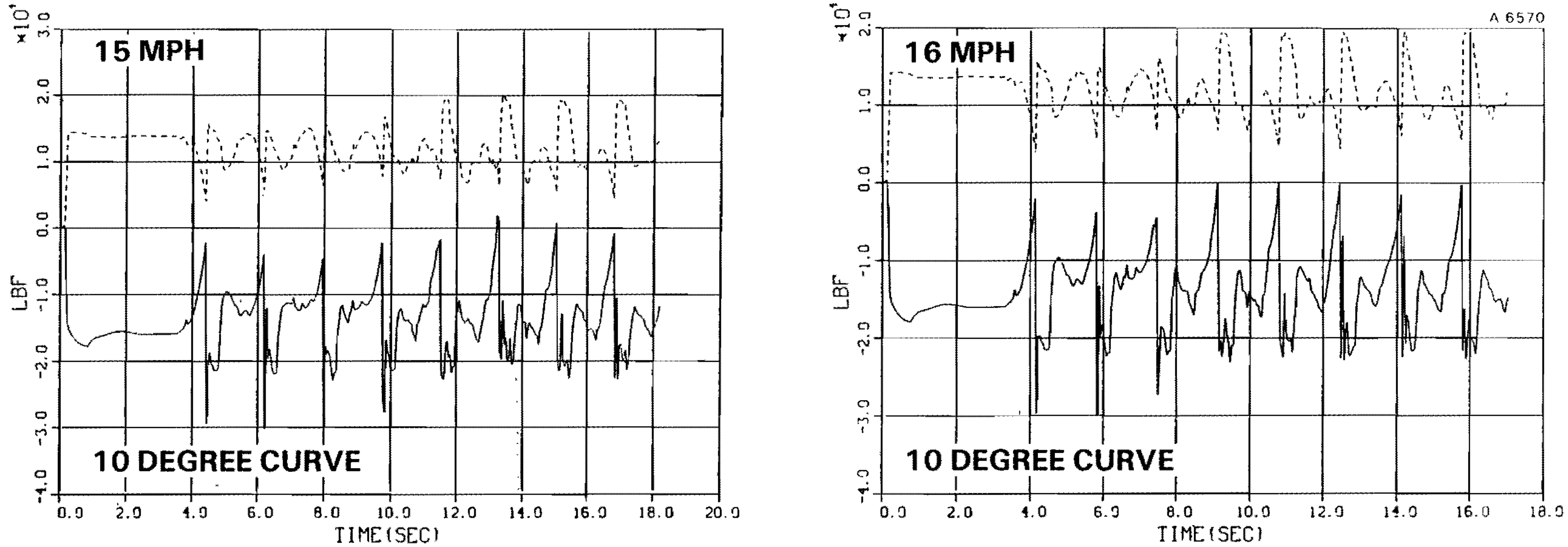

a) Lat. Cusp 1.25 in.

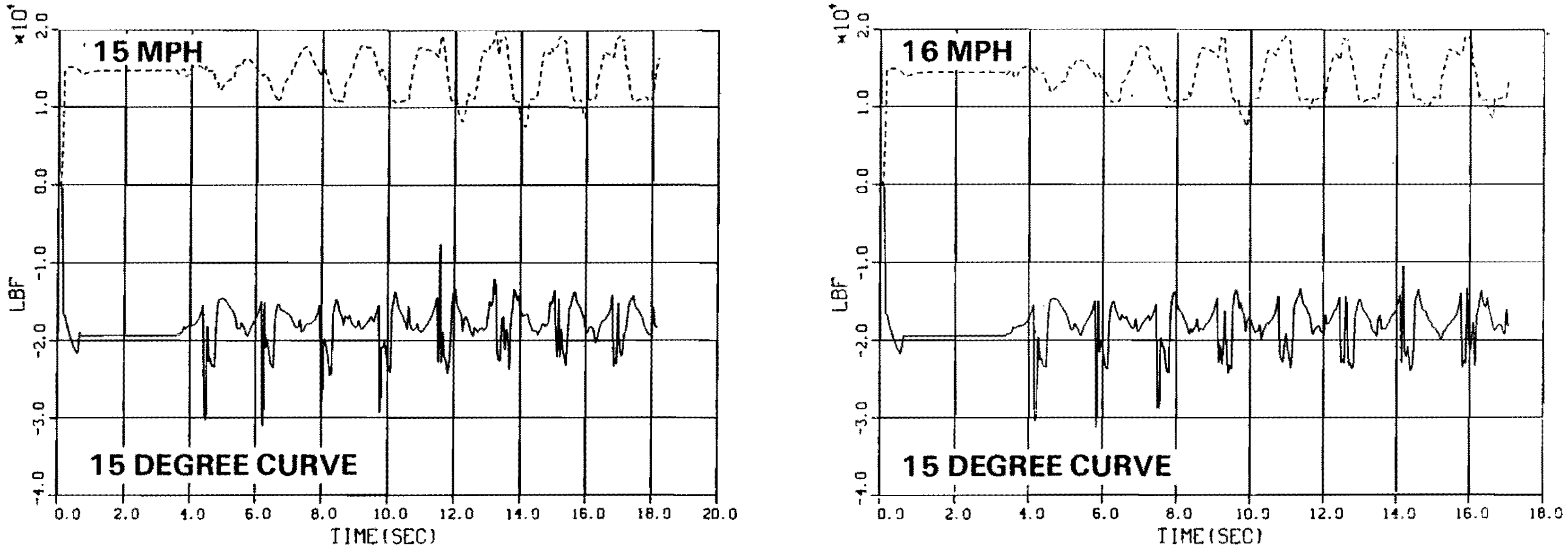

b) Lat. Cusp 1.0 in.

Figure 3.2-21 Lateral Forces on Leading Wheels (Response to Crosslevel and Gage Variation, Crosslevel Variation 1/2 in.)

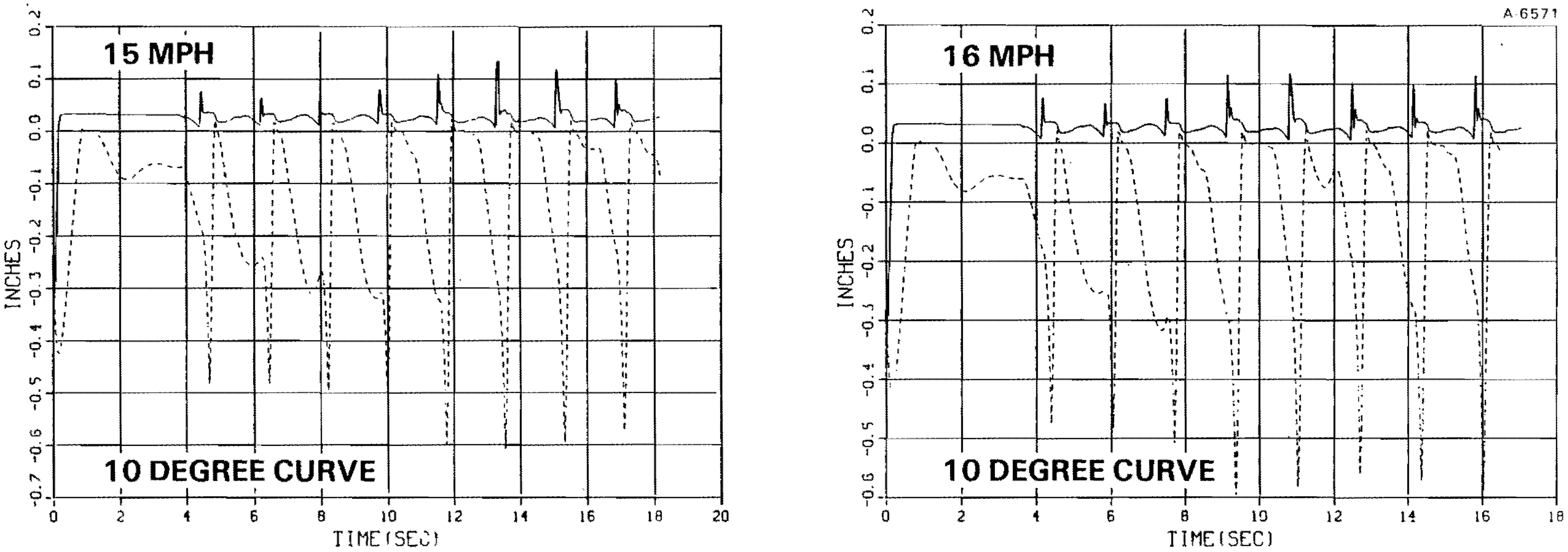

a) Lat. Cusp 1.25 in.

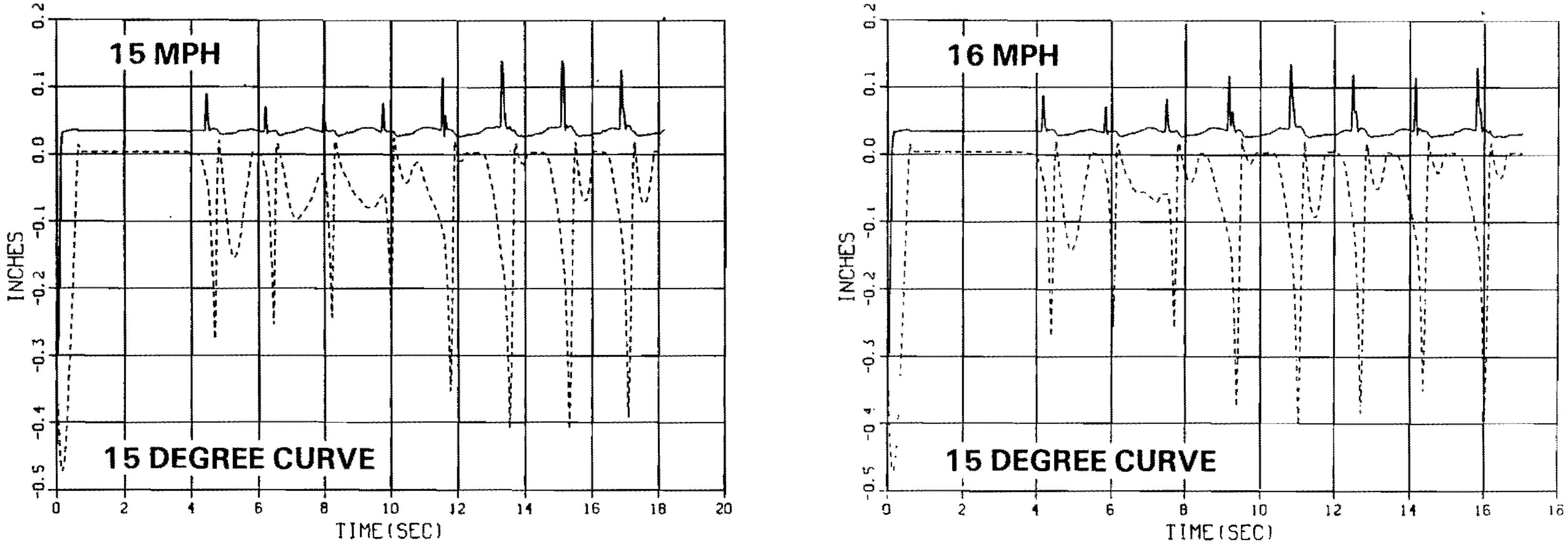

b) Lat. Cusp 1.0 in.

Figure 3.2-22 Wheel Climb Tendency (Response to Crosslevel and Gage Variation, Crosslevel Variation 1/2 in.)

TABLE 3.3-1
LIMITING VALUES OF ALIGNMENT AMPLITUDE
WHEEL DROP AT LOW SPEED ON TANGENT TRACK
HAVING A MINIMUM RESTRAINT CAPABILITY

WAVELENGTH, ft	PEAK/PEAK AMPLITUDE, in.
39	1.375
50	1.25
75	3.50
90	4.50

high lateral force levels. It is caused by the flanging wheel climbing beyond initial flange contact and permitting the non-flanging wheel to move across its rail head further, reducing DISTDROP.

The majority of the curving results discussed in this section are taken at balance speed. The change in lateral force resulting from different track elevation in curves is due to a transfer of vertical axle load between wheels. Figure 3.3-6 shows this effect for the loaded hopper at 25 mph in curves having a balance speed of 25 mph and 15 mph, respectively. The latter result at overbalance (a speed greater than balance) shows the separation of the curves of vertical force on inner and outer wheels. However, the curves of L/V on the low rail are almost identical and show a value near $\mu = 0.5$ for this saturated tight (15 degree) curving condition. Thus, the lateral force on the low rail is reduced, providing an apparent reduction in the tendency to gage spreading on this rail in the overbalance case. Figure 3.3-7, for the same conditions, shows little difference in the lateral force on the outer wheel but an apparent reduced tendency to wheel drop due to this reduction in force on the low wheel in the overbalanced condition (track superelevation 2.3 in.). It is felt that this exaggerates the result since the rail restraint curve does not reflect the additional lateral stiffness under increased vertical load. The results at balance speed are chosen to be representative of the worst conditions on track having a minimum restraint capability.

In curvatures of five degrees and above, the wheelset tends to follow the outer rail and cannot exhibit the flange-free path of tangent track previously shown in Fig. 3.3-2 even for wide gage (57.75 in.). Figure 3.3-8 shows the path of the leading wheelset in five, ten and 15 degree curves at a gage of 57.75 in. and sinusoidal alignment peak/peak amplitude of 1 in. Only the five degree curves shows periods of flange-free curving. All results are run at a balance speed of 25 mph. The wavelength for this illustration is 39 ft. The tendency to wheel drop is shown in Fig. 3.3-9 for the same conditions. As the curvature increases, the lateral force on the leading outer wheel also increases. However, the lateral force on the inner wheel decreases. This is due primarily to the increase in longitudinal force between the wheel and rail in the tighter curves which rotates the saturated (full slip) contact force more towards the longitudinal than lateral direction giving rise to a smaller lateral component. However, this reduction in inner wheel lateral force and its effect on the rail restraint curve are insufficient to compensate for the larger outer wheel force and hence the tendency to wheel drop is greater in the tighter curves.

The effect of curvature is seen more directly in Figs. 3.3-10 and 3.3-11, which plot the peak individual and the sum of the gage spreading lateral forces in zero, five, ten and 15 degree curves. Both show the increase in lateral force with curvature for a fixed gage of 57.75 in. It has been previously shown in Ref. 4 that the value of 34.5 kips for the sum of the gage spreading outward forces on both rails represents a limit to prevent a gage of 57.75 in. from spreading sufficiently to cause incipient wheel drop. Using this limiting value it may be seen that peak/peak sinusoidal amplitudes of 1.375 in., which do not lead to wheel drop on tangent track, must be reduced for curvatures of five degrees to 1.0 in. and for curvatures of ten degrees to 0.75 in. to prevent incipient wheel drop for the gage of 57.75 in.

The value of the gage is again shown to be of primary importance in this scenario. An increase in DISTDROP, the computed drop, is identical to the decrease in gage. For track with a minimum restraint capability, this represents an equivalent change in single wheel lateral force, at the wheel drop limit, of 15 kips for every inch. Thus, a reduction in gage of 0.25 in. permits an increase in force of just under four kips without causing a wheel drop derailment prediction. At the larger forces in tighter curves this becomes important and gages of both 57.75 in and 57.5 in were investigated in ten and 15 degree curves.

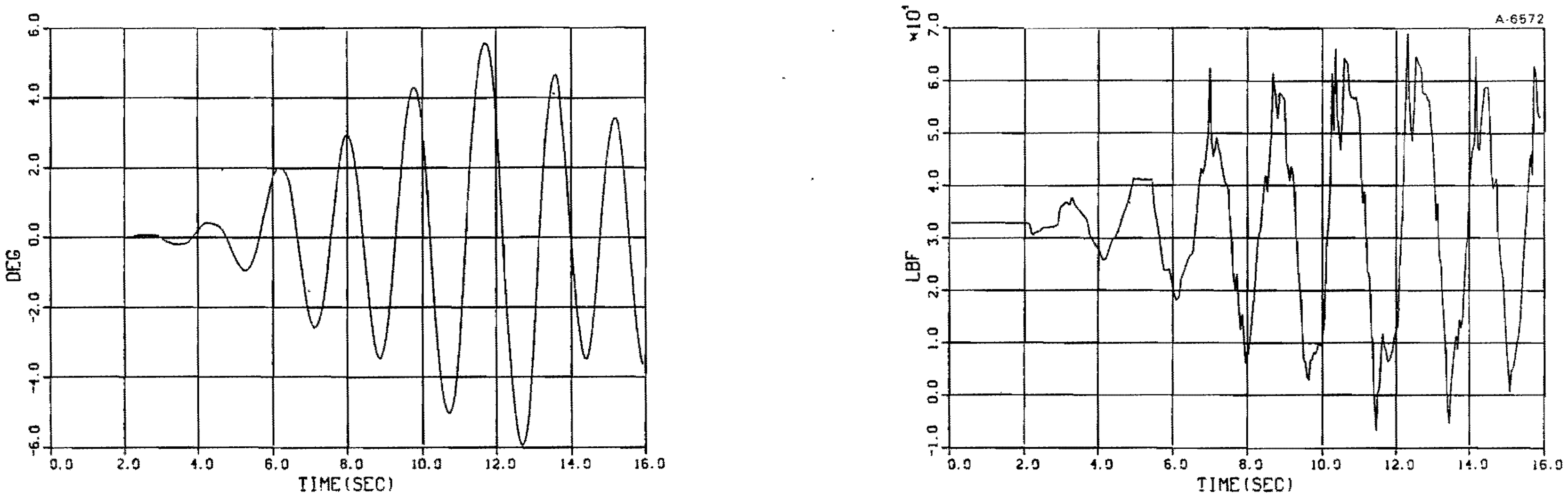

a) Body Roll Angle

b) Vertical Force on Right Wheel

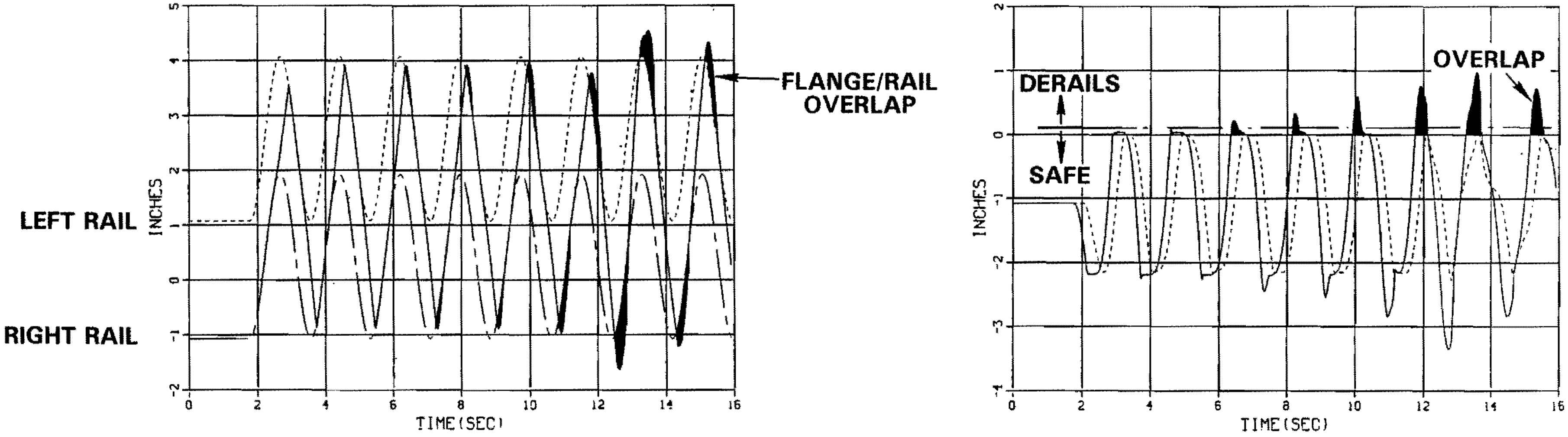

c) Lateral Motion of Axle 1 Within Track Clearance

d) Motion of Axles 1 and 2 Beyond Track Clearance

Figure 3.3-1 Severe Roll Response from 3 in. Peak/Peak Alignment Variation (15 mph/Tangent Track/Wavelength 39 ft/Gage 58.0 in.)

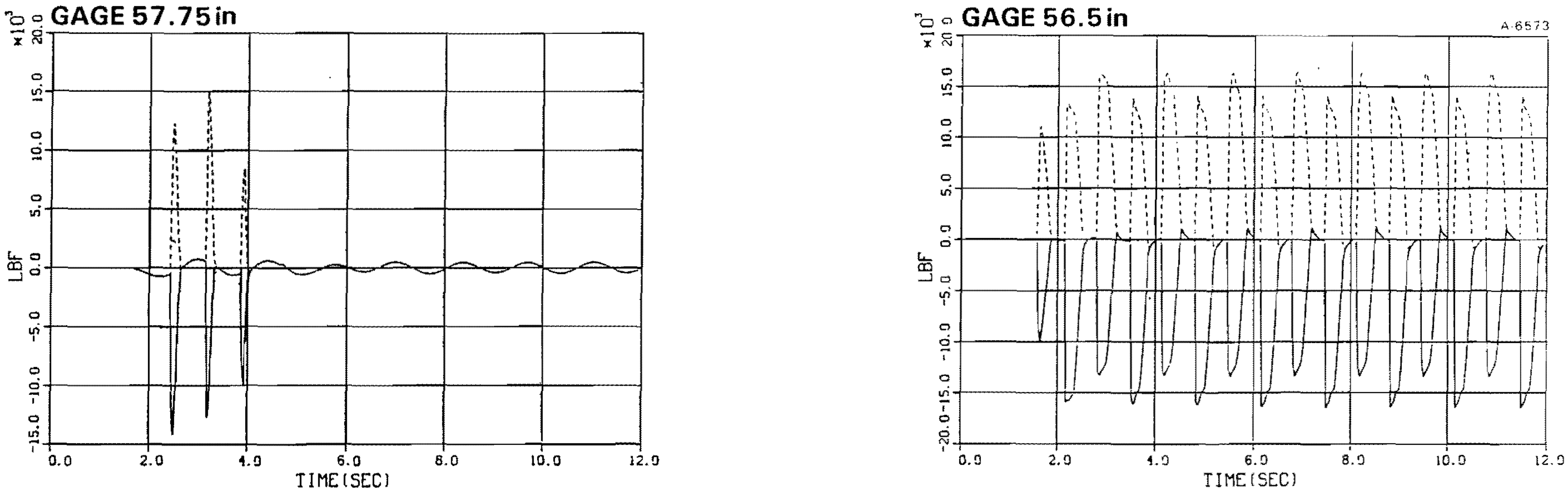

a) Lateral Forces on Axle 1

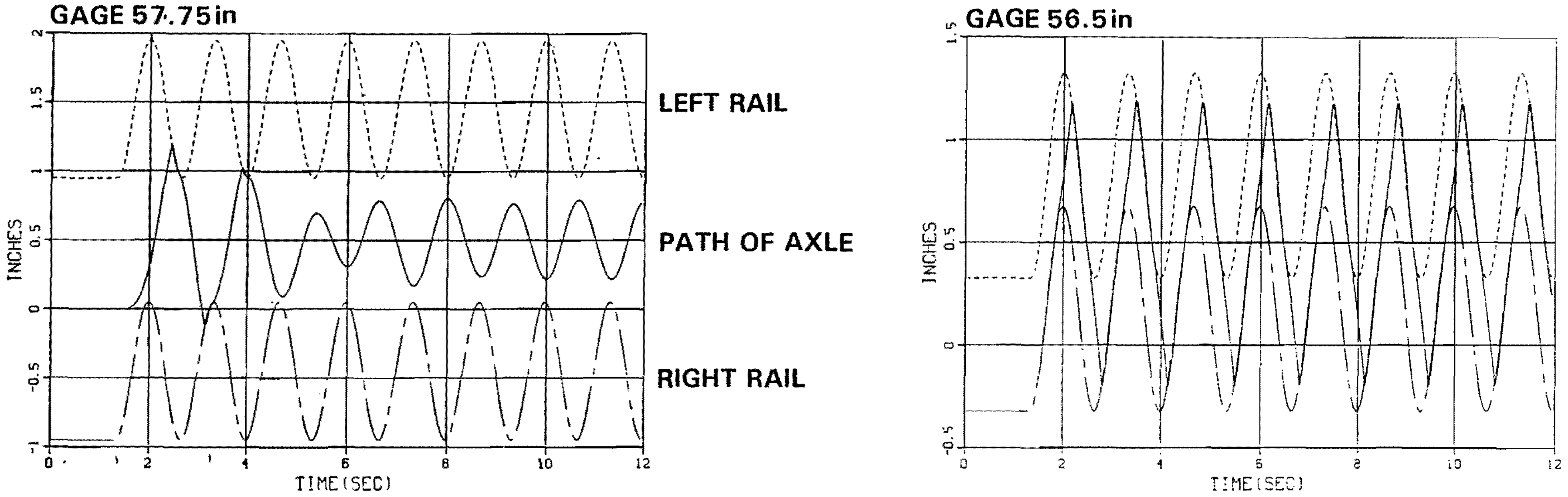

b) Lateral Motion of Axle 1

Figure 3.3-2 Response to Sinusoidal Alignment with Varying Gage (Tangent Track/Amplitude 3 in. Peak/Peak/Wavelength 39 ft/Speed 20 mph.)

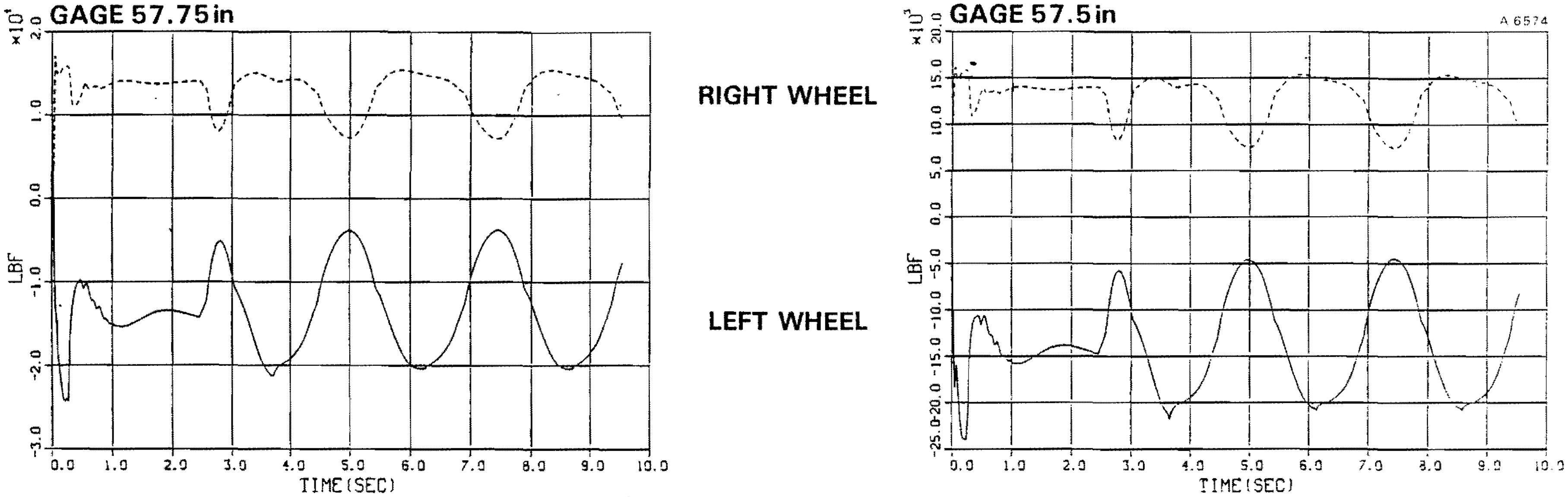

a) Lateral Forces on Axle 1

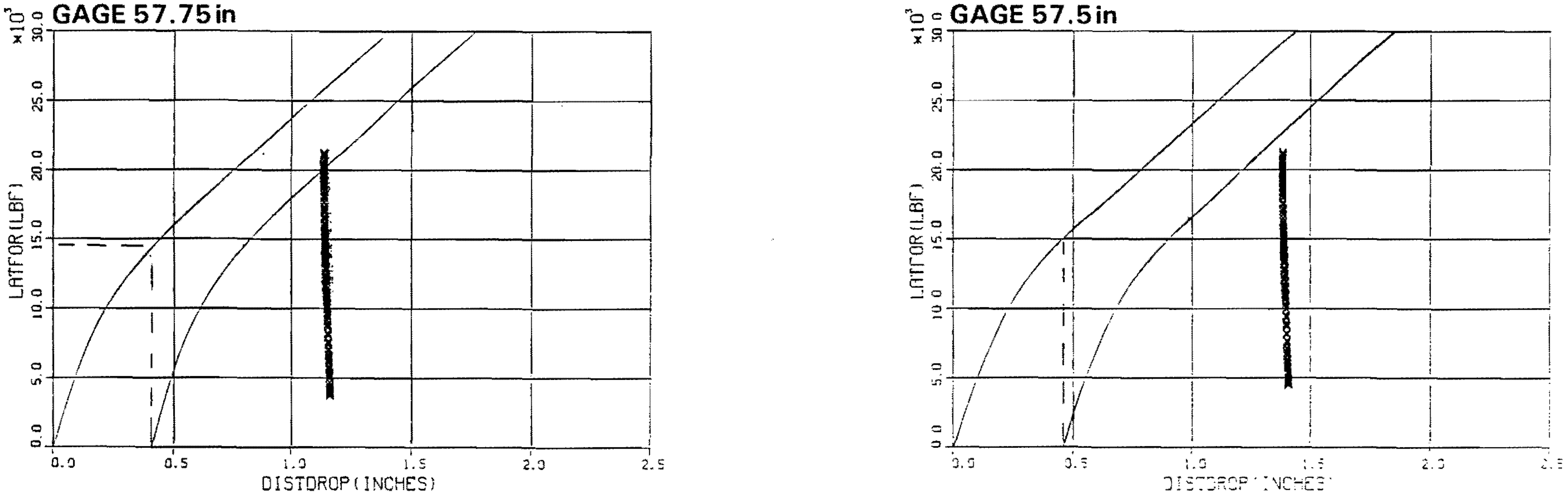

b) Wheel Drop Tendency on Axle 1

Figure 3.3-3 Response to Sinusoidal Alignment with Wide Gage (10 Degree Curve/Amplitude 4.5 in Peak/Peak/Wavelength 90 ft/Speed 25 mph at Balance)

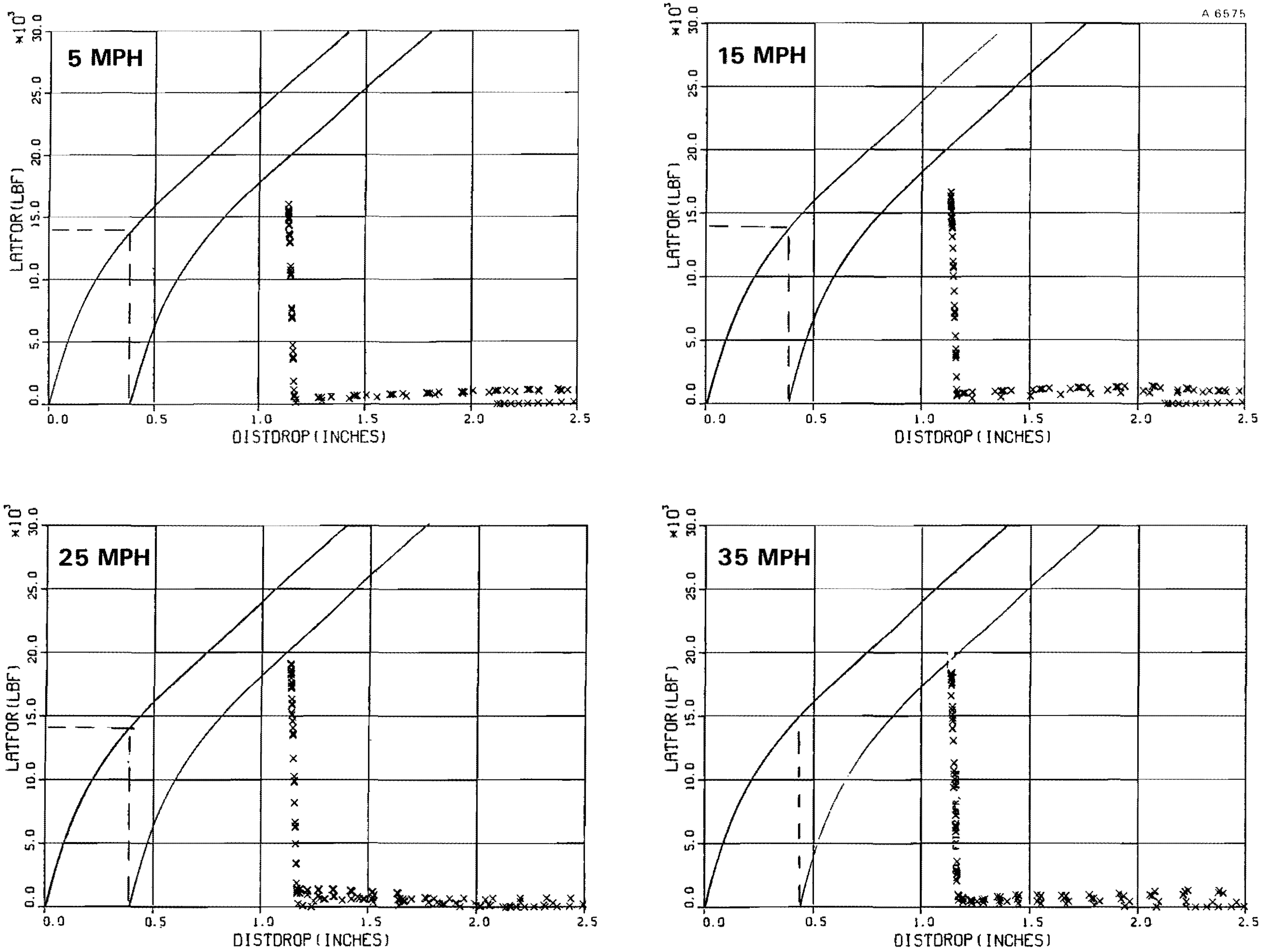

Figure 3.3-4 Variation in Wheel Drop Tendency with Speed (Tangent Track/ Amplitude 1.125 in. Peak/Peak/Wavelength 50 ft/Gage 57.75 in.)

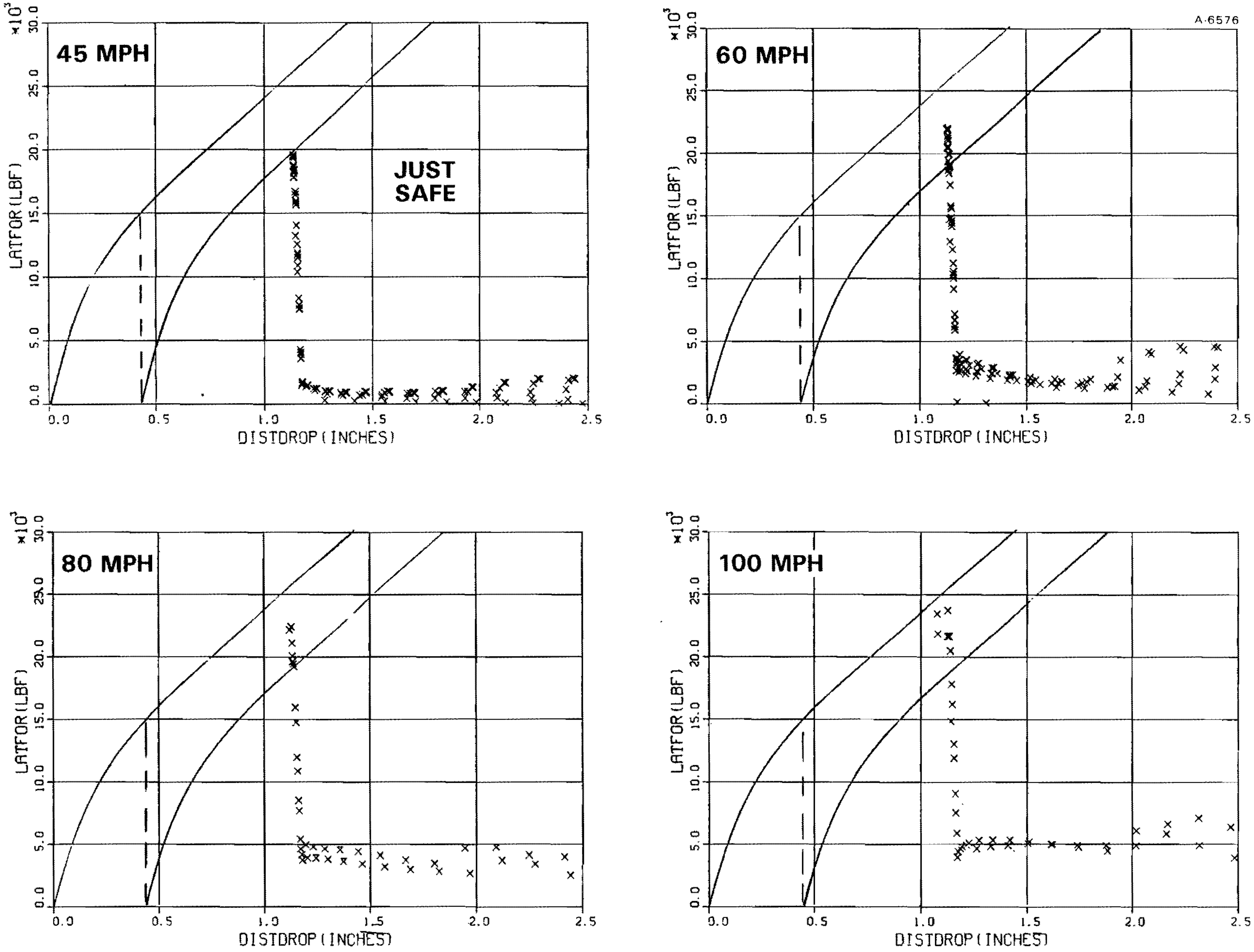

Figure 3.3-5 Variation in Wheel Drop Tendency with Speed (Tangent Track/Amplitude 1.125 in. Peak/Peak/Wavelength 50 ft/Gage 57.75 in.)

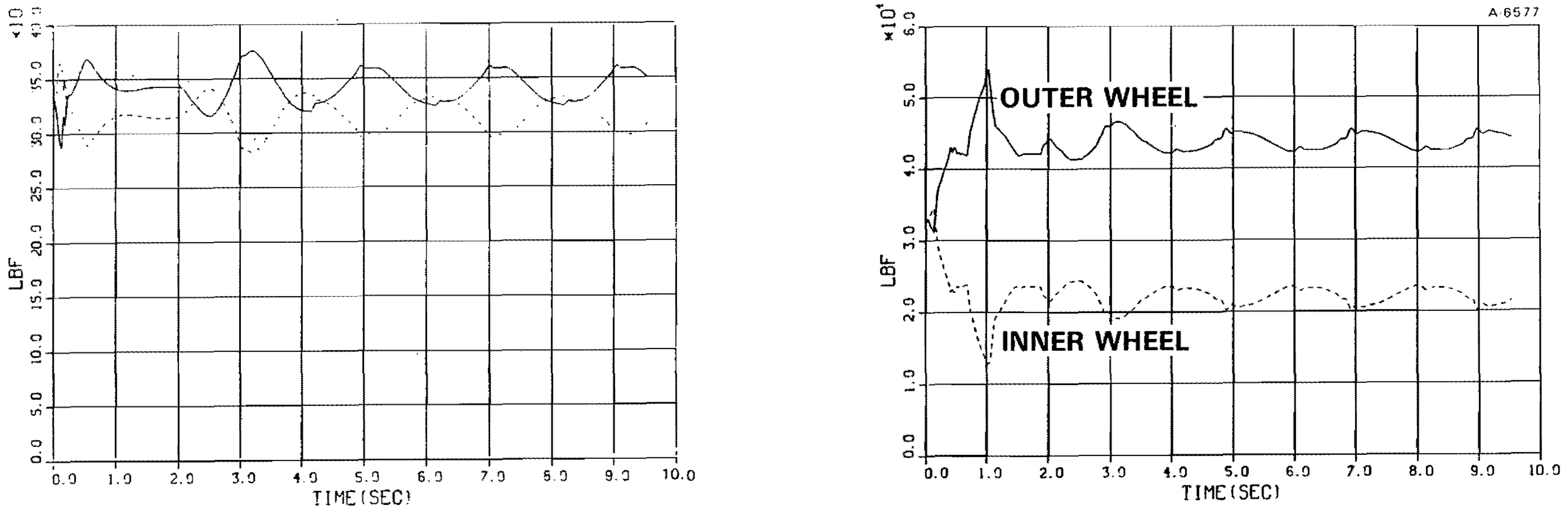

a) Vertical Force on Leading Axle (Track Superelevation 6.342 in., Balance Speed 25 mph)

b) Vertical Force on Leading Axle (Track Superelevation 2.283 in., Balance Speed 15 mph)

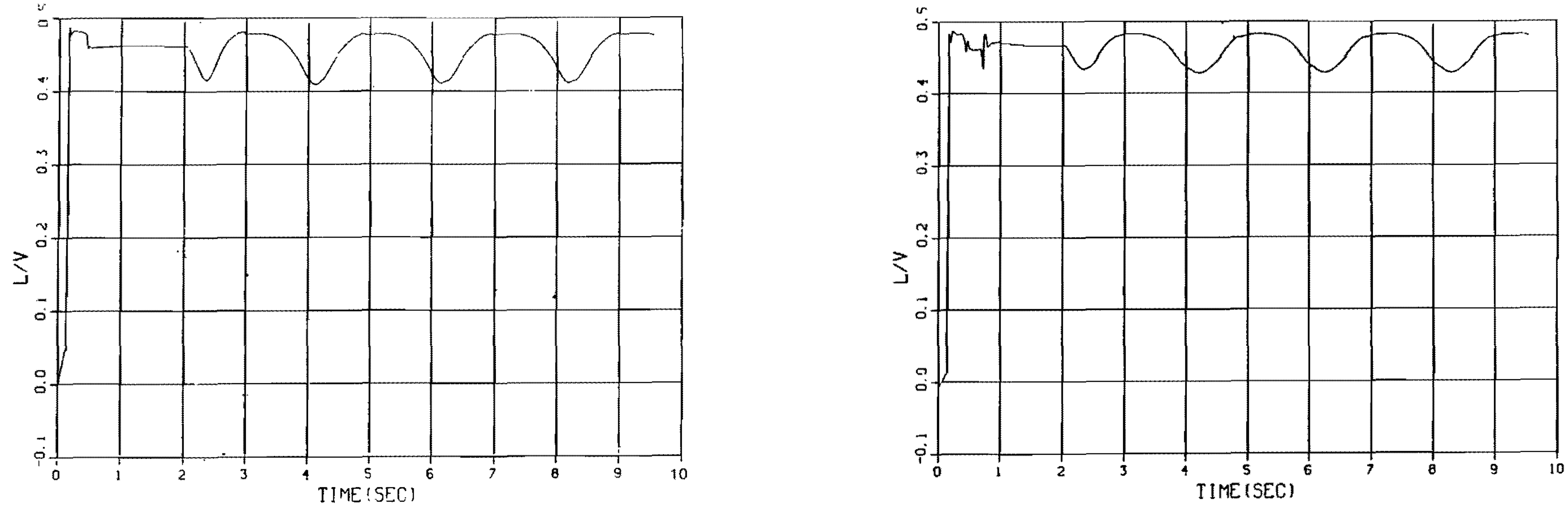

c) L/V Ratio (Track Superelevation 6.342 in., Balance Speed 25 mph)

d) L/V Ratio (Track Superelevation 2.283 in., Balance Speed 15 mph)

Figure 3.3-6 Variation in Vertical Force Due to Unbalance (15 Deg Curve/ Amplitude 3 in. Peak/Peak/Wavelength 75 ft/Run Speed 25 mph)

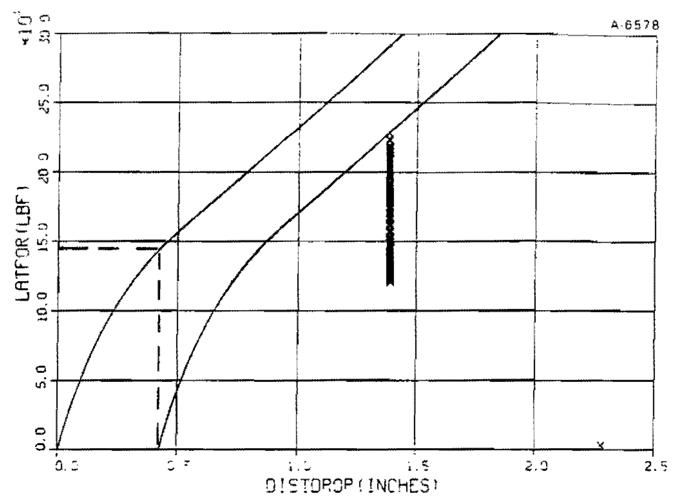

a) Track Superelevation 6.342 in., Balance Speed 25 mph

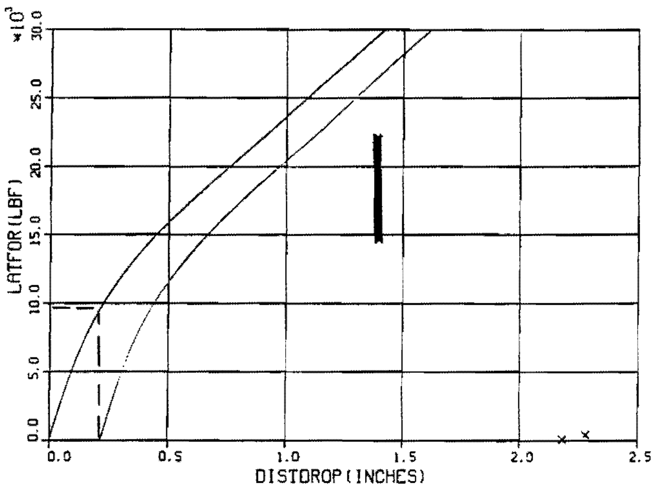

b) Track Superelevation 2.283 in., Balance Speed 15 mph

Figure 3.3-7 Effect of Unbalance on Wheel Drop Tendency (15 deg Curve/Amplitude 3 in. Peak/Peak/Wavelength 75 ft/Run Speed 25 mph)

The process by which the prediction of a limiting value of sinusoidal alignment peak/peak amplitude has been identified is given in Figs. 3.3-12 and 3.3-13. The lateral forces of Fig. 3.3-12 are reviewed to find the maximum value for the outer wheel and the simultaneous value for the inner wheel. The outer wheel lateral force is also a computer plotted output on the curves of Fig. 3.3-13. Added to this plot are the rail restraint curves, first for the inner wheel and with the knowledge of its lateral force, for the outer wheel. The runs were generally carried out by decreasing an alignment peak/peak amplitude until a case was found for which the wheel drop limit was not exceeded. In Fig. 3.3-11, this amplitude is seen to be 2.25 in.

The limiting sinusoidal alignment peak/peak amplitudes for which incipient wheel drop derailment is not predicted on track having a minimum restraint capability in the low speed regime for a 100 ton hopper car are presented in Figs. 3.3-14 through 3.3-19. Each figure shows the results for wavelengths of 39 ft, 50 ft, 75 ft, and 90 ft, selected to indicate the range of long wavelength alignment variations found in real track. Figures 3.3-14 through 3.3-17 are for tangent, five degree, ten degree and 15 degree curves at a gage of 57.75 in. Figures 3.3-18 and 3.3-19 are for ten degree and 15 degree curves at a gage of 57.5 in. From the figures it can be seen that the value of 4.5 in for the 90 ft wavelength is slightly below the computed limit for zero degree and five degree curves and 57.75 in. gage and for the ten degree curve and 57.5 in. gage. However, no larger values were considered necessary as part of this investigation on limits to track geometry specification. The reduction of track gage from 57.75 in. to 57.5 in. for curves of ten and 15 degrees is consistent with that found previously in runs with combined cross-level and gage variation. In particular, the tolerances the results suggest for the individual lateral rail alignment at the larger gage of 57.75 in. appear to be too restrictive for practical implementation although both gages were run and their results given.

The results for tangent track were used as the basis for planning the sinusoidal alignment variation tests at Bennington, New Hampshire, carried out in July and August 1982.

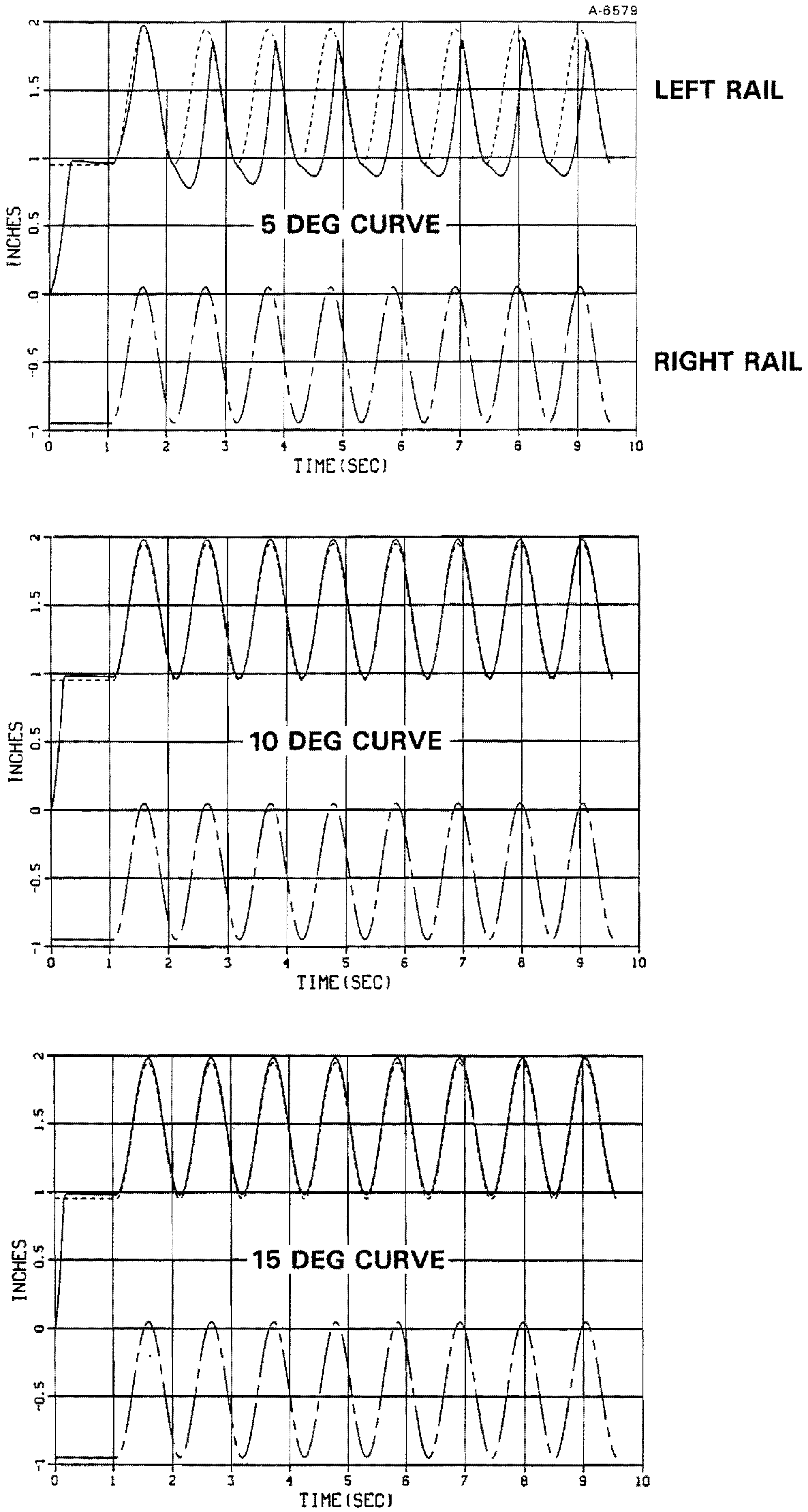

Figure 3.3-8 Lateral Motion of First Axle in Curves with Sinusoidal Alignment Variation (Amplitude 1 in. Peak/Peak/Wavelength 39 ft/Speed 25 mph at Balance/Gage 57.75 in.)

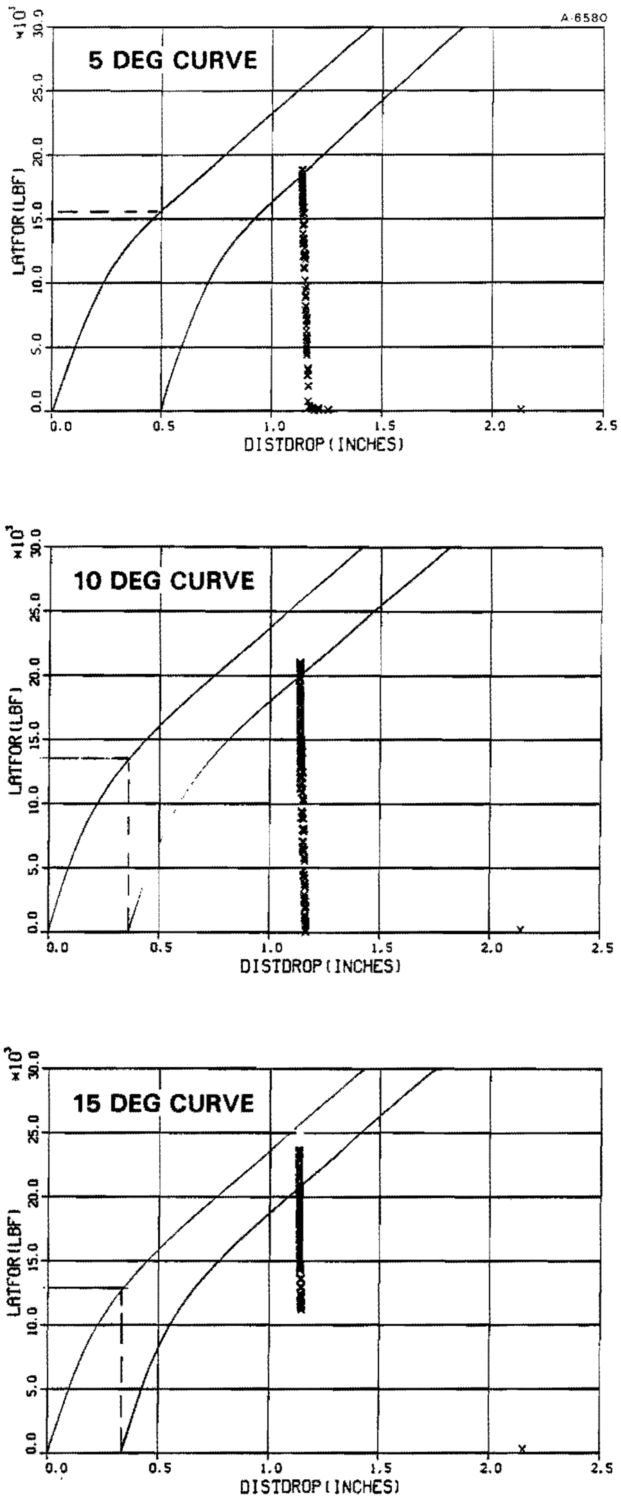

Figure 3.3-9 Wheel Drop Tendency of First Axle in Curves with Sinusoidal Alignment Variation (Amplitude 1 in. Peak/Peak/ Wavelength 39 ft/Speed 25 mph at Balance/Gage 57.75 in.)

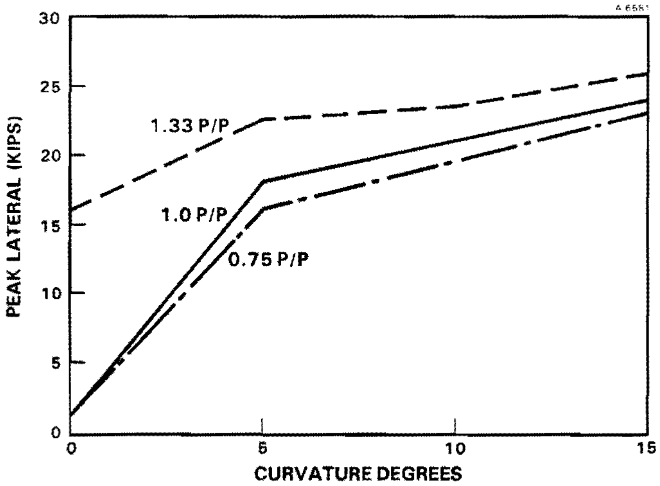

Figure 3.3-10 Lead Outer Wheel Peak Lateral Force with Increasing Curvature

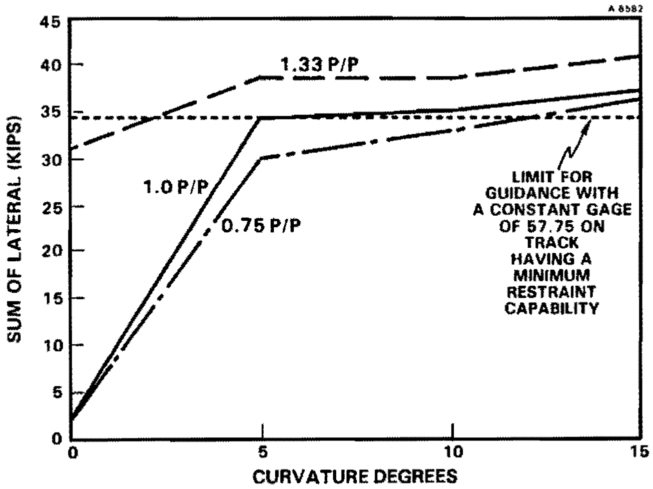

Figure 3.3-11 Maximum Combined Gage Spreading Force with Increasing Curvature

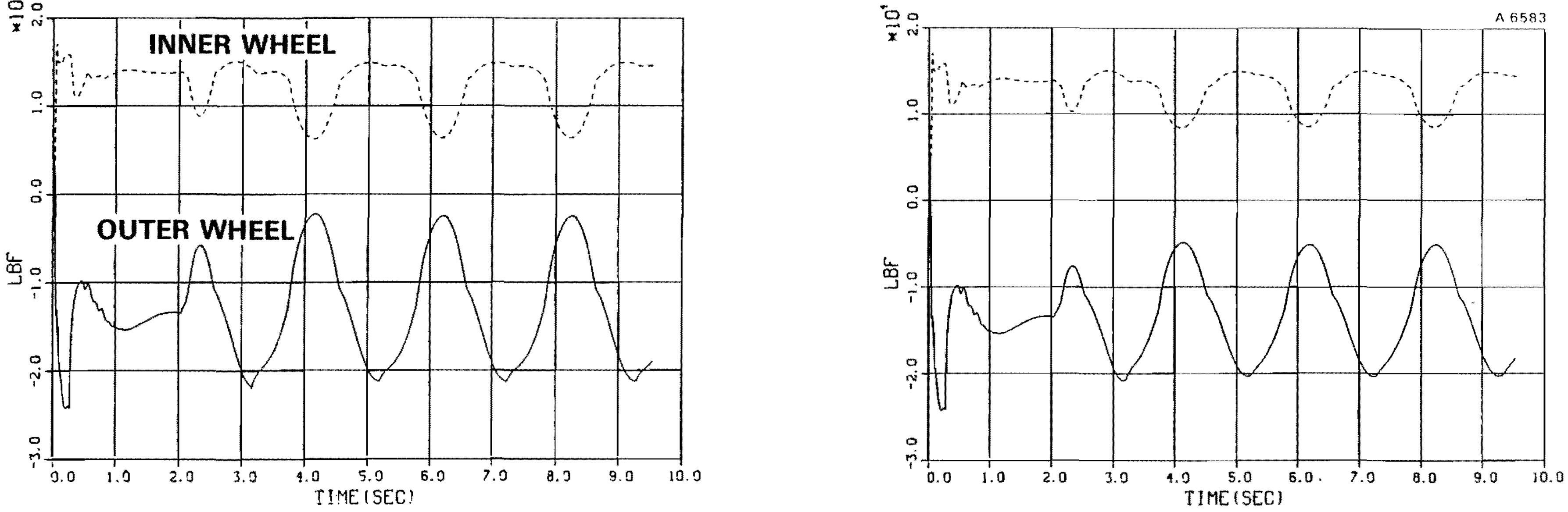

a) 3.25 in. Peak/Peak Amplitude

b) 2.7 in. Peak/Peak Amplitude

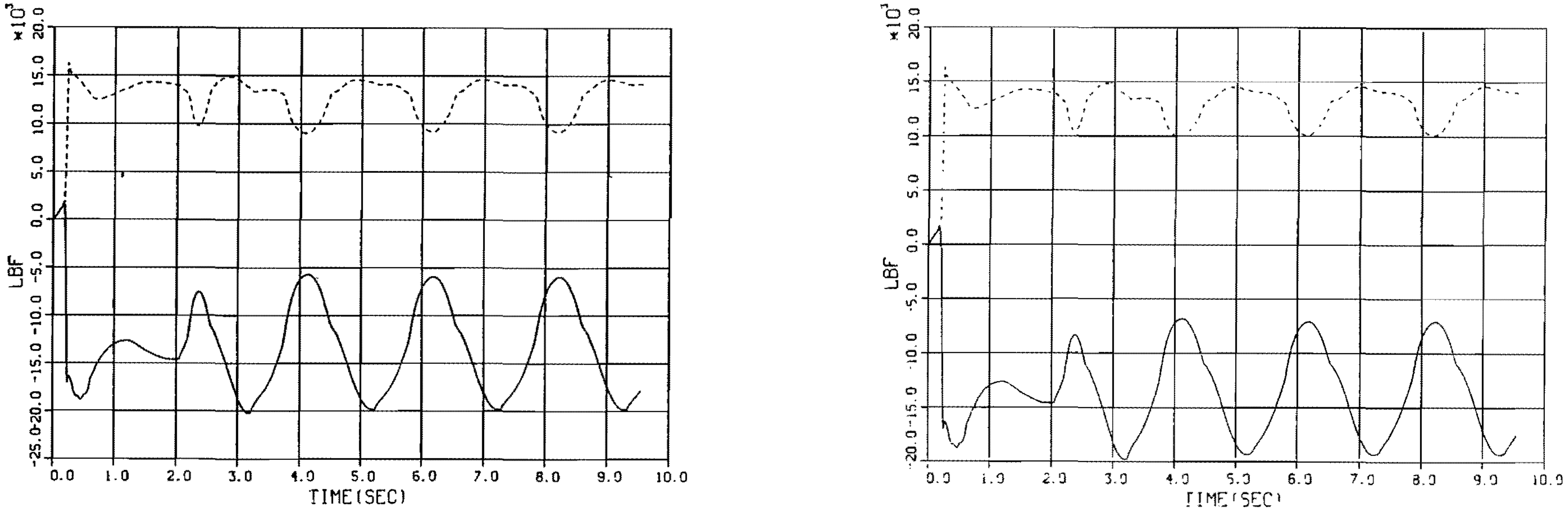

c) 2.5 in. Peak/Peak Amplitude

d) 2.25 in. Peak/Peak Amplitude

Figure 3.3-12 Variation of Lateral Force on First Axle with Amplitude of Sinusoidal Alignment (10 deg Curve/75 ft Wavelength/25mph at Balance/Gage 57.75 in.)

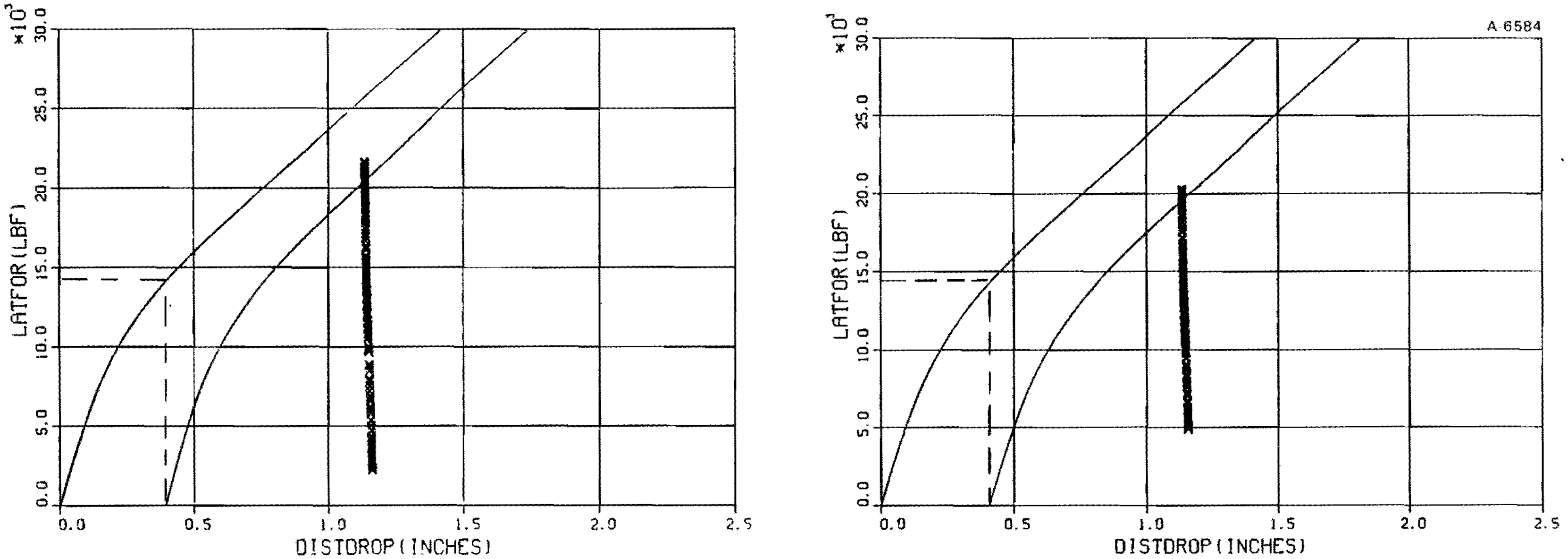

a) 3.25 in. Peak/Peak Amplitude

b) 2.7 in. Peak/Peak Amplitude

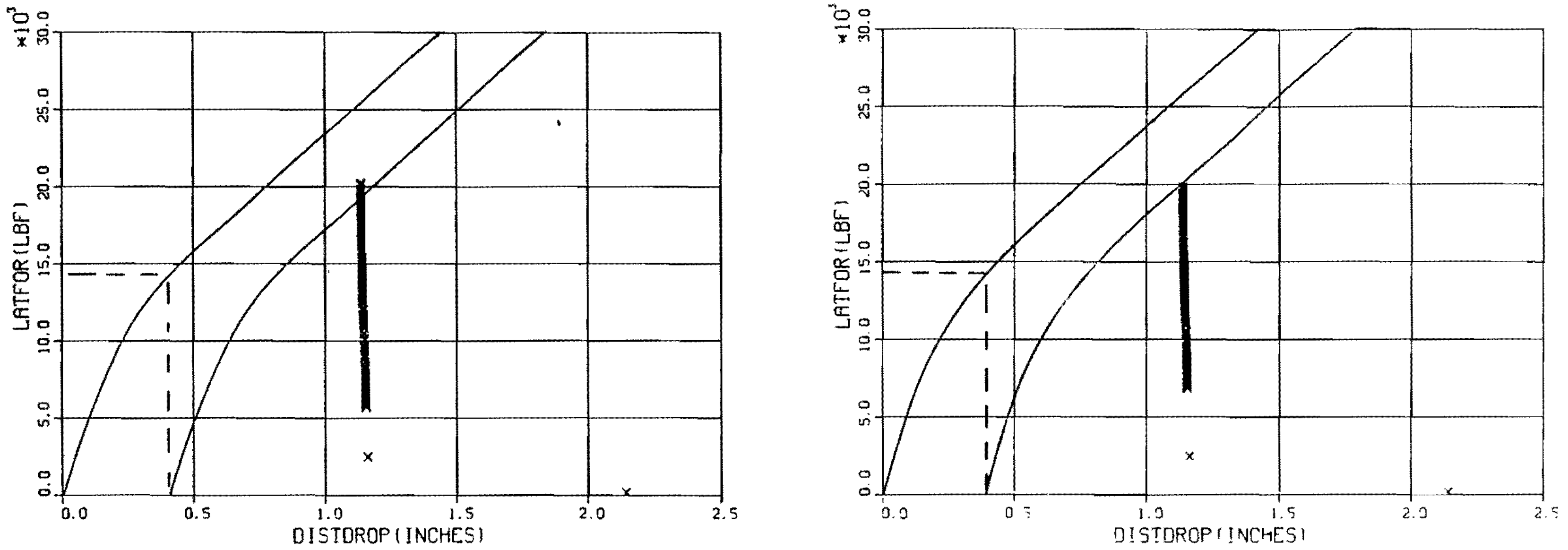

c) 2.5 in. Peak/Peak Amplitude

d) 2.25 in. Peak/Peak Amplitude

Figure 3.3-13 Wheel Drop Tendency on First Axle with Amplitude of Sinusoidal Alignment (10 deg Curve/75 ft Wavelength/25 mph at Balance/Gage 57.75 in.)

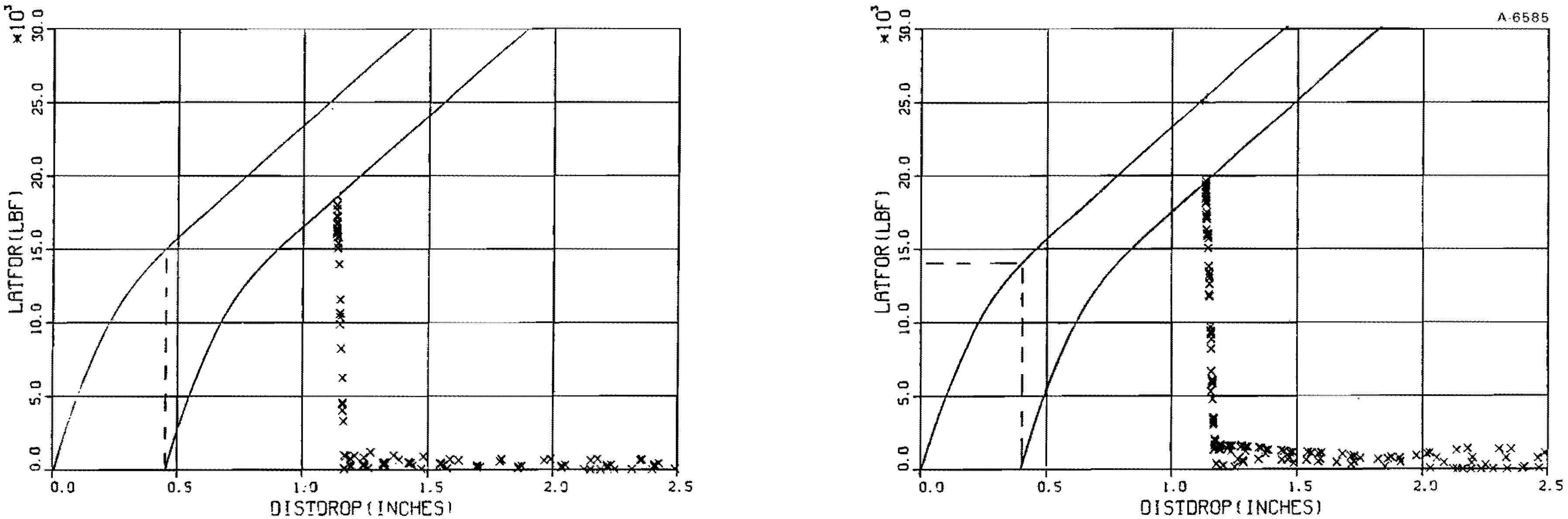

a) Wavelength 39 ft,
Amplitude 1.375 in. Peak/Peak

b) Wavelength 50 ft,
Amplitude 1.25 in. Peak/Peak

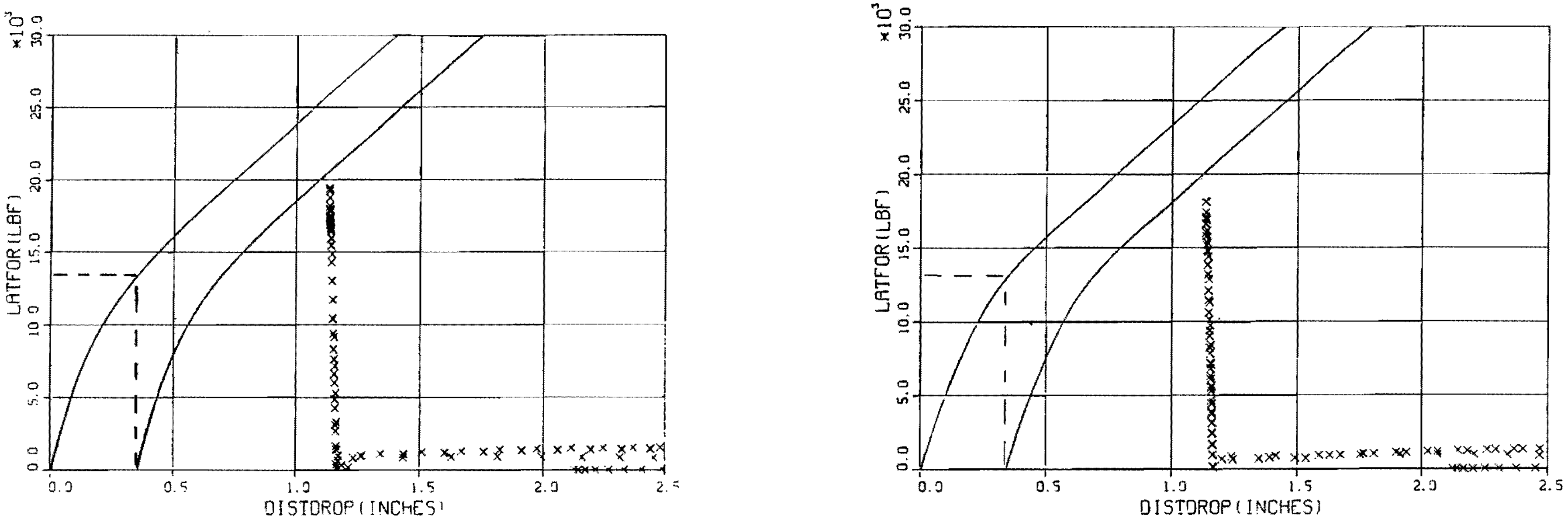

c) Wavelength 75 ft,
Amplitude 3.5 in. Peak/Peak

d) Wavelength 90 ft,
Amplitude 4.5 in. Peak/Peak

Figure 3.3-14 Limiting Cases for Wheel Drop Avoidance (Tangent Track/ 25 mph at Balance/Gage 57.75 in.)

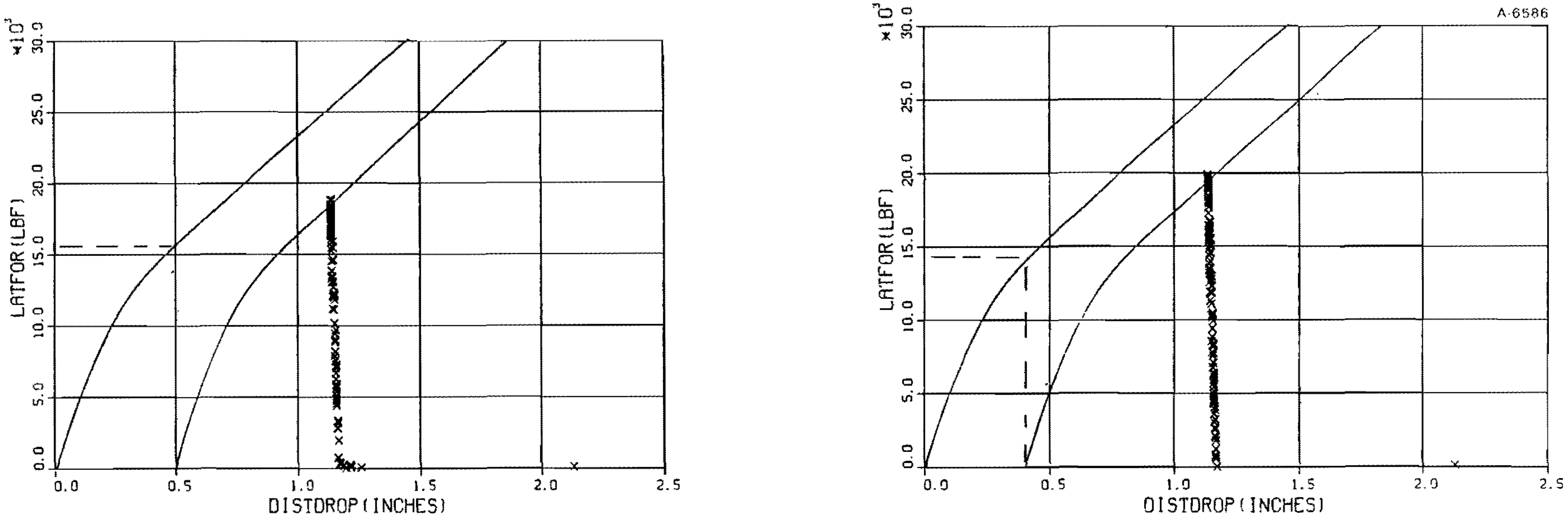

a) Wavelength 39 ft,
Amplitude 1.0 in. Peak/Peak

b) Wavelength 50 ft,
Amplitude 1.25 in. Peak/Peak

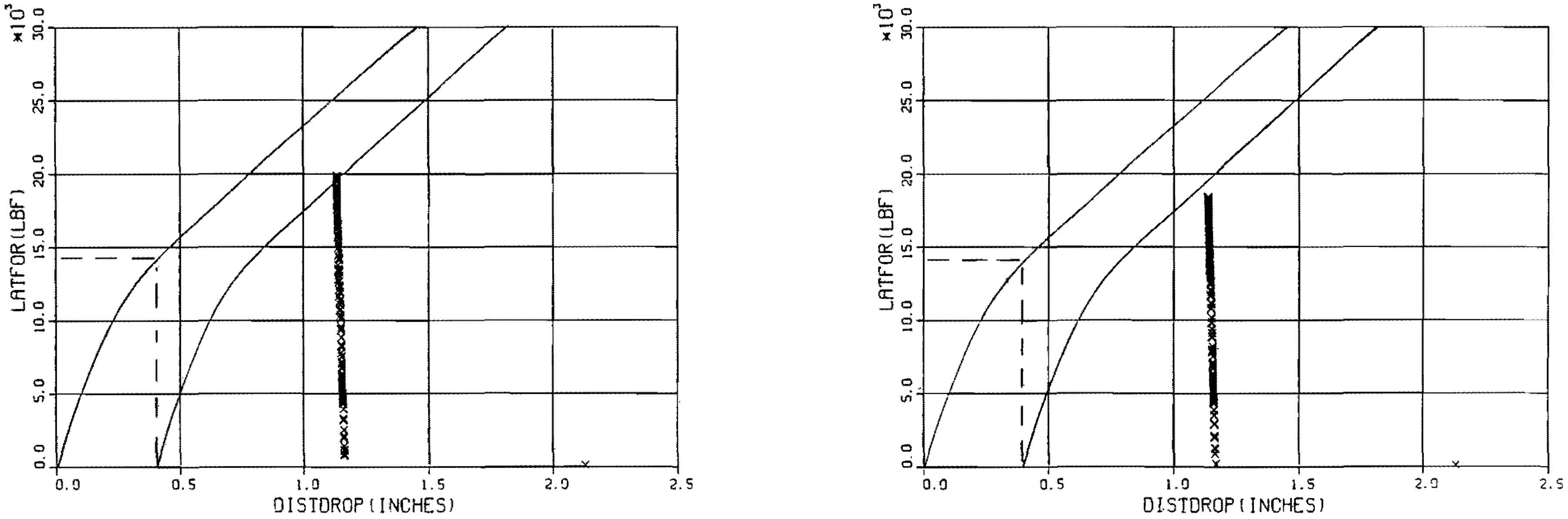

c) Wavelength 75 ft,
Amplitude 3.25 in. Peak/Peak

d) Wavelength 90 ft,
Amplitude 3.5 in. Peak/Peak

Figure 3.3-15 Limiting Cases for Wheel Drop Avoidance (5 deg Curve/
25 mph at Balance/Gage 57.75 in.)

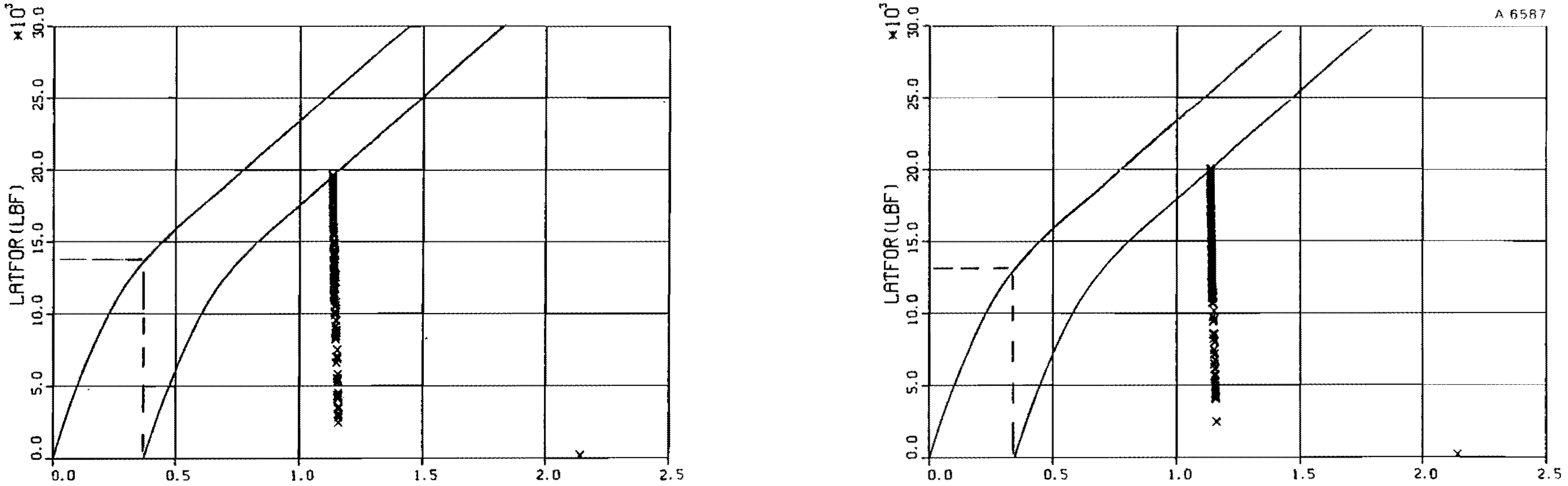

a) Wavelength 39 ft,
Amplitude 0.75 in. Peak/Peak

b) Wavelength 50 ft,
Amplitude 1.0 in. Peak/Peak

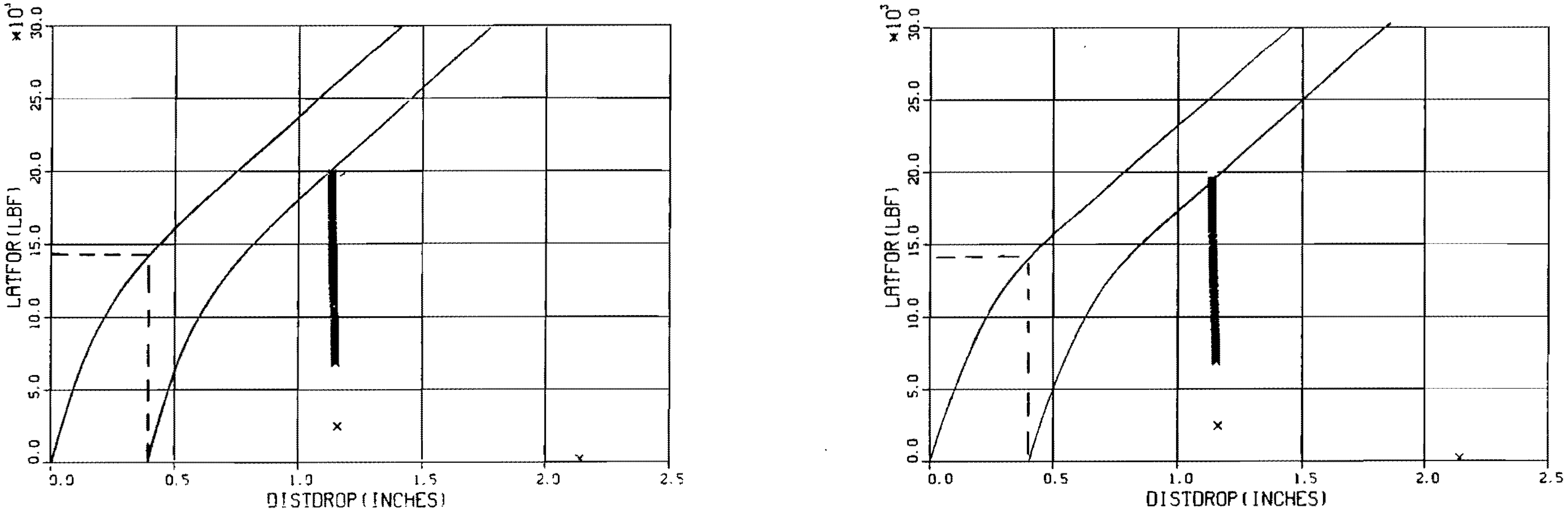

c) Wavelength 75 ft,
Amplitude 2.25 in. Peak/Peak

d) Wavelength 90 ft,
Amplitude 3.5 in. Peak/Peak

Figure 3.3-16 Limiting Cases for Wheel Drop Avoidance (10 deg Curve/
25 mph at Balance/Gage 57.75 in.)

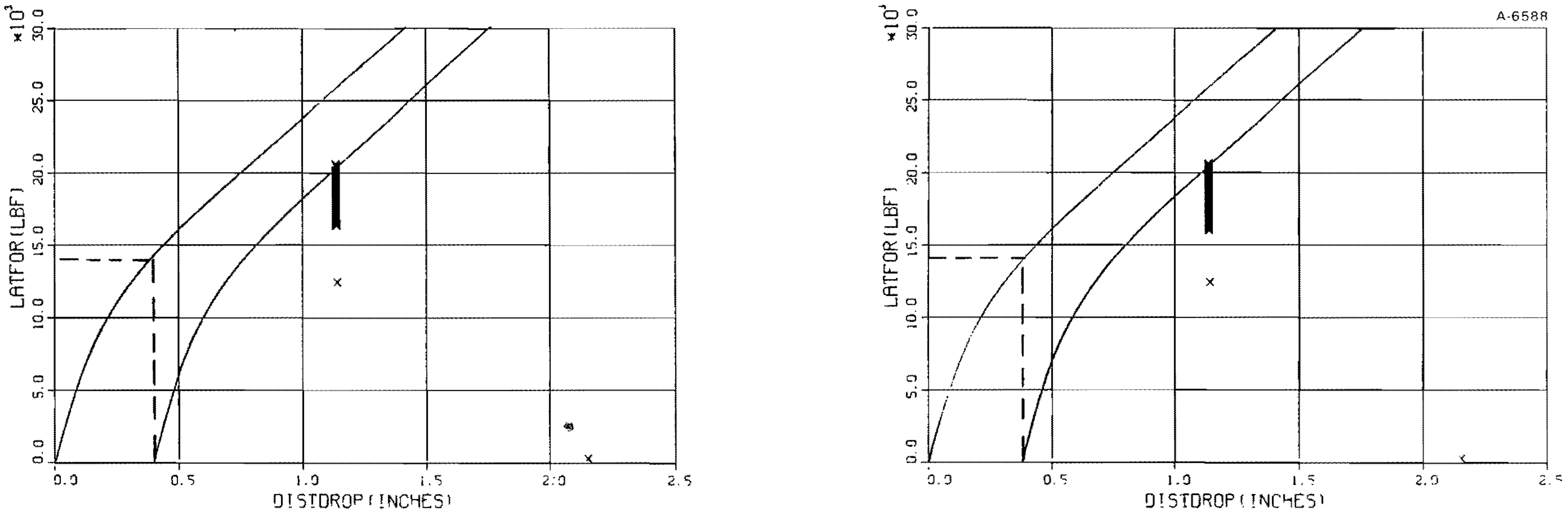

a) Wavelength 39 ft,
Amplitude 0.25 in. Peak/Peak

b) Wavelength 50 ft,
Amplitude 0.375 in. Peak/Peak

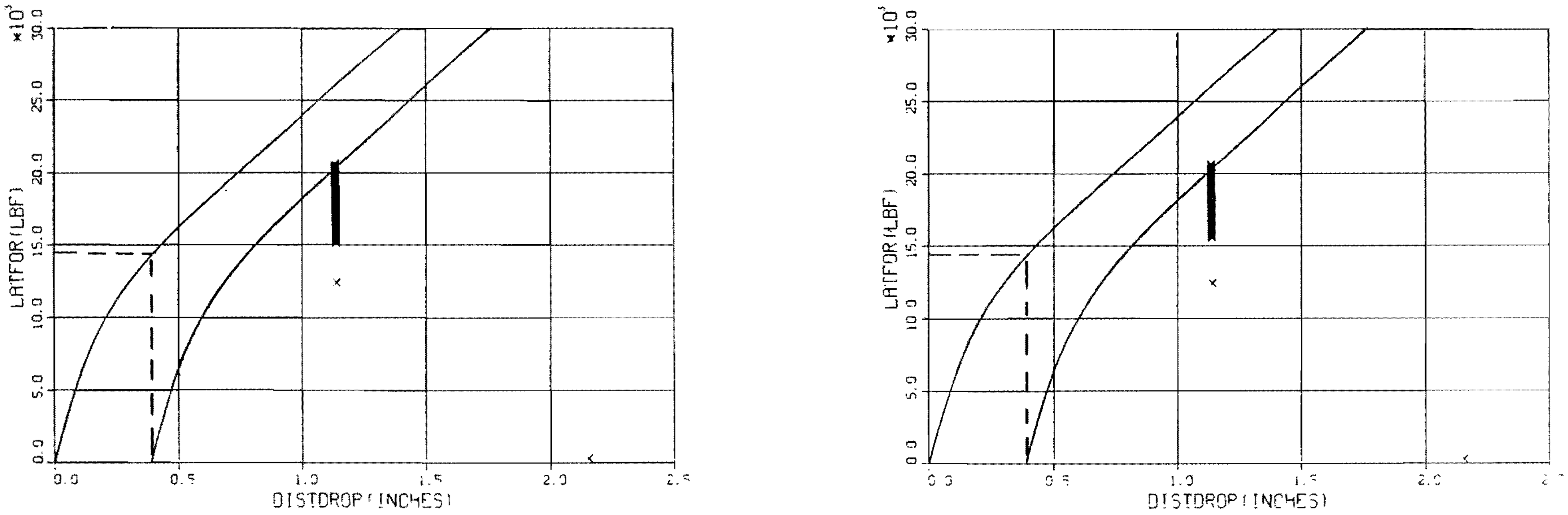

c) Wavelength 75 ft,
Amplitude 1.25 in. Peak/Peak

d) Wavelength 90 ft,
Amplitude 1.75 in. Peak/Peak

Figure 3.3-17 Limiting Cases for Wheel Drop Avoidance (15 deg Curve/
25 mph at Balance/Gage 57.75 in.)

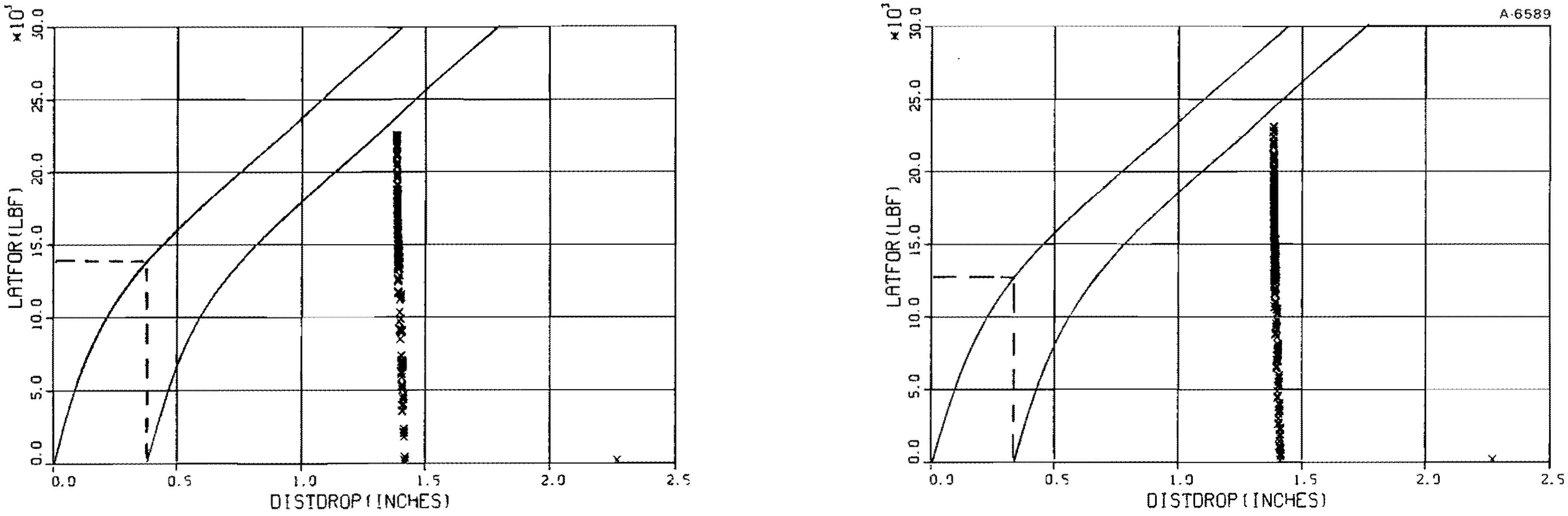

a) Wavelength 39 ft,
Amplitude 1.25 in. Peak/Peak

b) Wavelength 50 ft,
Amplitude 1.75 in. Peak/Peak

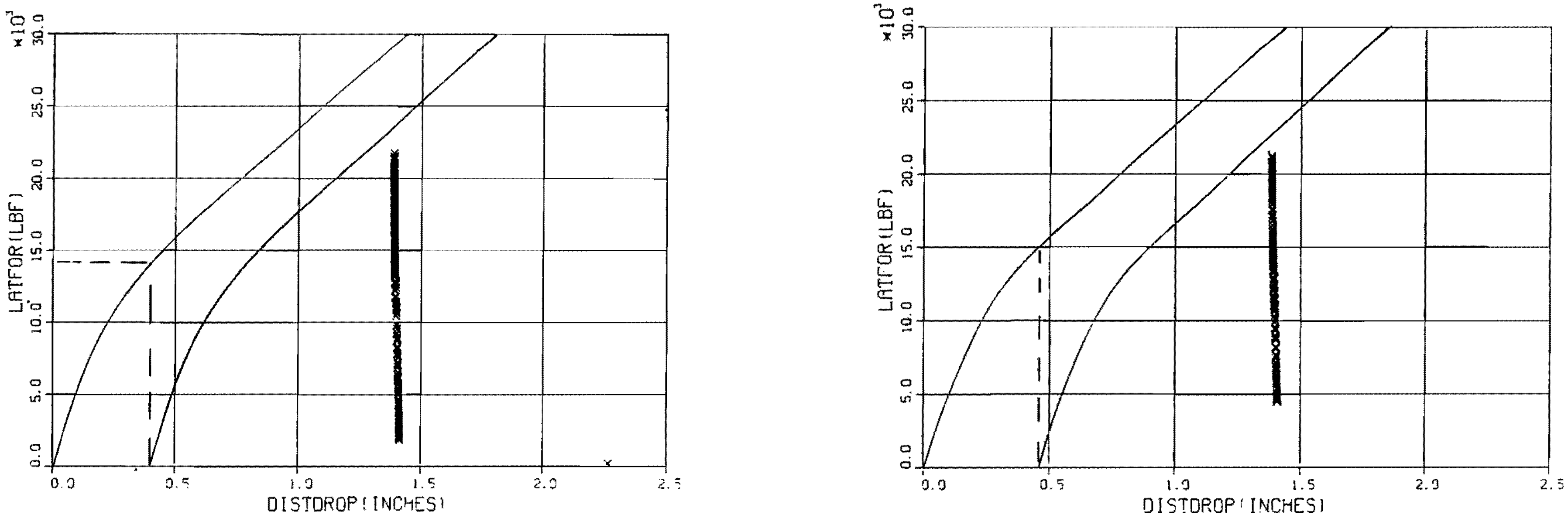

c) Wavelength 75 ft,
Amplitude 3.50 in. Peak/Peak

d) Wavelength 90 ft,
Amplitude 4.50 in. Peak/Peak

Figure 3.3-18 Limiting Cases for Wheel Drop Avoidance (10 deg Curve/ 25 mph at Balance/Gage 57.5 in.)

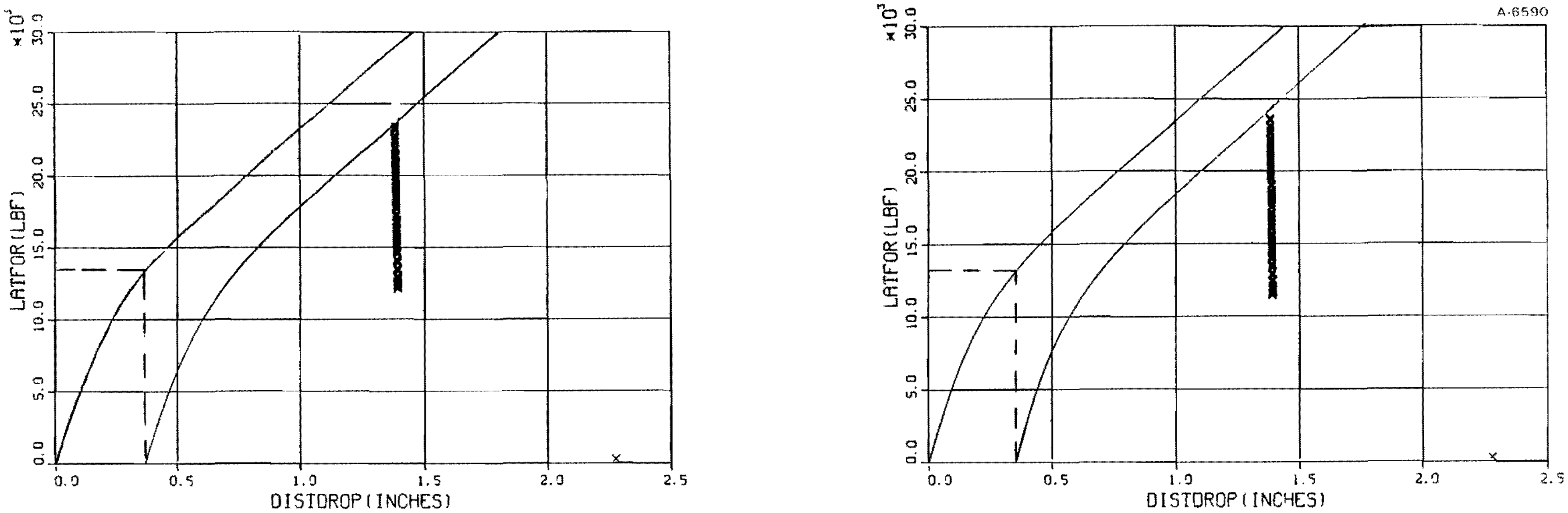

a) Wavelength 39 ft,
Amplitude 1.0 in. Peak/Peak

b) Wavelength 50 ft,
Amplitude 1.50 in. Peak/Peak

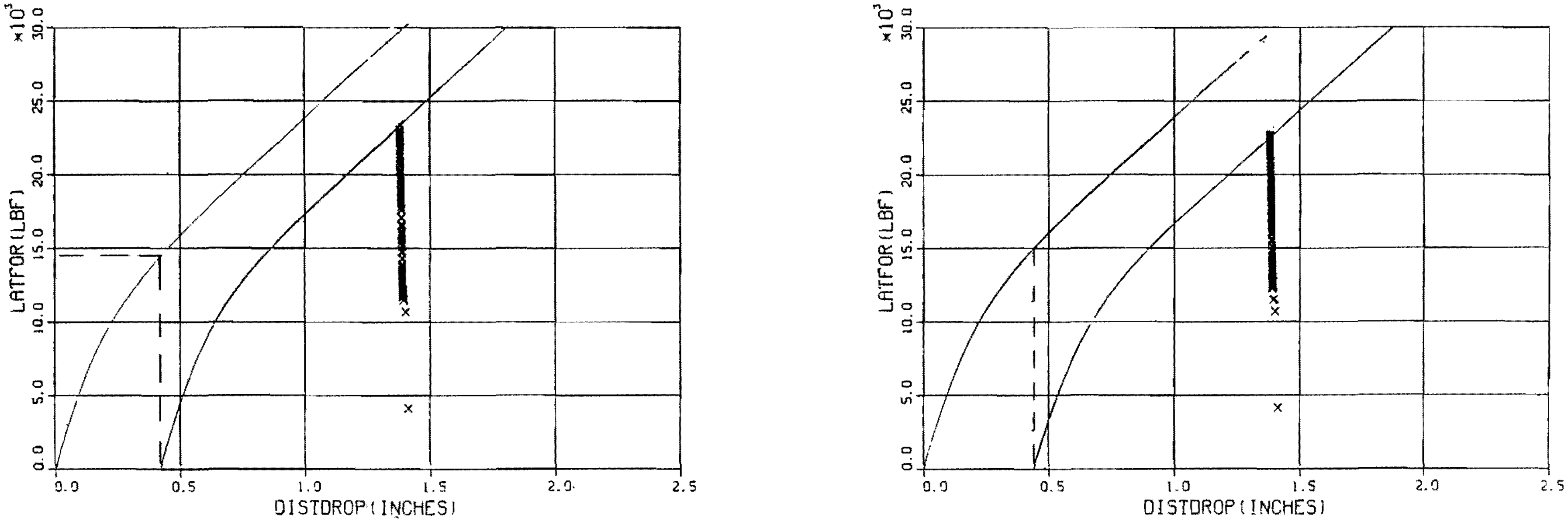

c) Wavelength 75 ft,
Amplitude 3.25 in. Peak/Peak

d) Wavelength 90 ft,
Amplitude 4.50 in. Peak/Peak

Figure 3.3-19 Limiting Cases for Wheel Drop Avoidance (15 deg Curve/
25 mph at Balance/Gage 57.5 in.)

4. SIMULATION RESULTS FOR BENNINGTON TEST

Simulation runs were carried out with SIMCAR following the tests at Bennington, New Hampshire. These runs used the modified car parameters given in Appendix A. Since there was no measurement of the height of the center of gravity or of the snubber friction, these quantities were estimated. The run list with the modified car data is given in Table 4-1. The design of the test included three sections: tangent track with alignment sinusoids of 39 ft, 50 ft and 90 ft wavelengths, a six degree curve with alignment sinusoids and outer rail cusps and a twelve degree curve with combined crosslevel and outer rail cusps. Results for the six degree curve were unavailable and have been simulated.

The two sections of the Bennington test track simulated were the tangent with alignment sinusoids and the twelve degree curve with outward cusps on the outer rail and crosslevel or downward cusps at the staggered rail joints.

4.1 ALIGNMENT SINUSOIDS ON TANGENT TRACK

Simulation of this scenario were carried out with 50 ft and 90 ft sinusoids but without crosslevel. The test used a lighter car than that assumed in the preceding chapter. The height of the body center of gravity was also reduced. A list of parameters for the car used in this scenario is given in Appendix A. The test results for the peak lateral forces and the SIMCAR values are given in Figs. 4.1-1 and 4.1-2. The simulated results compare well with those measured. However, Figs. 4.1-3 and 4.1-4 show the vertical force minima and dynamic peak/peak values for the same runs. These vertical forces show clear evidence of the roll resonance during the test runs. The actual resonance would not be at the sinusoidal alignment wavelength but at the rail length of 33 ft. This situation was not simulated. It is believed that the lateral transfer of load between wheels on the same axle would not greatly affect the results for the peak lateral force.

TABLE 4-1
RUN LIST FOR THE BENNINGTON TEST SIMULATIONS

RUN	BASIC CURVE		ALIGNMENT PERTURBATION		GAGE	SPEED	CAR	12 DEGREE CURVE		COMMENT
NO.	deg	BAL. SPEED	WAVE-LENGTH ft	P/P AMPLITUDE in.	CONST. in.	mph	HT in.	CROSSLEVEL in.	CUSP in.	
B1	0	-	90	4.5	57.0	10	60	-	-	
B2	↓			↓	↓	15	↓			Lateral Forces Good - Vert Force poor due to presumed zero Crosslevel
B3						20				
B4						25				
						30				
B5	12	21								
B6	↓	↓	-	-	56.5	15	60	0.3	1.25	
B7					↓		↓	0.625	↓	Inadequate Roll response with this Input and Ht
B8							70	↓		
B9						14	60	0.75		
B10						10	↓	↓		
B11	12	21	-	-	56.5	20	67	0.35	1.25	
B12	↓	↓			↓	14	↓	0.625	↓	
B13						10		0.80		Best Fit
B14						14		↓		
B15						14		0.90		
B16	0	-	50	1.25	57.0	20	67	-	-	No Crosslevel Input or Roll
B17	↓				↓	15	↓			
B18						10				

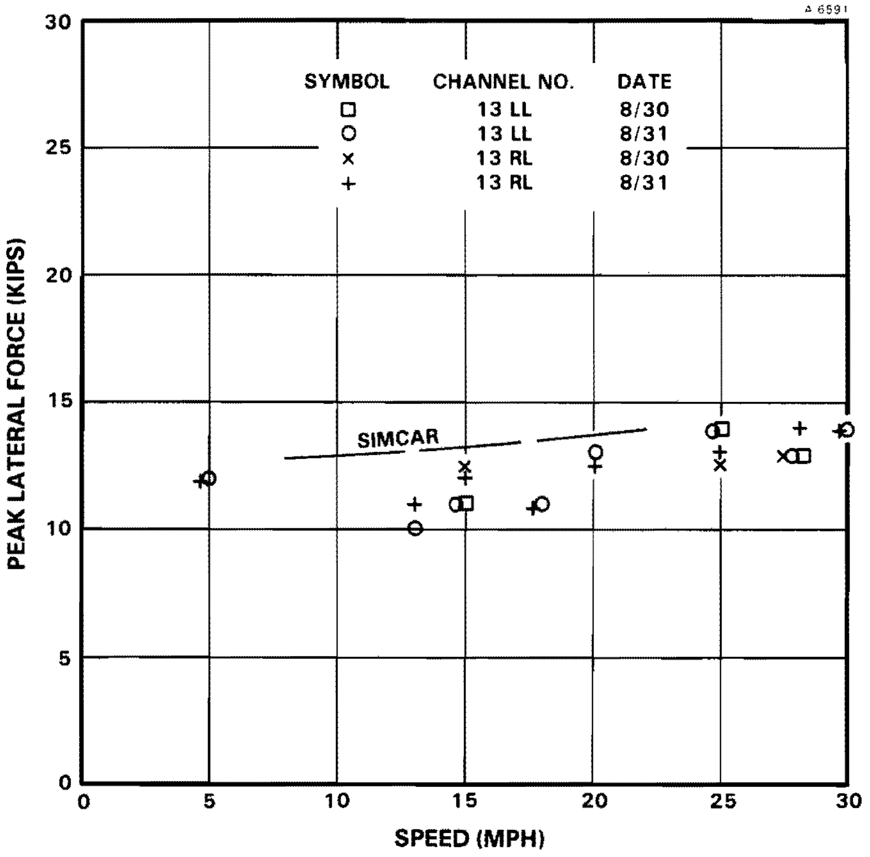

Figure 4.1-1 Comparison of Test with Simulated Peak Lateral Force in Alignment Sinusoids (Tangent Track/50 ft Wavelength/1.25 in. Peak/Peak)

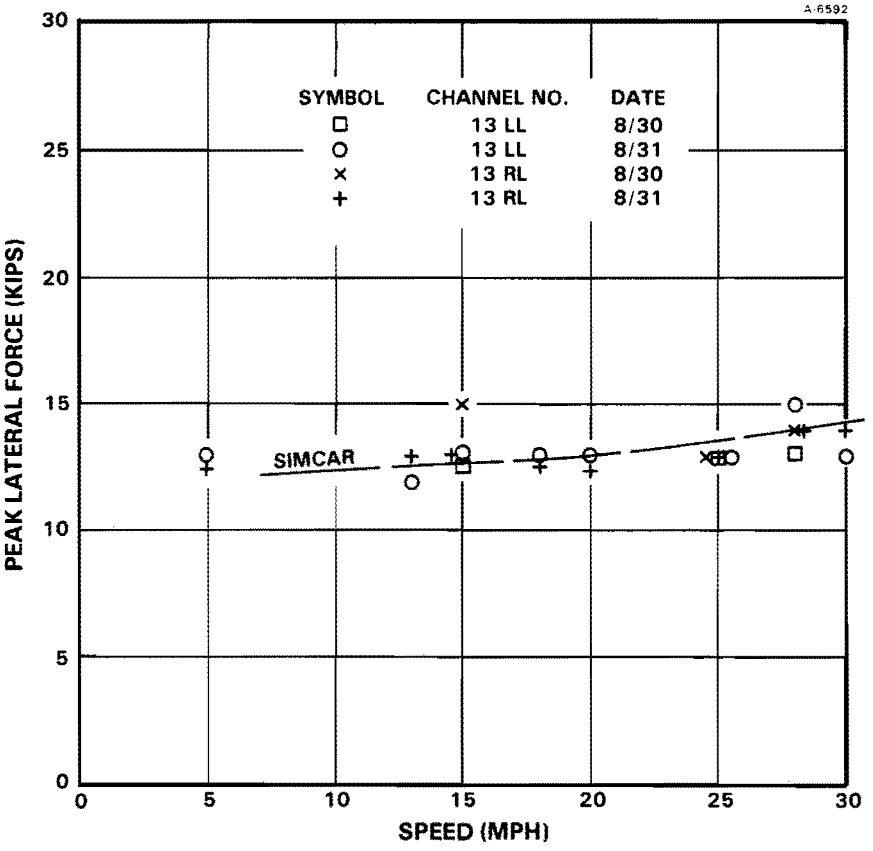

Figure 4.1-2 Comparison of Test with Simulated Peak Lateral Force in Alignment Sinusoids (Tangent Track/90 ft Wavelength/4.5 in. Peak/Peak)

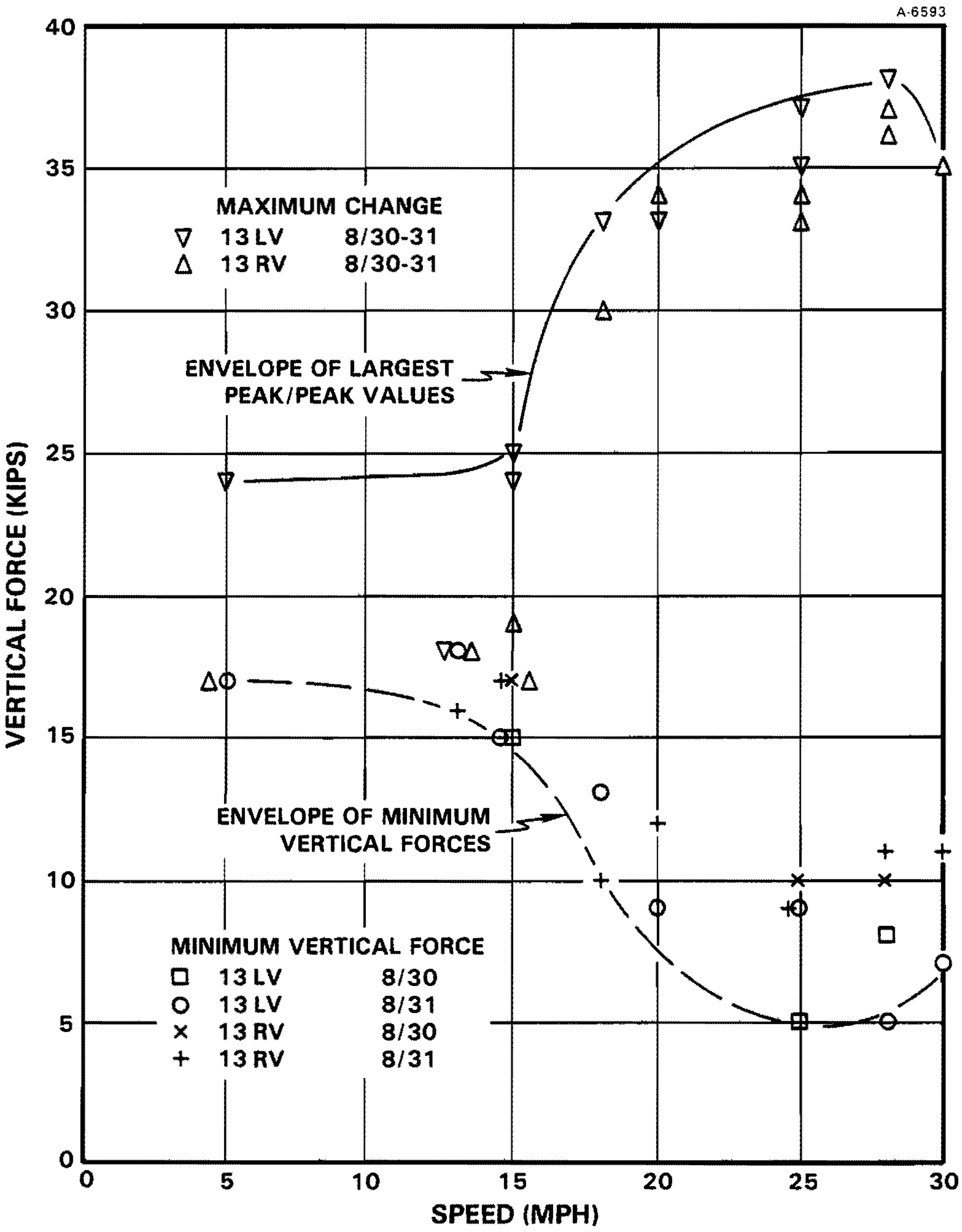

Figure 4.1-3 Comparison of Vertical Forces in Alignment Sinusoids (Tangent Track/50 ft Wavelength/ 1.25 in. Peak/Peak)

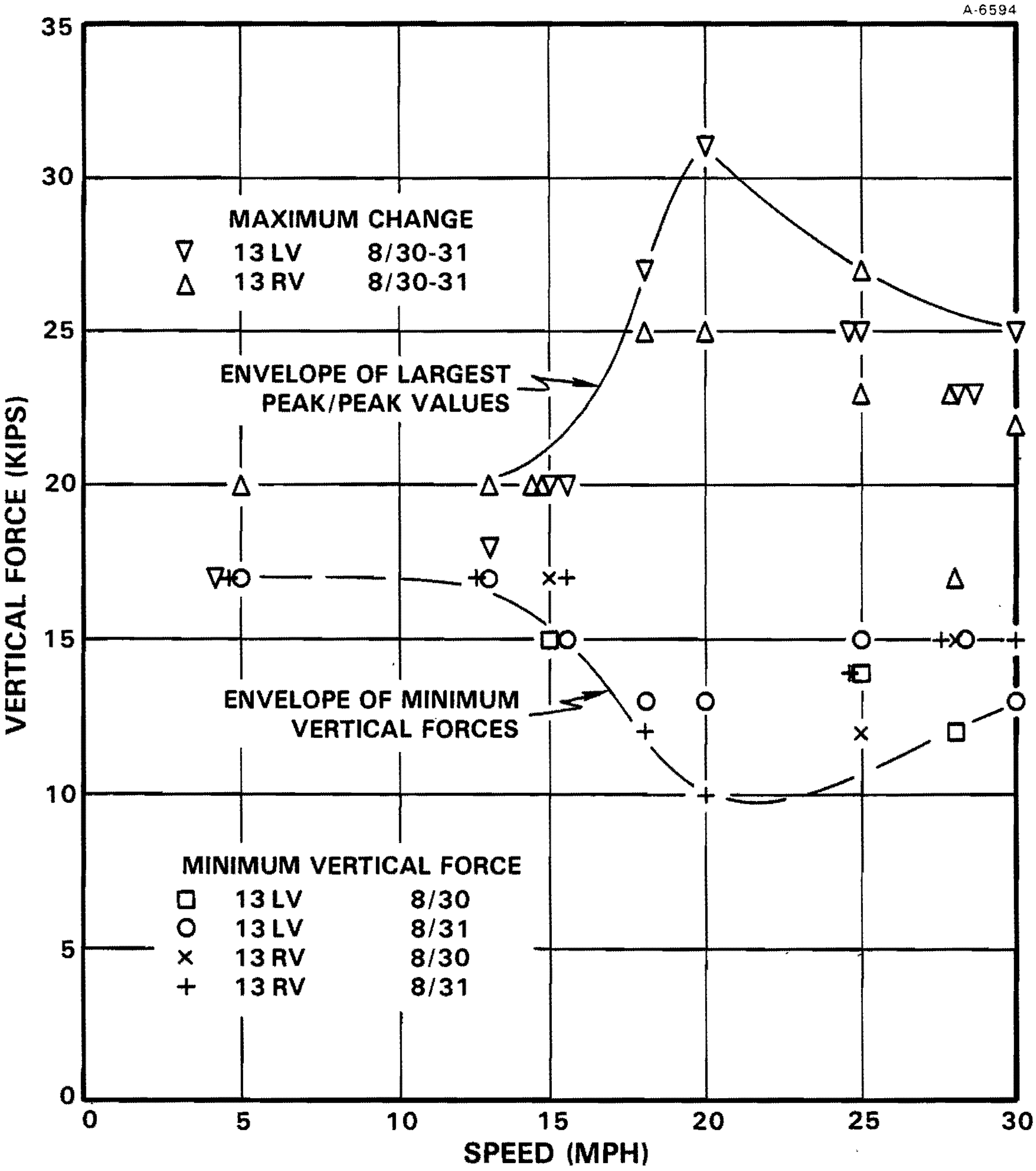

Figure 4.1-4 Comparison of Vertical Forces in Alignment Sinusoids (Tangent Track/90 ft Wavelength/ 4.5 in. Peak/Peak)

4.2 CUSPS AND CROSSLEVEL IN A TWELVE DEGREE CURVE

In this test, the large lateral to vertical force ratios developed, particularly by the locomotive, lead to an upper limit on speed of 14 mph. The results for peak lateral forces and vertical forces on the low and high rail are given in Figs. 4.2-1 through 4.2-3, respectively. The vertical forces again give evidence of the roll resonance estimated at about 17 mph or 0.75 Hz.

Very little information was available on the 100 ton hopper test car suspension characteristics. The static vertical wheel load of 25,000 lb was taken as an average over the wheels. An attempt was made to represent the vehicle using parameters given in Appendix A. The results are shown in the figures. The simulation vehicle has a lower resonant frequency at the amplitudes given. Furthermore, there appears to be a significant difference between the simulation and test results at 10 mph. This difference is seen principally in the amplitude of roll and hence vertical load transfer. The test result suggests a larger angle in roll for the almost static crosslevel input. This could be due to smaller suspension resistance to roll arising from reduced snubber friction or spring rate although the latter is also a contributor to the roll frequency. No attempt was made to "optimize" the simulation parameters. The trends are similar for both the test results and the simulation. The sensitivity of the simulation and known vehicular behavior to roll damping and the body to bolster roll moment characteristic are apparent in these results.

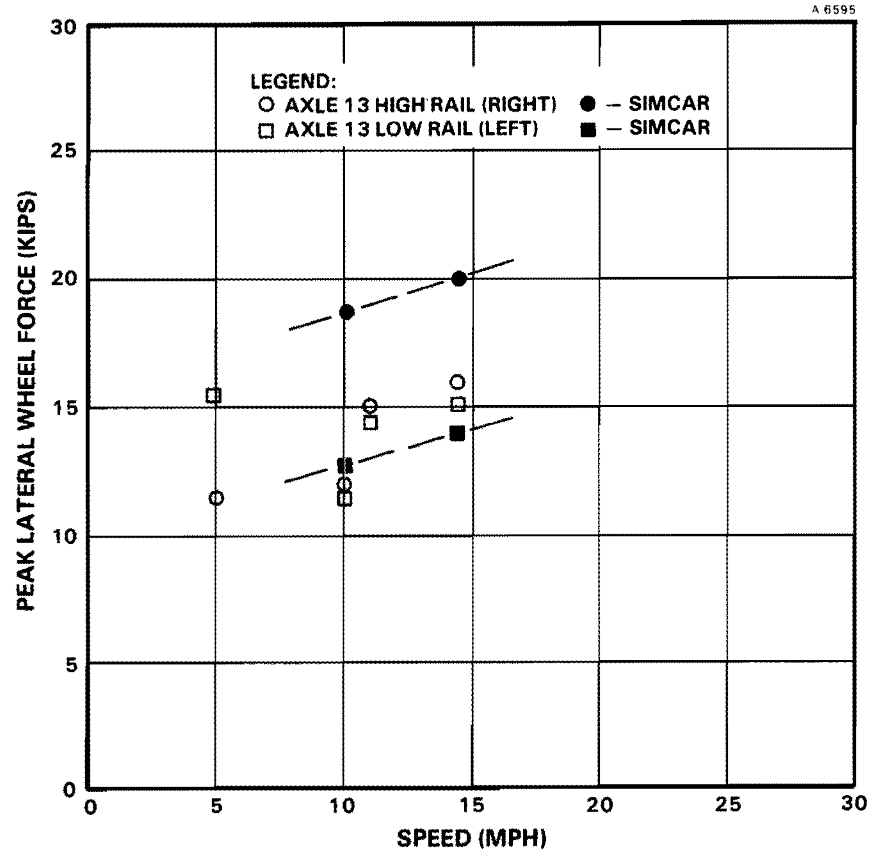

Figure 4.2-1 Peak Lateral Wheel Forces in the 12 Deg Curve (21 mph Balance/ Outer Rail Cusp 1.25 in./Crosslevel (Nominal) 0.75 in.)

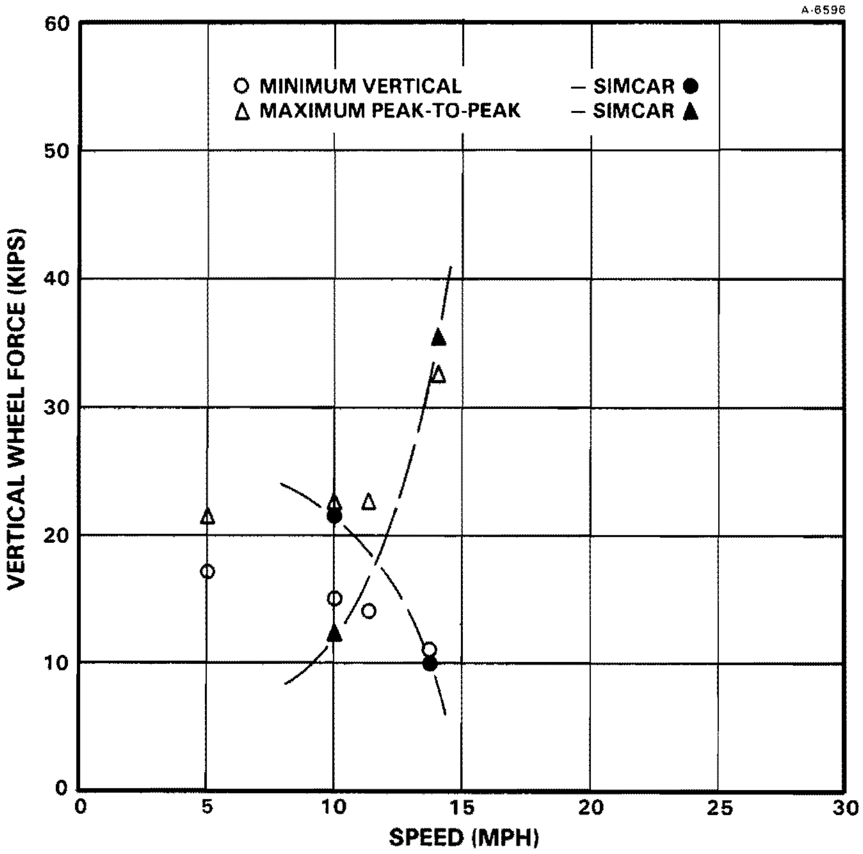

Figure 4.2-2 Vertical Wheel Forces on Low Rail in the 12 Deg Curve (21 mph Balance/Outer Rail Cusp 1.25 in./Crosslevel (Nominal) 0.75 in.)

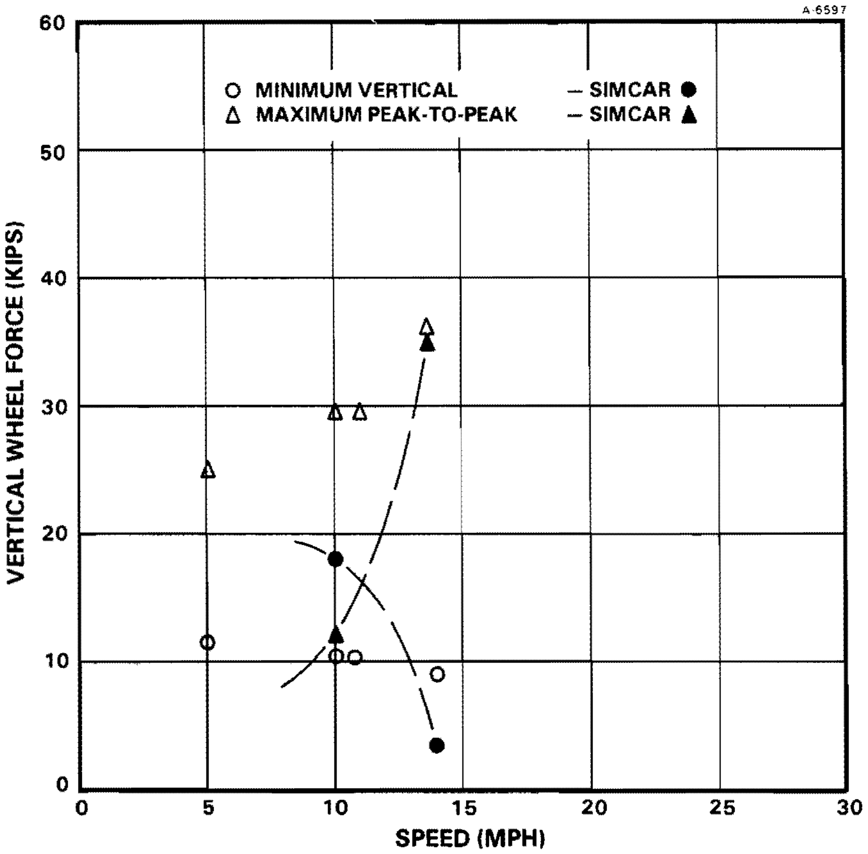

Figure 4.2-3 Vertical Wheel Forces on High Rail in the 12 Deg Curve (21 mph Balance/Outer Rail Cusp 1.25 in./Crosslevel (Nominal) 0.75 in.)

5. CONCLUSIONS AND RECOMMENDATIONS

The work described in Chapters 3 and 4 leads to conclusions concerning both the geometry beyond which either wheel climb or wheel drop is predicted in the low speed regime of 10 to 25 mph, especially in tight curves, and the recommendations already implemented on the value of geometric variables for tests on track with a minimum restraint capability carried out at Bennington, N.H. in August 1982.

5.1 DYNAMIC CURVING WITH CROSSLEVEL AND GAGE VARIATION IN TIGHT CURVES AT LOW SPEED

- In tight curves at low speed with track characterized by outer rail cusps at joints and crosslevel at both outer and inner rail joints, the results confirm that the response to the combined excitation provides a more severe condition than that resulting from either occurring separately.

- Under these conditions the limiting geometries which do not result in a wheel climb prediction under combined crosslevel and gage variation for the fully loaded 100 ton hopper car are given in Table 5.1-1.

- For the test at Bennington, New Hampshire, under conditions of track with a minimum restraint capability, a crosslevel of 0.75 in. combined with an outer rail cusp of 1.25 in. in a twelve degree curve provided a severe test of the ability of the vehicle/track system to resist wheel drop due to dynamic wide gage. However, the results are not conclusive due to the difficulty of obtaining a full characterization of the vehicle used.

- The particular circumstance which renders the combination of track crosslevel and gage and alignment variation hazardous in tight curves is the danger of having an unloaded wheel driven up the flange (wheel climb) by a heavily loaded non-flanging wheel with an angle of attack to the rail during a roll cycle.

TABLE 5.1-1
LIMITS PREDICTED FOR TRACK GEOMETRY FOR COMBINED OUTER RAIL CUSPS AND STAGGERED JOINT CROSSLEVEL IN CURVES*

CURVATURE deg	CROSSLEVEL in.	LAT. CUSP in.	MAX. GAGE in.
0-3	0.625	1.75	57.75
3-5	0.625	1.25	57.75
5-10	0.5	1.25	57.75
10-15	0.5	1.0	57.5

*100 ton loaded hopper, new wheel profiles.

5.2 DYNAMIC CURVING WITH ALIGNMENT SINUSOIDS AND CONSTANT GAGE AT LOW SPEED

- The sinusoidal alignment variation with constant gage provides to the 100 ton hopper a more severe response and potential for wheel drop derailment than the alignment amplitude due to outer rail cusps above. This is particularly true for wavelengths greater than 39 ft.

- Incipient wheel drop becomes more likely with increasing

  - speed
  - curvature
  - gage in curves
  - alignment amplitude

  It should be noted that this increase is not necessarily associated with an increase in lateral force.

- Under these conditions the limiting geometries which do not result in a wheel drop prediction for a 100 ton hopper car under excitation by sinusoidal alignments of varying amplitude and wavelength are given in Table 5.2-1.

- The lateral forces measured at Bennington, New Hampshire are close to those predicted using SIMCAR and confirm its accuracy in providing an assessment of wheel drop forces in sinusoidal alignment studies with the new wheel profile characteristics used in this study.

TABLE 5.2-1
MAXIMUM PEAK/PEAK AMPLITUDES OF SINUSOIDAL TRACK ALIGNMENT VARIATIONS WHICH DO NOT GIVE INCIPIENT WHEEL DROP DERAILMENTS ON TRACK HAVING A MINIMUM RESTRAINT CAPABILITY TO A LOADED 100 TON HOPPER CAR (25 mph at Balance Speed)

WAVELENGTH (ft)	CURVE (DEGREES)				TRACK GAGE (in.)
	0	5	10	15	
39	1.375	1.00	0.75	0.25	$57\frac{3}{4}$
50	1.25	1.25	1.00	0.375	
75	3.50	3.25	2.25	1.25	
90	4.50*	4.50*	3.50	1.75	
39	-	-	1.25	1.0	$57\frac{1}{2}$
50	-	-	1.75	1.50	
75	-	-	3.50	3.25	
90	-	-	4.50*	4.50	

* Very safe result - higher value possible.

5.3 RECOMMENDATIONS

- The simulation program (SIMCAR) presently has some deficiencies in representing wheel forces and therefore the results are difficult to interpret. These analytic problems may lead to inaccuracy in the interpretation of conditions of incipient derailment. It is recommended that the program be modified to provide a more accurate representation of wheel forces and an increase in computational efficiency.
- It is recommended that the present studies be extended to include higher speeds, a greater variety of car and locomotives in frequent usage, a wider range of rail/wheel profiles and additional track geometries so that safety specifications may be proposed which cover the full range of operating conditions found on the railroads.

APPENDIX A

PARAMETER VALUES USED IN THE SIMCAR MODEL

The values used in SIMCAR to represent the 100 ton hopper car for studies of the limiting conditions of track geometry and to represent the test vehicle at Bennington are given in Table A-1. A detailed description of the SIMCAR model may be found in Ref. 4.

TABLE A-1
PARAMETER VALUES USED FOR SIMCAR PREDICTIONS

SIMCAR VARIABLE NAME	DESCRIPTION	UNITS	LOADED HOPPER	BENNINGTON HOPPER
KY	Lateral stiffness	lb/in	2.04×10^4	2.04×10^4
BY	Lateral damping	lb-sec/in	3.242×10^3	3.242×10^3
KZ	Vertical stiffness	lb/in	4.422×10^4	4.422×10^4
BZ	Vertical damping	lb-sec-in	2.0×10^4	2.0×10^4
KZZ	Yaw stiffness	lb-in/rad	0.0	0.0
BZZ	Yaw damping	lb-in-sec/rad	0.0	0.0
KZT	Tram stiffness	lb-in/rad	3.43×10^7	3.43×10^7
BZT	Tram damping	lb-in-sec/rad	0.0	0.0
KXXR	Carbody to bolster roll stiffness	lb/in	1.0×10^9	1.0×10^9
LT	Half-length between truck centers	in	243.0	243.0
HT	Height from top of springs to body center of mass	in	82.0	67.0
GAMSX	Twist modal displacement at truck	----	0.9274	0.9274
GAMSY	Lateral bending modal displacement at truck	----	-0.6237	-0.6237
GAMSZ	Vertical bending modal displacement at truck	----	-0.6237	-0.6237
GAMPSZ	Lateral bending modal derivative at truck	----	-0.01028	-0.01028
A	Half wheelbase of truck	in	35.0	35.0
B	Half gauge	in	29.75	29.75
MC	Carbody mass	lb-sec^2/in	630.77	465.0
IXC	Carbody roll inertia	lb-in-sec^2	1.824×10^6	1.345×10^6
IYC	Carbody pitch inertia	lb-in-sec^2	1.68×10^7	1.24×10^7
IZC	Carbody yaw inertia	lb-in-sec^2	1.6657×10^7	1.23×10^7
MXC	Twist modal mass	lb-in-sec^2	9.12×10^5	9.12×10^5

TABLE A-1
PARAMETER VALUES USED FOR SIMCAR PREDICTIONS (Cont.)

SIMCAR VARIABLE NAME	DESCRIPTION	UNITS	LOADED HOPPER	BENNINGTON HOPPER
MYC	Vertical bending modal mass	$lb\text{-}sec^2/in$	317.2	317.2
MZC	Lateral bending modal mass	$lb\text{-}sec^2/in$	317.2	317.2
MW	Wheelset mass	$lb\text{-}sec^2/in$	7.731	7.731
MS	Sideframe mass	$lb\text{-}sec^2/in$	2.983	2.983
MB	Bolster mass	$lb\text{-}sec^2/in$	3.78	3.78
IW	Wheelset yaw inertia	$lb\text{-}in\text{-}sec^2$	5.889×10^3	5.889×10^3
IS	Sideframe yaw inertia	$lb\text{-}in\text{-}sec^2$	1.366×10^3	1.366×10^3
IBX	Bolster inertia, roll	$lb\text{-}in\text{-}sec^2$	2.757×10^3	2.757×10^3
IBZ	Bolster inertia, yaw	$lb\text{-}in\text{-}sec^2$	2.757×10^3	2.757×10^3
OMX	Twist frequency	rad/sec	44.08	44.08
OMY	Vertical bending frequency	rad/sec	108.45	108.45
OMZ	Lateral bending frequency	rad/sec	63.90	63.90
ALPHA	Conicity, centered	----	0.05	0.05
RO	Wheel radius, centered	in	18.0	18.0
F22	Lateral tread creep coefficient	lb	1.83×10^6	1.83×10^6
F11	Longitudinal tread creep coefficient	lb	1.96×10^6	1.96×10^6
GLOADZ	Influence of centrifugal load	----	0.0	0.0
WSG	Distance from center to spring group	in	39.52	39.52
HSG	Height of top of springs above rail	in	16.0	16.0
FLANG	Flange angle (relative to axle)	deg	67.0	67.0
CKGF	Coefficient of lateral force increase following flange contact	----	0.0	0.0
CR	Single-sided flange clearance at rail	in	0.325	0.325
MU	Coefficient of friction between wheel and rail	----	0.5	0.5
KGLEAD	Characteristic leading edge stiffness at flange	lb/in	1.0×10^6	1.0×10^6
CLSB	Clearance of the side bearers	in	0.25	0.25
LSB	Half lateral distance between sidebearers	in	25.0	25.0
RCP	Centerplace radius	in	7.0	7.0
FSND	Snubber force per side, downstroke	lb	4.0×10^3	4.0×10^3

TABLE A-1
PARAMETER VALUES USED FOR SIMCAR PREDICTIONS (Cont.)

SIMCAR VARIABLE NAME	DESCRIPTION	UNITS	LOADED HOPPER	BENNINGTON HOPPER
FSNU	Snubber force per side, upstroke	lb	4.0×10^{3}	4.0×10^{3}
DELCP	Centerplace free play rate	rad/sec	1.745×10^{-3}	1.745×10^{-3}
TCP	Centerplate torque	lb-in	5.619×10^{4}	5.619×10^{4}
PSNT	Tram free play	rad	0.05236	0.05236
KZZNT	Nonlinear truck tramming stiffness	lb-in/rad	3.43×10^{8}	3.43×10^{8}
K2Y	Lateral suspension stiffness on gibs	lb/in	1.02×10^{6}	1.02×10^{6}
DELHG	Suspension lateral clearance	in	0.375	0.375
K2Z	Vertical stiffness following spring closure	lb/in	2.406×10^{6}	2.406×10^{6}
COMSG	Close coiled compression of spring group	in	0.9104	0.9104
EXTSG	Extension to free length of spring group	in	2.7771	2.7771
CRINC	Incremental creepage change at flange contact	----	0.0105	0.0105
CRATE	Rate of creepage change with lateral displacement after flange contact	----	4.09	4.09
CLOAD	Coefficient of vertical force ratio in lateral force calculation	----	1.0	1.0

REFERENCES

1. DiMasi, F.P., "Correlation of Accident Data with Physical Characteristics of Derailed Freight Vehicles," TSC Report No. DOT-TSC-RR219-PM-82-6, June 1982.

2. DiMasi, F.P., Przybylinski, P.G., and Anderson, G.B., "Engineering Data Characterizing the Fleet of U.S. Railway Rolling Stock," DOT Report No. FRA/ORD-81/75.1 & 81/75.2 (2 vols.) NTIS: PB82-181546 and PB82-181553, 1981.

3. Hamid, A., Owings, R., and Kenworthy, M., "Characterization of Relatively Large Track Geometry Variations," DOT Report No. FRA/ORD-81/13, NTIS: PB82-169460, March 1982.

4. Blader, F.B., "Analytical Studies of the Relationship between Track Geometry Variations and Derailment Potential at Low Speed," DOT Report No. FRA/ORD-83/16, NTIS: PB84-129329, September 1983.

5. Platin, B.E., Beaman, J.J., Hedrick, J.K., and Wormley, D.N., "Computational Methods to Predict Railcar Response to Track Crosslevel Variations," MIT, Final Report, DOT Report No. FRA/OR&D-76/293, NTIS: PB 272-676/AS, September 1976.

☆ U. S. GOVERNMENT PRINTING OFFICE: 1985--502-199--20,107

79 copies

U.S. Department
of Transportation

**Research and
Special Programs
Administration**

Kendall Square
Cambridge, Massachusetts 02142

Postage and Fees Paid
Research and Special
Programs Administration
DOT 513

U.S. MAIL

Official Business
Penalty for Private Use $300

PROPERTY OF FRA
RESEARCH & DEVELOPMENT
LIBRARY